

**Characterization of the Interactions and Enzyme
Activities of the Type IV Secretion Components
VirB1 and VirB11 from
Brucella suis and *Agrobacterium tumefaciens***

**Dissertation
der Fakultät für Biologie
der Ludwig-Maximilian-Universität München**

**vorgelegt von
Christoph Höppner
am 3. Februar 2005**

1. Gutachter: Prof. Dr. Christian Baron

2. Gutachter: Prof. Dr. August Böck

Tag der mündlichen Prüfung: 22. März 2005

INTRODUCTION	1
1. A successful mechanism used for diverse applications	1
2. Similarity between the <i>A. tumefaciens</i> and <i>B. suis</i> T4SS	3
3. A dual role of the soluble lytic transglycosylase VirB1	7
3.1. The catalytic mechanism of SLTs	7
3.2. VirB1 interacts with T4SS components	9
4. The VirB11-like hexameric (d)NTPase of T4SS	9
4.1. General characteristics and role in the system	9
4.2. Choice of VirB11 orthologs as drug targets	11
5. Social and economic impact of some T4SS-mediated diseases	13
6. Aim of this work	18
MATERIALS AND METHODS	19
1. Bacterial strains, bacteriophages and plants	19
1.1. Bacterial strains	19
1.2. Bacteriophages and plants	20
2. Plasmids and genomic DNA	20
3. Oligonucleotides	25
3.1. PCR primers	25
3.2. Site-directed mutagenesis primers	27
3.3. Specialized sequencing primers	27
4. Growth media, supplements and antibiotics	28
4.1. Growth media	28
4.2. Supplements, antibiotics and inhibitors	29
5. Buffers and solutions	30
6. Growth conditions	30
6.1. <i>Escherichia coli</i>	30
6.2. <i>Agrobacterium tumefaciens</i>	31
7. Photometric methods	31
7.1. Optical density	31
7.2. Absorption	31
8. Molecular biology methods	31
8.1. PCR	31
8.2. DNA isolation	31
8.3. DNA <i>in vitro</i> modifications	32
8.3.1. Restriction cleavage and dephosphorylation	32
8.3.2. Removal of staggered ends	32
8.3.3. Ligation	32
8.4. Site-directed mutagenesis	32
8.5. DNA-sequencing	32
8.6. Transformation of plasmid DNA	32
9. Biochemical methods	33
9.1. (d)NTPase assay	33
9.2. Determination of protein-protein interactions	34
9.2.1. Strep-Tactin® Sepharose® pull-down assay	34

9.2.2.	Chemical crosslinking with DSS	34
10.	Electrophoretic methods	34
10.1.	Electrophoretic separation of DNA	34
10.2.	Protein separation by SDS-PAGE	34
10.3.	Electroelution	35
11.	Chromatographic methods	35
11.1.	Immobilized metal chelate affinity chromatography (IMAC)	35
11.2.	Strep-Tactin Sepharose chromatography	35
11.3.	Gel filtration	35
11.4.	Enrichment of proteins and dialysis	36
12.	Bacteriological methods	36
12.1.	Conjugation assay	36
12.1.1.	<i>A. tumefaciens</i>	36
12.1.2.	<i>E. coli</i>	36
12.2.	Virulence assay	37
12.3.	Phage infection assay	37
13.	Immunological methods	37
13.1.	Protein transfer	37
13.2.	Western blot	38
13.3.	Overlay assay	38
13.4.	Peptide array experiments	39
13.5.	Generation of polyclonal antisera	39
14.	Data processing	39
14.1.	Statistical and graphical data processing	39
14.2.	Protein sequence analysis	39
	RESULTS	41
1.	Characterization of structural and functional properties of VirB1	41
1.1.	Display of conservation between the VirB1 SLT domain and its orthologs LysG and Slr70	41
1.2.	An <i>in silico</i> analysis of VirB1 ortholog conservation	42
1.3.	Secondary structure prediction of the VirB1 C-terminus	43
1.4.	Biochemical analysis of <i>B. suis</i> VirB1 interactions	44
1.4.1.	Coproduction of VirB1 and other VirB proteins in bi-cistronic expression vectors	44
1.4.1.1.	Purification of C- and N-terminally affinity-tagged VirB1	47
1.4.1.2.	Analysis of VirB1-VirB8 bicistron products	51
1.4.1.3.	Analysis of VirB1-VirB9 bicistron products	51
1.4.1.4.	Analysis of VirB1-VirB10 bicistron products	51
1.4.1.5.	Analysis of VirB1-VirB11 bicistron products	52
1.4.1.6.	Analysis of VirB1-VirB4 bicistron products	52
1.4.2.	Strep-Tactin® Sepharose® pull-down assay	52
1.4.3.	Crosslinking of purified VirB1 to other VirB proteins	53
1.4.4.	Peptide-array analysis of VirB1 interactions	56
1.5.	Heterologous expression of the <i>B. suis</i> <i>virB</i> operon in <i>A. tumefaciens</i>	58
1.5.1.	Heterologous expression of different subsets of the <i>virB</i> operon	61
1.5.2.	Heterologous expression the <i>virB</i> operon encoding a VirB1 protein variant	65
1.6.	Genetic analysis of <i>A. tumefaciens</i> VirB1	66
1.6.1.	Heterologous complementation of the <i>virB1</i> deletion mutant PC1001	66
1.6.2.	Mutational analysis of the VirB1 processing-site	70
1.6.3.	Effect of the heterologous production of an HP0523-VirB1*-hybrid in PC1001.	74
2.	<i>In silico</i> , <i>in vitro</i> and <i>in vivo</i> analysis of T4SS traffic-(d)NTPase orthologs	78
2.1.	Sequence conservation among the studied VirB11 orthologs	78
2.2.	Purification and characterization of VirB11 orthologs from different T4SS	81
2.2.1.	Purification of VirB11 orthologs	81
2.2.2.	General Properties of the (d)NTPases	83

2.2.3.	<i>B. suis</i> StreptII-VirB11 ATPase activity in the presence of other VirB proteins	85
2.3.	Studies with VirB11-specific inhibitors	86
2.3.1.	<i>In vitro</i> studies of the effect of MTFPT	86
2.3.2.	<i>In vivo</i> studies of the MTFPT inhibitory effect	90
2.3.2.1.	Effect of MTFPT on the <i>A. tumefaciens</i> T4SS	91
2.3.2.2.	Effect of MTFPT on conjugative transfer of broad host range plasmids	93
2.3.2.3.	Effect of MTFPT on IncN pilus formation	94
2.3.3.	Effects of oleic and linoleic acid on VirB11 activity	95
2.4.	Complementation of an <i>A. tumefaciens</i> VirB11 mutant	97
2.5.	Protein-protein interactions of VirB11	99
2.5.1.	Strep-Tactin® Sepharose® pull-down assay	99
2.5.2.	Overlay assay of VirB11 and VirB5 orthologs	99
DISCUSSION		102
1.	Interactions of VirB1 with other T4SS components	102
1.1.	Common features of VirB1 from <i>B. suis</i> and <i>A. tumefaciens</i>	102
1.2.	Interactions of VirB1 with other VirB proteins	102
1.3.	VirB1 is an important component of the <i>B. suis</i> T4SS	106
1.4.	Structure-function analysis of VirB1	108
1.5.	Multiple roles of VirB1	110
2.	VirB11, the hexameric traffic (d)NTPase from T4SS	112
2.1.	Structural conservation in diverse systems	112
2.2.	Similar enzymology of VirB11 orthologs from T4SS	113
2.3.	Inhibitors act on all VirB11 orthologs	114
3.	Complementation of a VirB11 mutant	115
4.	Interaction of VirB11 and VirB5	116
SUMMARY		118
REFERENCES		120

Abbreviations

AA	amino acid
antibiotic ^R	resistant to the indicated antibiotics
AS	acetosyringone (3',5'-dimethoxy-4'-hydroxyacetophenone)
<i>bla</i>	β-lactamase gene
bhr	broad host range
bp	base pairs
carb	carbenicillin
CLB	crosslink buffer
cm	chloramphenicol
CTD	C-terminal domain
CV	column volume
DSS	disuccinimidyl suberate
DTT	dithiothreitol
(d)NTP	(2'-deoxy)nucleoside-5'-triphosphate
ery	erythromycin
GlcNAc	N-acetylglucosamine
His ₆	hexa-histidine
IMAC	immobilized metal affinity chromatography
kan	kanamycin
kDa	kilo dalton (1000 g/mol)
kb	kilo basepairs
MTFPT	4-methyl-2-[4-(trifluoromethoxy)phenyl]-1,2,4-thiadiazolane-3,5-dione
MurNAc	N-acetylmuramic acid
MW	molecular weight
NTD	N-terminal domain
PBS	phosphate-buffered saline
PMSF	phenylmethylsulfonylfluoride
PSB	protein storage buffer
psi	pounds per square inch
RT	room temperature
SB	sample buffer
SDS	sodium dodecyl sulfate
SDS-PAGE	SDS polyacrylamide gel electrophoresis
SLT	soluble lytic transglycosylase
spc	spectinomycin
str	streptomycin
T4SS	type IV secretion system
tm	trimethoprim

Introduction

1. A successful mechanism used for diverse applications

When David Bruce was rewarded with a knighthood in 1908, this was not only for his achievements in discovering the transmission mode of the sleeping sickness. Having started his career in the English Army Medical Service twenty-five years earlier on the island of Malta, the occurrence of “Malta fever” not only caught the attention but, fortunately, also challenged the investigative talent of the young surgeon. While conducting examinations on his Mediterranean post, he discovered that the cause for this disease, which sometimes resembled typhoid fever and sometimes malaria, was an organism he called *Micrococcus melitensis*. It became later known as *Brucella melitensis*. The reservoir of infection was traced to the Maltese goat, and drinking milk from infected animals seemed to be the main cause of infection. The genus *Brucella* is characterized by species like *B. melitensis*, *B. abortus* and *B. suis*, which all reside within animal hosts. They are also pathogens of humans, where they cause zoonotic infections. The symptoms of this long-lasting febrile illness are severe, but brucellosis is rarely fatal for humans. Patients who have experienced the disease, which requires antibiotic treatment for nine months or longer, describe it to be like having “the flu times ten” (Winstead, 2004; LSHTM, 2004).

This debilitating nature of brucellosis encouraged the US-military’s interest in the disease and more importantly in properties of its causative agent. In the 1950s the cold-war superpowers attempted to weaponize a number of pathogenic bacteria and the US military, among other projects, focused on creating bioweapons that would not kill but rather disable attacking troops for a prolonged period. *B. suis*, typically isolated from pigs, was cultivated, processed and filled into bomb shells, which were never used for other goals than maintaining the balance of power. These bombs were destroyed in 1969 when the bioweapon program was abandoned (Winstead, 2004). Aside from such questionable applications, the military contributed to progress in the life sciences and medicine by being a driving force in the development of antibiotics and vaccines. Nevertheless, the mechanisms of bacterial virulence remained unknown until the late 20th century, when techniques of biochemistry and molecular biology started to unravel the molecular basis of bacterial pathogenicity.

In the last 30 years, research conducted with the plant pathogenic bacterium *Agrobacterium tumefaciens* brought a number of fundamental insights for both the fields of plant science and bacterial pathogenesis (reviewed by Zupan and Zambryski, 2000; Baron *et al.*, 2002; Binns, 2002). *A. tumefaciens* was shown to transfer single stranded DNA (T-DNA)

to plant cells where it is stably integrated into the genome (Zambryski, 1992). Due to the genes encoded in the T-DNA, the plant cell is forced to proliferate while producing certain organic compounds called opines, which can be preferably utilized by the *Agrobacteria* (Petit *et al.*, 1970). This example of gene transfer into eukaryotic species by a bacterium is unique. The *virB* operon was identified to be important for this process (Kuldau *et al.*, 1990), and ten of the eleven genes encoded in it are indispensable for virulence (Berger and Christie, 1994). The operon-encoded proteins VirB1 to VirB11 build up the VirB-complex, a macromolecular membrane-spanning apparatus responsible for secretion of the T-DNA into the plant cell. With the onset of efficient DNA-sequencing techniques the growing amount of sequence data led to the discovery that many proteobacteria possess orthologous genes coding for proteins that constitute similar membrane-spanning machineries. The obvious similarities between the *A. tumefaciens virB* operon, the *tra* operon of broad host range plasmid pKM101 and the *ptl* operon from *Bordetella pertussis* were among the first findings in this area (Weiss *et al.*, 1993; Winans *et al.*, 1996). In order to distinguish them from other common secretion machineries in bacteria, the *vir*-encoded membrane-spanning translocation apparatus was denominated type IV secretion system (T4SS). It is apparent that proteobacteria generally take advantage of T4SS for three different purposes.

First, in *A. tumefaciens* and broad host range (bhr)-plasmid-carrying bacteria the T4SS serves to transfer ssDNA together with associated proteins to recipient eukaryotic and prokaryotic cells, respectively. Second, many bacterial pathogens utilize T4SS to deliver effector molecules to the host, thus ensuring their survival and propagation inside the host cell (e.g. *Legionella pneumophila*, *Brucella spp.* and *Bartonella spp.*) and outside of the host cell (e.g. *Bordetella pertussis* and *Helicobacter pylori*). Third, it was observed that the transfer of IncQ plasmids between *A. tumefaciens* cells is drastically improved when recipient cells display the *virB*-encoded T4SS (Bohne *et al.*, 1998) and *H. pylori* obtains natural transformation competence by expression of an operon that encodes T4SS core components VirB4, VirB8, VirB9 and VirB10 (Hofreuther *et al.*, 2001). Together, these data show the importance of T4SS not only for DNA delivery to other cells, but also for DNA uptake into cells.

An ecologically diverse group of proteobacteria utilizes T4SS for an equally diverse set of applications (Table 1), and the different lifestyle of *A. tumefaciens* and *B. suis* is obvious though there are many similarities between the two organisms. After completion of the genomic sequence of the intracellular animal pathogen *B. suis*, it became apparent that this organism is in fact a close relative of extracellular plant pathogen *A. tumefaciens*. Despite their preference for hosts belonging to different kingdoms, these organisms share

genes, have a similar genome structure and biological pathways, a fact that is also exemplified by comparison of the T4SS of the two organisms (Paulsen *et al.*, 2002; Tsolis, 2002).

Table 1. Diversity of T4SS utilization by different proteobacteria. (Nagai and Roy, 2003; Christie and Vogel, 2000; Masui *et al.*, 2000; Shamaei-Tousi *et al.*, 2004, Baron *et al.*, 2002; Brock *et al.*, 1997; Harb *et al.*, 2000).

genus	proteobacteria group	host relation	habitat	lifestyle	<i>virB</i> operon localization	VirB orthologs	substrate(s)
<i>Agrobacterium</i>	α	pp	soil, plants	ec	Ti plasmid, cryptic plasmid	1-11	ssDNA-VirD2, VirE2, VirF
<i>Bartonella</i>	α	p	mam. blood, arthropods	ic	genome	2-11	unknown
<i>Bordetella</i>	β	p	upper respiratory tract	ec	genome	2-4,6-11	Pertussis toxin (Ptx)
<i>Brucella</i>	α	p	soil, animals	ic	genome	1-11	unknown
<i>Escherichia</i>	γ	s/c/p	gastrointestinal tract	ec	broad-host-range plasmids	1-11	ssDNA, proteins
<i>Helicobacter</i>	ϵ	c/p	stomach, duodenum	ec	genome	1,4,9-11	CagA
<i>Legionella</i>	γ	c/p	protozoa, animals	ic	genome	10,11	RalF, DotA
<i>Wolbachia</i>	α	s/c/p	arthropods, nematodes	ic	genome	4+8-11	unknown

pp: plant pathogenic, p: human and animal pathogenic, s: symbiotic, c: commensal, ec: extracellular, ic: intracellular, mam.: mammalian.

2. Similarity between the *A. tumefaciens* and *B. suis* T4SS

The 11.8 kb *virB* operon of *B. suis* was identified following the observation that Tn*bla*M insertion mutants in that region were unable to multiply in the intracellular environment of macrophages. The DNA sequence flanking the transposon insertion showed significant sequence similarities to genes encoding *B. pertussis* PtlG and *A. tumefaciens* VirB9. Sequence determination of the surrounding region identified the *virB* operon and its 12 *orfs*, which was subsequently proven to be also present in *B. abortus*, *B. canis*, *B. melitensis*, *B. neotomae* and *B. ovis*. Comparison of the *virB* region of *A. tumefaciens* and *B. suis* showed that the newly discovered operon consists of genes encoding orthologs to all VirB proteins of *A. tumefaciens* plus an additional gene for the putative lipoprotein VirB12 (O'Callaghan *et al.*, 1999). The structures of the *virB* operons of *B. suis* and *A. tumefaciens*

are almost identical (Fig. 1A). While many genes overlap the preceding one either with their Shine-Dalgarno sequence or their start codon like in the *A. tumefaciens* *virB* operon, the presence of intergenic regions between *virB1* and *virB2*, *virB5* and *virB6*, *virB6* and *virB7* is special for *B. suis*. This raised the question whether the 12 genes constitute an operon. Moreover, there are two degenerate *Brucella*-specific repeat regions denominated BruRS1 and BruRS2 (Halling and Bricker, 1994), which succeed *virB1* and *virB12*. Finally, sequence comparison of orthologous *B. suis* and *A. tumefaciens* VirB proteins showed good conservation of their general predicted properties, such as export signals, lipoprotein modification signals, membrane-spanning domains and membrane topology (Fig. 1B).

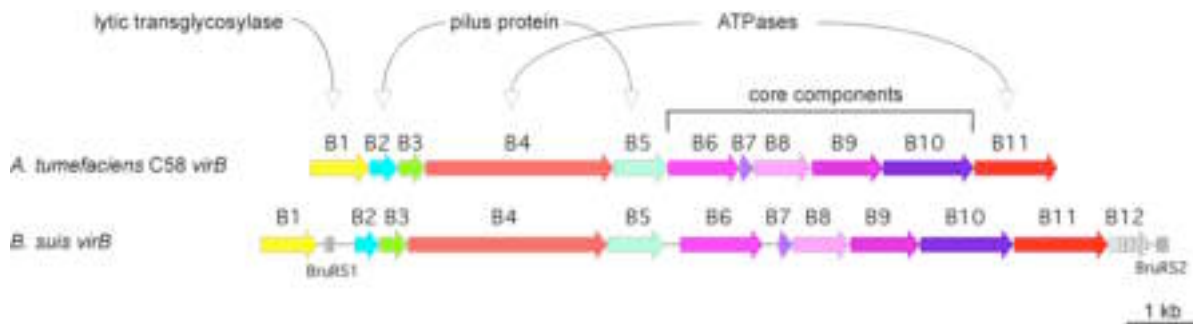
Due to the presence of a highly conserved sequence motif, **VirB1** was identified as a putative lytic transglycosylase. The orthologs from *A. tumefaciens* and *B. suis* both possess a signal sequence and are therefore directed to the periplasmic space by the general secretion pathway (*sec* pathway) (O'Callaghan *et al.*, 1999; Llosa *et al.*, 2000), where their enzymatic activity likely leads to localized cell wall lysis, creating space for accommodation of the T4SS (Mushegian *et al.*, 1996). The sequence identity between the two proteins as determined by a ClustalW-alignment is 22%. In *A. tumefaciens*, VirB1 is the only protein that is non-essential for action of the T4SS since its absence merely causes a 10- to 100-fold attenuation of virulence (Berger and Christie, 1994). A similar observation was made for *B. abortus* VirB1 (den Hartigh *et al.*, 2004).

The identity values between the T4SS core components of *A. tumefaciens* and *B. suis* are 21.5% for **VirB3**, 21% for **VirB6**, 27% for **VirB7**, 24.5% for **VirB8**, 26.5% for **VirB9** and 32.5% for **VirB10** (O'Callaghan *et al.*, 1999). Genetic and biochemical experiments suggest that these proteins constitute a membrane-spanning pore, which connects the outer and the inner membrane through periplasmic interactions and homo-oligomer formation (Cascales and Christie, 2003). These proteins are indispensable both for virulence of *A. tumefaciens* and for *Brucella*'s ability to reach the proper intracellular niche and to replicate within HeLa cells or macrophages (Berger and Christie, 1994; O'Callaghan *et al.*, 1999; Siera *et al.*, 2000; Comerchi *et al.*, 2001).

The proteins constituting the T-pilus in *A. tumefaciens* are required for all functions of the T4SS. It is interesting to note that the lowest values of identity between the *A. tumefaciens* and *B. suis* VirB orthologs were found in case of **VirB2** (18%) and **VirB5** (19%) (O'Callaghan *et al.*, 1999). VirB2 is exported via the *sec* pathway, but may subsequently remain associated with the inner membrane where it undergoes a number of post-translational modifications in *A. tumefaciens* (Eisenbrandt *et al.*, 1999), resulting in a cyclic

peptide, which is the main constituent of the T-pilus and it is likely responsible for plant cell contact (Hwang and Gelvin, 2004). VirB5, which is also directed to the periplasm by a classical N-terminal apolar leader peptide, is an indispensable part and minor component of the T-pilus. The protein, which is supposedly rich in α -helices, was proposed to be either membrane-associated (Schmidt-Eisenlohr *et al.*, 1999a), or to act as a chaperone for VirB2 (Sauer *et al.*, 2000). Certain mutants of the VirB5 ortholog TraC from the *tra* region of the IncN-plasmid pKM101 (29% identical to *B. suis* VirB5) were unable to promote DNA transfer and to serve as receptor for the donor-specific bacteriophage IKe (Yeo *et al.*, 2004). Nevertheless, incorporation of the protein variants into the pilus occurred normally, suggesting a role of VirB5 for pilus biogenesis and adhesion (Yeo and Waksman, 2004). The outer membrane lipoprotein VirB7 was shown to interact with VirB9, and VirB6 participates in formation of this complex while exerting a stabilizing effect on VirB2 (Jakubowski *et al.*, 2003). Moreover, VirB2, VirB5 and VirB7 were co-isolated from *vir*-induced *A. tumefaciens* cells suggesting that VirB7 links the pilus structure to the membrane-spanning structure constituted by the core components (Krall *et al.*, 2002). It is unknown whether *B. suis* produces a pilus under virulence-inducing conditions (Boschiroli *et al.*, 2002). If this should be the case, VirB2 and VirB5 may establish contact with the host. This would explain the relatively low conservation of these proteins in the two species compared here, reflecting suspected differences of receptor molecules on the plant cell surface and inside mammalian cells.

A)



B)

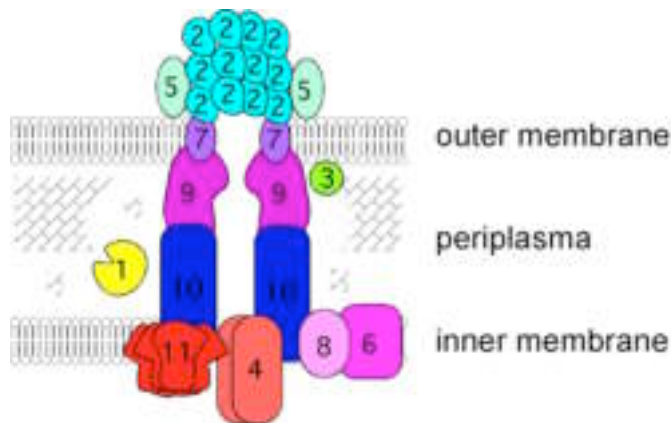


Fig. 1. The *virB* regions from *A. tumefaciens* and *B. suis* and the hypothetical structure of the membrane-spanning T4SS.

Comparison of the *A. tumefaciens* and *B. suis* *virB* region (A). The functions of the proteins are indicated. Orthologs are in the same colour. Intergenic regions are symbolized by a dash, *Brucella*-specific regions are depicted as grey boxes (O'Callaghan *et al.*, 1999; modified). (B) The localization of VirB protein is suggested by different lines of experimental evidence (Cascales and Christie PJ, 2003). The color code for the proteins is the same as in A.

The *virB* operons of *A. tumefaciens* and *B. suis* each encode two NTPases, **VirB4** (30% identity) and **VirB11** (29.5% identity). VirB4 forms dimers and homo-multimers embedded in the inner membrane and *A. tumefaciens* requires an intact NTPase site of VirB4 for substrate secretion. Enzyme activity could not be demonstrated *in vitro*, but there is little doubt that the protein hydrolyzes NTPs in the context of the T4SS (Rabel *et al.*, 2003). Parts of VirB4 may traverse the inner membrane to contact periplasmatic VirB proteins (Dang *et al.*, 1999). In fact, interactions with VirB1, VirB8, VirB10 and VirB11 were suggested based on the results of a dihybrid study (Ward *et al.*, 2002). VirB11-like proteins seem to be especially important, since orthologs of VirB11 are found not only in T4SS but also in a wide range of gram-negative and gram-positive bacteria and even in Archaea (Planet *et al.*, 2001). The hexameric ATPase VirB11 is located in the inner membrane and is essential for *A. tumefaciens* virulence. It was proposed that this protein either acts as an assembly factor for the T4SS or that it is responsible for driving pilus subunits or substrate molecules across the envelope. Like proteins VirB2-VirB10, VirB11 is required both for pilus biogenesis and substrate secretion, but certain amino acid substitutions in VirB11 cause uncoupling of the two features, enabling T-DNA transfer without pilus formation (Sagulenko *et al.*, 2001). This observation can be rationalized if VirB11 indeed carries out two tasks.

3. A dual role of the soluble lytic transglycosylase VirB1

3.1. The catalytic mechanism of SLTs

Despite the well-known area of lysozyme biochemistry, proposals for the catalytic mechanism of lytic transglycosylases were published only recently. While the well-known lysozymes like hen egg white lysozyme (HEWL), goose egg white lysozyme (GEWL) or the human lysozyme break up murein by hydrolysis of the $\beta(1\rightarrow4)$ -glycosidic bond between the MurNAc C1 and the GlcNAc C4, the lytic transglycosylases lyse this substrate in a transglycosylation reaction utilizing the C6-OH residue of the same MurNAc. Thus, no water is required for the reaction that produces a 1,6-anhydromuramic acid terminal residue (Fig. 2). Special features of the active site that distinguish the lytic transglycosylases from lysozymes must explain the mechanistic difference.

The classical mechanism of murein/chitin degradation by lysozyme was described as follows: A hexa-glycosidic stretch of a murein fiber binds to lysozyme, each GlcNAc and MurNAc residue is positioned to certain subsites in the active site cleft of the enzyme, denominated A-F. MurNAc residues cannot bind to subsite C since their large lactyl side chain will not fit into that position. This leaves only one possible arrangement of the substrate, with MurNAc in subsites B, D, F and GlcNAc at A, C, E. Cleavage is catalysed by an E (Glu) and a D (Asp) residue and occurs at the glycosidic bond connecting C1 of MurNAc (subsite D) and C4 of GlcNAc (subsite E). The E (Glu) residue donates a proton and thus cleaves the glycosidic bond under formation of a carbenium ion at C1 that is stabilized by the deprotonated D (Asp) residue. The positively charged C1 subsequently attracts a water molecule leading to completion of hydrolysis and re-protonation of E (Glu) (Stryer, 1995).

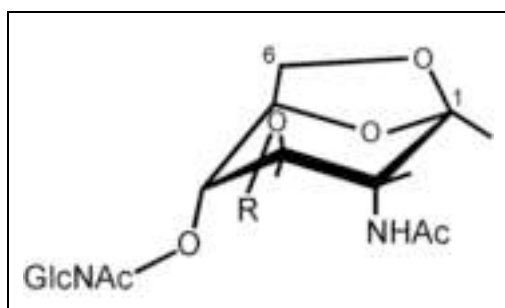


Fig. 2. The 1,6-anhydromuropeptide. GlcNAc: N-acetylglucosamine, R: lactyl-peptidyl sidechain (Höltje, 1998; modified)

There are three major differences that might explain why the C1 carbenium ion is not attacked by water but instead by the 6-OH group of the same molecule. First, lytic transglycosylases do not possess a D (Asp) residue in the right position to ensure stabilization of the carbenium ion. Second, in contrast to lysozyme, the GlcNAc residue at subsite E is deeply buried inside the active site crevice and forms numerous interactions with the enzyme. In lysozyme

the saccharides at sites E and F are able to quickly dissociate, allowing water to enter into the active site, whereas no water is available during catalysis in the lytic transglycosylases. Third, MurNAc needs to be heavily distorted into the half chair conformation to fit into subsite D, bringing 6-OH into proximity of the carbenium-ion (Leung *et al.*, 2001). Thus, by necessity,

complete degradation of a murein strand by a lytic transglycosylase results in the formation of 1,6-anhydromuropeptides (Fig. 2).

Since VirB1 orthologs present in the T4SS of many pathogenic bacterial species are members of the lytic transglycosylase family, it is noteworthy that the 1,6-anhydromuropeptide is known to cause a vast number of physiological responses. The 1,6-anhydromuropeptide N-acetylglucosaminyl-1,6-anhydro-N-acetylmuramyl-L-alanyl-D-glutamyl-*meso*-diaminopimelyl-D-alanine is released by *B. pertussis* and causes cell damage. Somnogenic, arthriogenic and pyrogenic effects have been reported and moreover, release of interleukin-1 β , interleukin-6 and granulocyte colony-stimulating factor was induced by 1,6-anhydromuropeptides (Leung *et al.*, 2001).

3.2. VirB1 interacts with T4SS components

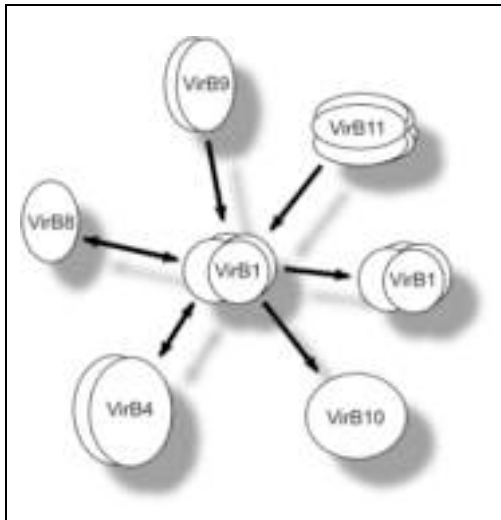


Fig. 3. Interactions of *A. tumefaciens* VirB1 as found by yeast dihybrid analysis. Arrows indicate interactions among VirB-proteins from bait to prey (Ward *et al.*, 2002)

When VirB1 was identified as a lytic transglycosylase, its importance for the *A. tumefaciens* T4SS was largely attributed to its proposed catalytic activity. This notion was repeatedly confirmed by the observation that active site mutants of the protein failed to complement *virB1* deletion strains (Mushegian *et al.*, 1996; Höppner *et al.*, 2004). VirB1 of *A. tumefaciens* is processed in the periplasm, yielding a C-terminal processing product denominated VirB1*. VirB1* and the N-terminus representing the SLT domain independently enhanced tumorigenicity, which implied an additional function of VirB1 (Llosa *et al.*, 2000). Further evidence for this hypothesis was generated when it was shown by co-immunoprecipitation, that VirB9

interacts with VirB1* in *A. tumefaciens* (Baron *et al.*, 1997). A high-resolution dihybrid screen with protein components of the *A. tumefaciens* T4SS suggested self-interaction and a number of uni- and bi-directional interactions between VirB1 and VirB4, VirB8, VirB9, VirB10 and VirB11 (Fig. 3). Unfortunately, the study failed to further narrow down the interaction domain within the VirB1 protein and biochemical evidence for the interactions was not presented (Ward *et al.*, 2002).

4. The VirB11-like hexameric (d)NTPase of T4SS

4.1. General characteristics and role in the system

Gram-negative bacteria utilize a number of macromolecular secretion machineries, which contribute to their virulence and pathogenicity. Dependent on their general characteristics (number of protein components, sequence similarities and membrane localization), the secretion systems were classified as type I through type V, and their task is to translocate proteins or nucleoprotein complexes across the two membranes and the peptidoglycan layer of the bacterial cell (Thanassi and Hultgren, 2000). Whereas fundamental differences exist between the systems, there are mechanistic similarities like the utilization of (d)NTPases to energize assembly of the apparatus and substrate secretion (Planet *et al.*, 2001). The VirB11-PulE (d)NTPase-family comprises a vast number of (d)NTPases. Many of the orthologs identified to date are not only essential components of the *sec*-independent type IV secretion systems but also are constituents of the main terminal

branch of the *sec*-dependent type II secretion systems. Other functions are the participation in naturally competence-related DNA uptake systems and a role in twitching motility (Cao and Saier, 2001).

Studies on the T4SS (d)NTPases HP0525 from *H. pylori*, TrwD from the R388 and TrbB from the RP4 conjugative systems have yielded fundamental insight into general properties of these enzymes. In addition, research conducted on (d)NTPases from type II secretion systems, which are implicated in the formation of type IV pili, confirm common features of a number of proteins that belong to this family (Krause *et al.*, 2000a; Sakai *et al.*, 2001; Machón *et al.*, 2002). The amino acid sequences of proteins belonging to the VirB11-PulE family is characterized by four sequence motifs, namely the Walker A and Walker B nucleotide binding site, a D box (Asp Box) and a H box (His Box). Functional studies suggested multimer formation since dominant negative mutants could be created by site-directed mutagenesis (Sagulenko *et al.*, 2001), and native protein was purified in assemblies of much larger molecular mass than the monomer. Characterization of the enzymology of T4SS ATPases yielded a multitude of results concerning substrate specificity, optimal pH and other factors that influence activity, like fatty acids and phospholipids (Machón, unpublished; Krause *et al.*, 2000a).

It was demonstrated that cardiolipin (CL) and phosphatidylglycerol (PG) stimulate the enzymatic activity of the VirB11 orthologs HP0525 from *H. pylori* and TrbB from pRP4. TrwD from pR388 was shown to promote the hemifusion of lipid vesicles consisting of CL and PG. Hemifusion (also coined close apposition) of vesicles is a process in which the outer monolayers of vesicles are mixed whereas the inner aqueous content is not. The membrane-destabilizing action of TrwD is required during the process of T4SS assembly or DNA transfer (Machón *et al.*, 2002). Electron-micrographic images of the hexameric protein TrwD were obtained and it was discovered that ATP binding effects large conformational changes in the hexamer (Krause *et al.*, 2000a; Krause *et al.*, 2000b). This observation could be explained after determination of the structure of the hexameric VirB11 ortholog from *H. pylori* (Yeo *et al.*, 2000). Analysis of the X-ray structure showed that an ATP binding and hydrolysis cycle effects rigid body rotation of the N-terminal domain of some monomers around the linker region, a flexible AA stretch around R133 that is interconnecting the two domains of HP0525. Certain non-functional variants of HP0525 had enhanced ATPase activity and a reduced ability to form the native hexameric shape. Together, these data led to the postulation of a four-step mechanism of HP0525 dynamic action. The main characteristics of this mechanism are:

- 1) Occurrence of a nucleotide-free asymmetric form in which the C-terminal domain (CTD) is responsible for maintaining the pseudohexameric scaffold while the N-terminal domain (NTD) uses its general flexibility to contact potential target molecules.
- 2) Upon binding of three molecules of ATP, an equal number of subunits are locked in a rigid conformation.
- 3) Hydrolysis and binding of three additional ATP molecules to the remaining nucleotide-free subunits creates a rigid symmetric hexamer.
- 4) After hydrolysis of all ATP molecules, the symmetric hexamer regains its flexibility (Savvides *et al.*, 2003).

Whereas VirB11-PulE orthologs were reported to reside in the inner membrane (Possot and Pugsley, 1994), the outer membrane or the cytoplasm (Rivas *et al.*, 1997), the NTD of inner membrane protein HP0525 was proposed to contact the periplasmic space where it might be involved in interactions with proteins of the core complex, possibly acting as an assembly factor (Ward *et al.*, 2002; Cascales and Christie, 2003). Recent studies showed that VirB11 and VirB4, the two multimeric ATPases common to most T4SS, not only interact with each other but also seem to coordinate their actions which are required for substrate secretion (Ward *et al.*, 2002; Cascales and Christie, 2004).

4.2. Choice of VirB11 orthologs as drug targets

A growing concern of modern medicine is the massive spread of antibiotic resistance that has occurred ever since the classical antibiotics were widely applied, not only for the treatment of microbial infections, but also as growth promoters in animal breeding facilities. The problem will become even bigger since a considerable innovation gap in antibiotic development is obvious as indicated by a recent inspection of drug candidates that are being advanced through clinical trials (Walsh, 2003). Targeting bacterial cell functions that are non-essential for microbial growth could drastically reduce the velocity by which selection and horizontal gene transfer cause resistance to spread. Classical antibiotics exert a broad-spectrum effect by targeting processes essential for bacterial cell viability while anti-infective drugs could specifically target pathogenic species possessing characteristic virulence factors. If successfully applied, it can be anticipated that the favorable property of reduced resistance development would be combined with reduced negative impact of antimicrobial chemotherapy on the commensal and symbiotic microorganisms colonizing the human body (Alksne and Projan, 2000).

VirB11-PulE orthologs from type IV and type II secretion machineries are found in a number of pathogenic bacteria. Among them are enteropathogenic *E. coli* and *Pseudomonas*

aeruginosa, which causes nosocomial infections in hospitalized patients. T4SS are the major virulence factors in an impressive number of Gram-negative pathogenic bacteria, but also the spread of antibiotic resistance genes can be attributed to this mechanism (Cascales and Christie, 2003). While other components, like the ATPases VirB4 and VirD4, are often not present in the virulence-related T4SS of pathogens, VirB11 is highly conserved. The enzymatic activity was shown to be required for its role in the secretion system. Moreover, the structure of a representative member of the family was solved and the 3-dimensional shape of the active site was modeled. VirB11 orthologs were purified either by classical purification methods or by affinity purification of N-terminally tagged fusion proteins, and (d)NTPase properties were determined (Krause *et al.*, 2000a; Sakai *et al.*, 2001). Target molecules from different T4SS are therefore available, which is an important prerequisite to assay broad-spectrum effects in *in vitro* assays. Due to the essential function(s) of VirB11 orthologs and the large amount of available information, they constitute ideal targets for the development of drugs, which will disarm but not kill many bacterial pathogens. The knowledge gained concerning these (d)NTPases must be especially appreciated considering the number of diseases that are caused by organisms utilizing T4SS as important virulence factor.

5. Social and economic impact of some T4SS-mediated diseases

Brucellosis,

also called undulant or Malta fever is a zoonotic disease mostly caused by one of the three species *B. melitensis*, *B. abortus* or *B. suis* (Corbel, 1997) The disease is endemic (*def.*: constantly present to a low degree) in countries of the Mediterranean basin, the Arab peninsula, western Asia, the Indian subcontinent, parts of Africa and in Latin America. The causative agent is spread by the common domestic animals in these countries.

This severe, and long-lasting but rarely fatal disease was almost eradicated in countries possessing an effective and standardized public and domestic animal health program. Tests for seropositivity in humans and the number of reported cases allow estimates of the actual importance of Brucellosis in the human population. However, due to inaccurate diagnosis, the disease might remain unrecognized in many cases, resulting in an actual infection rate 10 to 25 times higher than suspected. Countries like the USA, which by virtue of a rigorous eradication program managed to reduce the disease to very low levels, now report less than 0.1 cases annually per 100,000 people (Ragan and Gilsdorf, 2001). Estimates for disease prevalence in endemic areas are in the range of 1.2 to 70 annual cases per 100,000 people and might go as high as the 540 annual cases per 100,000 reported for Kuwait. Nevertheless, serological evidence of exposure to *Brucella* can be found in approximately 5% to 20% of the population in these areas, and in up to 55% of the population reported for Nigeria (Rust and Worrell, 2004)

The World Health Organisation (WHO) recommends 45 days doxycycline/rifampine therapy for treatment that costs \$225.96 for a dosage sufficient to cure an adult (FAO, 1986). Assuming that 2 billion people live in areas of endemic Brucellosis and a hypothetical low prevalence of 10 annual cases per 100,000 would bring the cost to a sum of \$45 million per year, just to finance treatment. This does of course not take into account the cost of lost labor power, which is undoubtedly much more severe when no treatment is pursued.

Although a number of formulations had been used for vaccination of humans with limited efficacy (Corbel, 1997), the main effort to prevent infection is through controlling the disease in the animal host. This strategy is useful since major savings can be achieved in the livestock and dairy industry by successful eradication. In 1952, annual losses from lowered milk production, aborted calves and pigs and reduced breeding efficiency in the USA accounted for more than \$400 million. In contrast, today, after more than fifty years of the “Federal Brucellosis Eradication Program”, the annual loss is only \$1 million (Ragan and

Gilsdorf, 2001). Consistent with these data are estimates that *B. abortus* alone accounts even nowadays for an annual veterinary toll of \$700 million in South America (Rust *et al.*, 2004). Since data on human and veterinary cases of the disease are not available for all countries with endemic Brucellosis, an estimation of the overall impact is difficult. A simple approach to assess the overall veterinary cost is to compare the overall number of domestic animals (buffalo, cattle, goat, pig and sheep) in Latin America with the total number of these animals in other countries and regions with endemic Brucellosis (Africa, India, the Arab peninsula, Eastern Europe, Iran, Greece, Spain, Portugal and Italy) and suppose the same cost per animal of Brucellosis as in Latin America. Whereas 573 million of the mentioned domestic animals live in Latin America, about 1.6 billion are estimated in the other countries (FAO, 2004). This would imply a yearly loss of \$1.95 billion for these countries, a total of \$2.65 billion globally. Though all statements are based on assumptions, it is clear that the veterinary toll of Brucellosis by far outruns the cost of human treatment.

Crown gall or Hairy Root

is the plant disease named after the morphological manifestation of an *Agrobacterium* infection. Although reviews sometimes underscore the economically significant crop loss that *Agrobacterium* is responsible for, it is very hard to obtain data supporting this notion. The genus is present in soil all over the planet but the only significant damage occurs in fruit and nut orchards, vineyards, and nurseries situated in areas that experience drastic temperature variations in winter and spring. The resulting frost damage together with the manipulative techniques applied in cultivation creates lesions on the plants that enable *Agrobacterium* to infect the stem and cause the formation of tumors, called crown galls. Relative to the large impact of other plant pathogens like insects and fungi on agriculture, *Agrobacterium* plays no major role. Data concerning agriculture in the state of Georgia/USA shows that formation of crown galls plus costs of controlling of the disease account for 2.7% of the total financial loss in the bunch grape harvest (Williams-Woodward, 2002). Interestingly, crown gall disease caused by plant pathogenic *A. tumefaciens* can be controlled with agrocin producing *Agrobacterium radiobacter* K84, the first reported example of successful biocontrol (Jones *et al.*, 1991). *A. tumefaciens* has no severe impact as compared to other pests and there are no reports of other crops damaged.

In an economical sense, a different aspect of *A. tumefaciens*' capability to transform plants is much more important. Transformation of plants with *Agrobacterium* has evolved to be one of the most important techniques that are used to create genetically modified crops by inserting exogenous genes into the plant genome (Binns, 2002). The fate of transgenic plants with advantageous properties is still an issue of discussion between authorities in the USA and the EU. The debate is about labeling and traceability requirements for genetically

manipulated foods (GM foods). Nevertheless, it is clear that *Agrobacterium* plays a mayor role in the creation of crops that in the future might be of global importance in an effort to solve urgent problems of food production (Evenson and Santaniello, 2004).

Bartonellosis

shares many characteristics with Brucellosis. The causative agents *B. bacilliformis*, *B. tribocorum*, *B. quintana*, *B. henselae* and *B. vinsonii* are predominantly found in animal hosts, typically feline, canine and rodent species. While direct transmission of *Bartonella* from animal to human seems to be rather exceptional, insect vectors like the sand fly (*Lutzomyias sp.*), the human body louse (*Pedicular humanis*), cat fleas (*Ctenocephalides felis*) and ticks (*Ixodes sp.*) seem to play an important role for the spread of this intracellular pathogen (Breitschwerdt and Kordick, 2000). Clinical manifestations are rather broad, including Carrion's disease (Verruga peruana), trench fever, cat scratch disease, bacillary angiomatosis peliosis, bacteraemia and endocarditis. Especially immunocompromised patients may suffer from the formation of vasoproliferative tumors due to the organism's proliferation in endothelial cells (Dehio, 2001), where it causes increased production of vascular endothelial growth factor (VEGF) (Kempf *et al.*, 2001).

There are no reliable data on the frequency of the disease in the human population but seroprevalence as a measure for the risk of infection ranges between 2% and 6% in healthy blood donors from the USA. However, seroprevalence of 30% in homeless patients from Marseille and 51.1% in a group of European veterinarians were reported, which demonstrates that risk groups with a very different socioeconomic background may be found due to the transmission mode of Bartonellosis (Breitschwerdt and Kordick, 2000).

Gastric ulcer

can be caused by *H. pylori*, an organism which has infected approximately half of the world population (Covacci *et al.*, 1999). This ϵ -proteobacterium was identified to be a causative agent of gastric adenocarcinoma and duodenal ulcer disease. Prevalence of infection is linked to many factors such as socioeconomic status, sex and age and males over 40 years of age that live in developing countries are the most likely infected by the organism. A number of diseases have been ascribed to *Helicobacter* infection, best documented are duodenal ulcer, gastric ulcer, gastric adenocarcinoma and gastric lymphoma (Pisani *et al.*, 1997). Though there are also other reasons, it was estimated that 5 million new cases of these diseases occur due to *Helicobacter* infection worldwide *per annum* (Parsonnet, 1998). A different study that tried to assess the economics of ulcer disease in the USA estimated

annual health care costs of approximately \$ 6 billion, consisting of physician office visits, hospitalization and decreased productivity (Sonneberg and Everhart, 1997).

Whooping Cough

caused by *Bordetella pertussis* was largely controlled by global vaccination programs, but for some years the number of infections has been on the rise again. Since an all time low in 1976, with only 1,000 reported cases in the USA, the number rose to more than 8,000 cases in 2002 (CDC, 2004). About 20% of the infected patients require hospitalization, but the rate is much higher in infants younger than 6 months (63%), which are especially prone to the infection (CDC, 2003). The disease is fatal in 0.04% of the cases in developed countries and in 3% of the cases in developing countries (Galazka, 1991), but the many complications that the primary symptoms create drastically increase the impact. Apart from hemorrhages in the eye, nosebleeds, hernias and physical damage to the lungs there is a considerable danger of encephalopathy, seen in 0.7% of all cases and often leading to brain damage (Siber and Samore, 1998).

Onchocerciasis and Wolbachia

Another important example for the impact of T4SS comes from the genus *Wolbachia*. *Wolbachia spp.* are α -proteobacteria and have an extremely broad host range, which enables them to reside within host-derived vacuoles in the cytoplasm of arthropods and filarial nematodes (Taylor and Hoerauf, 1999). Whereas it is still discussed whether the species is beneficial or detrimental to the arthropod host, *Wolbachia spp.* are essential endosymbionts in filarial nematodes, where their abundant presence in tissues of all developmental stages was shown to be essential for nematode embryogenesis (Hoerauf *et al.*, 2003). *Wolbachia* harbors a functional T4SS (Masui *et al.*, 2000), and there are strong indications that, like in other intracellular pathogens of the proteobacteria, the T4SS is essential for establishment and maintenance of intracellular survival (McGraw and O'Neill, 2004).

About 200 million individuals worldwide suffer from filarial nematode parasites like *Brugia malayi*, *Wucheria bancrofti* and *Onchocerca volvulus*, the causative agent of onchocerciasis, due to its transmission by riverbank inhabiting mosquitoes also called “river blindness”. This disease, which is endemic in 35 countries throughout Africa, the Americas and the Arab peninsula, accounts for the debilitating infection of 18 million people annually, which suffer from skin and ocular lesions caused by the high titer of filarial nematodes that are released into the blood by an adult nematode residing under the skin (WHO/TDR, 2002). 450,000 people worldwide are suspected to have lost their vision due to the disease. The

depopulation of fertile river valleys in the African savannah is a direct result of the disease, and constitutes a major obstacle to socioeconomic development in that region (The Carter Center, 2002-2003).

Eradication of *Wolbachia* from *O. volvulus* by doxycyclin treatment drastically improved all disease symptoms, which is due the inhibition of filarial development. Even more importantly, the treatment reduced the blindness-promoting inflammatory response in the cornea, which seems to be caused by *Wolbachia* antigen alone (Saint André *et al.*, 2002). The current control strategy of this disease is based on a single microfilaricidal drug (Ivermectine), but treatment that negatively affects the endosymbiosis between *O. volovulus* and *Wolbachia spp.* should be a viable alternative to fight onchocerciasis. This example shows that by promotion of endosymbiosis, the *Wolbachia* T4SS might contribute to one of the major global health problems.

6. Aim of this work

Type IV secretion systems have an important role for the virulence of many obligate and opportunistic pathogens. Studies in many laboratories have yielded fundamental insights into the roles of the participating proteins (reviewed in: Baron *et al.*, 2002; Cascales and Christie, 2003, Zupan and Zambryski, 2000).

Lytic transglycosylases similar to *A. tumefaciens* VirB1 were of special interest in a number of studies (Mushegian *et al.*, 1996; Bayer *et al.*, 2001), but their actual task in the function of the T4SS was not elucidated in detail. Many of the T4SS known to date do not possess VirB1-like proteins and even if they are present, they are most likely non-essential. Dihybrid data indicated multifold interactions of VirB1, but biochemical data were not provided (Ward *et al.*, 2002). Experiments with purified recombinant *B. suis* proteins have the potential to demonstrate VirB1 interactions, while functional studies conducted with the *A. tumefaciens* model should permit insights into the importance of the active site requirements and the processing site of the protein.

In contrast to VirB1, the traffic NTPase VirB11 has orthologs in all T4SS described so far. Thus, the protein is an excellent target for anti-infective drugs, which could block either the NTPase activity or the formation of homo-oligomers, both essential features of VirB11 action (Savvides *et al.*, 2003). A potential inhibitor of NTPase activity of VirB11 orthologs was identified in a high throughput screen conducted at CHIRON (Emeryville, USA and Siena, Italy). Different *in vitro* and *in vivo* analyses were conducted to clarify the effect of this compound on VirB11 orthologs from different T4SS. In addition, the analysis of interactions of VirB11 with other components of the secretion apparatus could further define its role as a drug target, and its contribution to T4SS function. The development of an effective broad-spectrum VirB11 inhibitor with good pharmaceutical properties would provide an alternative drug for the treatment of a number of severe and long-lasting bacterial infections. The presented work should lay the foundation for the development of such an inhibitor.

Materials and Methods

1. Bacterial strains, bacteriophages and plants

1.1. Bacterial strains

Table 2. Bacterial strains

strain	genotype or description	source or reference
<i>Escherichia coli</i>		
DH5 α	F' Φ 80d <i>lacZ</i> Δ M15 Δ (<i>lacZYA-argF</i>)U169 <i>deoR recA1 endA1 hsdR17</i> (r _K ⁻ m _K ⁺) <i>phoA supE44</i> λ - <i>thi-1 gyrA96 relA1</i>	Woodcock <i>et al.</i> , 1989
JM109	F' (<i>traD36 proAB+ lacIqZ</i> Δ M15) <i>recA1 endA1 gyrA96 thi-1 hsdR17 relA1 supE44</i> Δ (<i>lac-proAB</i>)	Yanisch-Perron <i>et al.</i> , 1985
WL400	cm ^R , str ^R <i>araD139</i> Δ (<i>araF-lac</i>)U169 <i>ptsF25 deoC1 relA1 flb5301 rpsL150</i> Δ <i>selD204::cat</i>	W. Leinfelder
FM433	spc ^R <i>araD139</i> Δ (<i>argF-lac</i>)U169 <i>ptsF25 deoC1 relA1 flbB5301 rpsE13</i> Δ (<i>srl-recA</i>)306::Tn10	Zinoni <i>et al.</i> , 1990
GJ1158	<i>ompT hsdS gal dcm</i> Δ <i>malAp510 malP::</i> (<i>proUp-T7</i> RNAP) <i>malQ::lacZhyb11</i> Δ (<i>zhf-900::Tn10dTet</i>)	Bhandari and Gowrishankar, 1997
BMH71-18 <i>mutS</i>	<i>thi supE</i> Δ (<i>lac-proAB</i>) [<i>mutS::Tn10</i>] [F' <i>proAB lacI^qZ</i> Δ M15]	Wallace <i>et al.</i> , 1981
TOP10	F- <i>mcrA</i> Δ (<i>mrr-hsdRMS-mcrBC</i>) Φ 80 <i>lacZ</i> Δ M15 Δ <i>lacX74 recA1 deoR araD139</i> Δ (<i>ara-leu</i>)7697 <i>galU galK rpsL</i> (str ^R) <i>endA1 nupG</i>	Invitrogen
<i>Agrobacterium tumefaciens</i>		
A348	Wild type, pTiA6NC	Garfinkel <i>et al.</i> , 1981
UIA143	A348, ery ^R	Bohne <i>et al.</i> , 1998
UIA143pTiA6	UIA143, pTiA6NC	Bohne <i>et al.</i> , 1998
PC1001	pTiA6NC carrying an in frame deletion of <i>virB1</i>	Berger and Christie, 1994
PC1011	pTiA6NC carrying an in frame deletion of <i>virB11</i>	Berger and Christie, 1994

1.2. Bacteriophages and plants

The donor-specific bacteriophage IKE (Kathoon *et al.*, 1972) was used to assess the functionality of IncN-determined conjugative pili. Four to six week old plants of *Kalanchoë diargremontiana* were used to assay the virulence of *A. tumefaciens* strains.

2. Plasmids and genomic DNA

Table 3. Plasmids

plasmid	genotype	reference
pTrc200	str ^R , spc ^R , pVS1 origin, <i>lacI</i> ^q , <i>trc</i> promotor expression vector	Schmidt-Eisenlohr <i>et al.</i> , 1999b
pTrc300	pTrc200 with <i>NcoI</i> -site deleted	Schmidt-Eisenlohr <i>et al.</i> , 2002
pTrc300-VirB3-B6	pTrc300 expressing <i>virB3-B6</i> of the <i>B. suis</i> <i>virB</i> operon (Fig. 14)	Q. Yuan
pTrc300-VirB7-B12	pTrc300 expressing <i>virB7-B12</i> of the <i>B. suis</i> <i>virB</i> operon (Fig. 14)	Q. Yuan
pTrc300-VirB3-B12	pTrc300 expressing <i>virB3-B12</i> of the <i>B. suis</i> <i>virB</i> operon (Fig. 14)	Q. Yuan
pTrc300-VirB2-B12	pTrc300 expressing <i>virB2-B12</i> of the <i>B. suis</i> <i>virB</i> operon (Fig. 14)	this work
pTrc300-VirB1-B12	pTrc300 expressing <i>virB1-B12</i> of the <i>B. suis</i> <i>virB</i> operon (Fig. 14)	this work
pTrc300-VirB1+B3-B12	pTrc300 expressing <i>virB1</i> and <i>virB3-B12</i> of the <i>B. suis</i> <i>virB</i> operon, 56 bp insert after <i>virB1</i> (Fig. 14)	this work
pTrc300-VirB1+B2-B12	pTrc300 expressing <i>virB1</i> and <i>virB2-B12</i> of the <i>B. suis</i> <i>virB</i> operon, 56 bp insert after <i>virB1</i> (Fig. 14)	this work
pTrc300-VirB1 ^{E27A} -B12	like pTrc300-VirB1-B12, <i>virB1</i> active site variation (Fig. 14)	this work
pTrcB11	pTrc200, <i>A. tumefaciens</i> <i>virB11</i> treated <i>BspHI/XbaI</i> , for expression	this work
pTrcB11s	pTrc200, <i>B. suis</i> <i>virB11</i> treated <i>BspHI/XbaI</i> , for expression	this work

pTrcB1	pTrc200 with 759 bp <i>NcoI/BglII</i> <i>virB1</i> fragment from <i>A. tumefaciens</i>	Schmidt-Eisenlohr <i>et al.</i> , 1999a
pTrcB1s	pTrc200 with 717 bp <i>NcoI/Scal</i> <i>virB1</i> fragment from <i>B. suis</i>	this work
pTrcTraL	pTrc200 with 735 bp <i>NcoI/Scal</i> <i>traL</i> fragment from pKM101	this work
pTrcF169	pTrc200 with 507 bp <i>NcoI/Scal</i> <i>orf169</i> fragment from the F plasmid	this work
pTrcHP0523	pTrc200 with 507 bp <i>NcoI/Scal</i> <i>hp0523</i> fragment from <i>H. pylori</i> chromosomal DNA	this work
pTrcB1 ^{E→A}	pTrcB1 active site variant E60A	this work
pTrcB1s ^{E→A}	pTrcB1s active site variant E27A	this work
pTrcTraL ^{E→A}	pTrcTraL active site variant E53A	this work
pTrcB1*	pTrc200 with 222 bp <i>NcoI/BglII</i> <i>virB1</i> fragment from <i>A. tumefaciens</i>	this work
pTrcB1 ^{ΔAA}	pTrcB1 cleavage site variant A172, A173 deleted	this work
pTrcB1 ^{A→D}	pTrcB1 cleavage site variant A172D	this work
pTrcB1 ^{Q1→E}	pTrcB1 cleavage site variant Q174E	this work
pTrcB1 ^{Q2→E}	pTrcB1 cleavage site variant Q175E	this work
pTrcB1 ^{Q1→E/Q2→E}	pTrcB1 cleavage site variant Q174E, Q175E	this work
pTrcB1 ^{A→P}	pTrcB1 cleavage site variant A173P	this work
pTrcB1 ^{E→P/T→W}	pTrcB1 cleavage site variant E170P, T171W	this work
pTrcHP0523-B1*	pTrc300 with 507 bp <i>EcoRI/NcoI</i> fragment from <i>H. pylori</i> chromosomal DNA and 225 bp <i>NcoI/Acc65I</i> <i>virB1*</i> fragment from <i>A. tumefaciens</i>	this work
pTrcSP-HP0523-B1*	pTrcHP0523-B1* with 90 bp SP fragment of <i>A. tumefaciens</i> <i>virB1</i> inserted into <i>EcoRI</i> site	this work
pLS1	carb ^R , IncQ plasmid for VirB/D4-mediated transfer experiments	Stahl <i>et al.</i> , 1998
pKM101	carb ^R , <i>mucA</i> , <i>mucB</i> IncN conjugative plasmid	Langer and Walker, 1981

pRP4	kan ^R , IncP α conjugative plasmid	Pansegrau <i>et al.</i> , 1994
pR388	tm ^R , IncP α conjugative plasmid	Datta and Hedges, 1972
pT7-7	carb ^R , vector for T7-promotor controlled expression	Tabor and Richardson, 1985
pT7-7NcoI	carb ^R , pT7-7, NdeI-site substituted with NcoI	Schmidt-Eisenlohr <i>et al.</i> , 2001
pT7-StrepII	carb ^R , pT7-7NcoI with 50 bp NcoI fragment coding for StrepII-Tag and factor X α cleavage site	Balsiger <i>et al.</i> , 2004
pT7-StrepII-VirB11 <i>B. suis</i>	pT7-StrepII with full-length Acc65I/ HindIII fragment of <i>virB11</i> from <i>B. suis</i>	this work
pT7-StrepII-VirB11 <i>A. tumefaciens</i>	pT7-StrepII with full-length Bsp1407I/NcoI fragment of <i>virB11</i> from <i>A. tumefaciens</i> C58	this work
pT7-StrepII-TrwD	pT7-StrepII with full-length Acc65I/PstI fragment of <i>trwD</i> from pR388	this work
pT7-StrepII-TraG	pT7-StrepII with full-length Acc65I/PstI fragment of <i>traG</i> from pKM101	this work
pT7-StrepII-HP0525	pT7-StrepII with full-length Acc65I/PstI fragment of <i>hp0525</i> from <i>H. pylori</i>	this work
pT7-7-VirB4	pT7-7 with 2499 bp NcoI/EcoRI fragment of <i>virB4</i> from <i>B. suis</i>	this work
pT7-StrepII-VirB8	pT7-StrepII with 492 bp Acc65I/PstI fragment of <i>virB8</i> from <i>B. suis</i>	N. Domke
pT7-StrepII-VirB9	pT7-StrepII with 813 bp Acc65I/PstI fragment of <i>virB9</i> from <i>B. suis</i>	N. Domke
pT7-StrepII-VirB10	pT7-StrepII with full-length 1020 bp Acc65I/PstI fragment of <i>virB10</i> from <i>B. suis</i>	N. Domke
pT7-H ₆ TrxFus	carb ^R , for T7-based expression of N-terminal hexa-histidine and <i>trxA</i> (thioredoxin)-fusions	Kromayer <i>et al.</i> , 1996
pT7-H ₆ Trx-VirB7	pT7-H ₆ TrxFus with 126 bp PstI/XbaI fragment of <i>B. suis virB7</i>	A. Carle
pT7-H ₆ Trx-VirB8	pT7-H ₆ TrxFus with 492 bp Acc65I/PstI fragment of <i>B. suis virB8</i>	N. Domke

pT7-H ₆ Trx-VirB9	pT7-H ₆ TrxFus with 813 bp <i>Acc65I/PstI</i> fragment of <i>B. suis virB9</i>	N. Domke
pT7-H ₆ Trx-VirB10	pT7-H ₆ TrxFus with 1020 bp <i>Acc65I/PstI</i> fragment of <i>B. suis virB10</i>	N. Domke
pT7-H ₆ Trx-VirB11	pT7-H ₆ TrxFus with full-length <i>Acc65I/HindIII</i> fragment of <i>VirB11</i> from <i>B. suis</i>	this work
pT7-StrepII-VirB1	pT7-StrepII with 654 bp <i>Acc65I/PstI</i> SP-less fragment of <i>virB1</i> from <i>B. suis</i>	this work
pT7-StrepII-VirB1/VirB4	pT7-StrepII-VirB1 with 2499 bp <i>NotI/EcoRI</i> fragment of <i>virB4</i> from <i>B. suis</i>	this work
pT7-StrepII-VirB1/VirB8	pT7-StrepII-VirB1 with 524 bp <i>PstI/HindIII</i> fragment of <i>virB8</i> from <i>B. suis</i>	this work
pT7-StrepII-VirB1/VirB9	pT7-StrepII-VirB1 with 776 bp <i>NotI/EcoRI</i> fragment of <i>virB9</i> from <i>B. suis</i>	this work
pT7-StrepII-VirB1/VirB10	pT7-StrepII-VirB1 with 1011 bp <i>NotI/EcoRI</i> fragment of <i>virB10</i> from <i>B. suis</i>	this work
pT7-StrepII-VirB1/VirB11	pT7-StrepII-VirB1 with 1194 bp <i>NotI/EcoRI</i> fragment of <i>virB11</i> from <i>B. suis</i>	this work
pET21b-BC	carb ^R , pET21b derivative with two RBS in the polylinker for T7-driven bi-cistronic expression, determines hexa-His tagged C-terminus of second ORF	S. Höppner
pET24d-VirB1-His ₆	kan ^R , pET24d with 654 bp <i>NdeI/EcoRI B. suis virB1</i> fragment	this work
pET21b-VirB8/VirB1-His ₆	pET21b-BC with 524 bp <i>NcoI/NotI virB8</i> and 654 bp <i>NheI/EcoRI B. suis virB1</i> fragment downstream	this work
pET21b-VirB9/VirB1-His ₆	pET21b-BC with 776 bp <i>virB9</i> and 654 bp <i>B. suis virB1</i> fragment downstream	this work
pET21b-VirB10/VirB1-His ₆	pET21b-BC with 1011 bp <i>virB10</i> and 654 bp <i>B. suis virB1</i> fragment downstream	this work
pET21b-VirB8	pET21b-VirB8/VirB1-His ₆ , <i>virB1</i> gene removed with <i>Sall/XhoI</i> and religated	this work
pET21b-VirB9	pET21b-VirB9/VirB1-His ₆ , <i>virB1</i> gene removed with <i>Sall/XhoI</i> and religated	this work
pET21b-VirB10	pET21b-VirB10/VirB1-His ₆ , <i>virB1</i> gene removed with <i>Sall/XhoI</i> and religated	this work

pUC18VirB	carb ^R , <i>virB</i> region from <i>B. suis</i> 1330	O'Callaghan <i>et al.</i> , 1999
pGK217	carb ^R , <i>virB</i> region from <i>A. tumefaciens</i> C58	Kuldau <i>et al.</i> , 1990
pCR®2.1-TOPO	carb ^R , kan ^R for direct cloning of PCR fragments	Invitrogen
pCR®2.1-TOPO-VirB1	pCR®2.1-TOPO with 733 bp <i>virB1</i> fragment of <i>B. suis</i>	this work
pCR®2.1-TOPO-VirB1-II	pCR®2.1-TOPO with 733 bp <i>virB1</i> fragment of <i>B. suis</i> , SacI-site mutated to NheI (proximal to the <i>virB1</i> stop codon)	this work
pCR®2.1-TOPO-VirB1 E27A	pCR®2.1-TOPO with 733 bp <i>virB1</i> fragment of <i>B. suis</i> featuring active site mutation	this work

Genomic DNA from *Helicobacter pylori* 26695 (ATCC 700392) was used as template for PCR (K.A. Eaton).

3. Oligonucleotides

3.1. PCR primers

Table 4. PCR primers

primer name	sequence
primers for construction of bi-cistronic vectors:	
VirB1suisNcoIBC5':	5'-GCGCGCCCATGGCAGCAATCGTGCAGGTCGAGT-3'
VirB1suisBC3':	3'-GACTGCGGCCGCGAAAACAACACTACGCCGTCCG-3'
B1suisExp-5':	5'-CGATGGTACCCGCAATCGTGCAGGTCGAGTCGG-3'
B1suisExp-3':	5'-CGATCTGCAGTTAGAAAACAACACTACGCCGTCCG-3'
StrepBCVirB8- 5':	5'-GGGGGGCTGCAGTAATTAAGGAGCGGCCGCA TGCGCGTCAACGCACAGAC-3'
VirB8 3':	5'-GGGGGGAAGCTT/GAATTCTCATTGCACCACTCCCATT TCTGG-3'
VirB8 suisBC5':	5'-GCGCGCTAGCCGCGTCAACGCACAGAC-3'
VirB8 suisBC3':	5'-GCGCGAATTCTCATTGCACCACTCCCATTCTGG-3'
VirB9-5':	5'-GATCGAGTGCGGCCGCATGATTCAAGTATGTCGATTAC-3'
VirB9suisBC5':	5'-GCGCGCTAGCATTCAAGTATGTCGATTACAATTC-3'
VirB9suisBC3':	5'-GCGCGAATTCTCATTGCAGGTTCTCCCCGGGC-3'
VirB10-5':	5'-GCGCGCGCGCGGCCGCATGGGCAATGCAGAGAATAA-3'
VirB10suisBC5':	5'-GCGCGCTAGCGGCAATGCAGAGAATAATCACC-3'
VirB10suisBC3':	5'-GCGCGAATTCTCATTGCAGGTTCTCCCCGGGC-3'
VirB11-5':	5'-GCGCGCCTGCAGTAATTAAGGAGCGGCCGCA TGATGTCCAACCGAAGT-3'
VirB11suisBC3':	5'-GCGCGAATTCTTATATGCGTGATATGCGGCTGCAC-3'
VirB4sNcoI 5':	5'-GCGCGCCCATGGGCGCTCAATCCA-3'
VirB4-5':	5'-GCGCGCGCGCGGCCGCATGATGGGCGCTCAATCCA-3'
Strep VirB4-5':	5'-GCGCGCGGTACCCATGATGGGCGCTCAATC-3'
VirB4suisBC3':	5'-GCGCGAATTCTCATTGCAGGTTCTCCCCGGGC-3'
primers for construction of the <i>hp0523-virB1*</i> -fusion:	
523-5' <i>EcoRI</i> :	5'-CGATGAATTCTTGTTCGAGAAATGGATTGGTC-3'
523-3' <i>NcoI</i> :	5'-GCTACCATGGCTCGTTATATCGCACTTGAGA-3'
B1*-5' <i>NcoI</i> :	5'-CTAGCCATGGGCGGCTCAACAGCTCGTCCCC-3'
B1*-3' <i>Acc65I</i> :	5'-GATCGGTACCTTATTGCGGACCTCCTTGATTTAA-3'
SPVirB1-5':	P-5'-AATTCATGAGCTTGGGGAGATGGGGAATGTTGAAGG CAACAGGGCCGCTGTCGATTATCTTACTGGCCTCCACGT GCCCGTCGAGTGGTGCTGCCG-3'

SPVirB1-3':	P-5'-AATTCGGCAGCACCACCTCGACGGGCACGTGGAGGC CAGTAAGATAATCGACAGCGGCCCTGTTGCCTTCAACAT TCCCCATCTCCCAAGCTCATG-3'
primers for the pTrc300 <i>B. suis</i> <i>virB</i> constructs:	
pTrc1+2-12:5':	5'-GCGCGAGCTCAGAAGGAGACGATCCTATGGTGCCA-3'
pTrc1+2-12:3':	5'-GCGCGAGCTCTTAGAAAACAACACTACGCCGTCC-3'
VirBsuis2-5':	5'-GATGCGGCAGAGCTCGACATAAGGAATAAAGATCATG AAAAC-3'
VirBsuis6-3':	5'-GACTGCGAGGTCTAGAAAGGCCCTAATCCCTGTTGAA CTG-3'
primers for <i>virB11</i> ortholog-encoding genes:	
pVSBAD11suis5':	5'-GCTACGTCATGATGTCCAACCGAAGTGACTTTATTG-3'
pVSBAD11suis3':	5'-GCTACGCTAGATTATAAATTTGTGCAGCATATGC-3'
pVSBAD11Agro5':	5'-GCTACGCCATGGAGGTGGATCCGCAATTACGA-3'
pVSBAD11Agro3':	5'-GCTACGCTAGACTACTGCTGGTTAAGAAGATC-3'
VirB11suis>:	5'-GCGCGGTACCCATGATGTCCAACCGAAGTGAC-3'
T7-7VirB11suis3':	5'-CGTCAGAAGCTTATAAATTTGTGCAGCATATGCGT-3'
TraG>:	5'-GCGCGGTACCCATGACTGATGCAGCTTTCTATC-3'
TraG<:	5'-CGCGCTGCAGTTACAGGCTCCCGTTCA-3'
TrwD>:	5'-GCGCGGTACCCATGTCTACAGTCTCGAAAGCAT-3'
TrwD<:	5'-GCGCCTGCAGCTAAGCCATCTTGGAATTGG-3'
HP0525>:	5'-GCGCGGTACCCATGACTGAAGACAGATTGGA-3'
Hp0525<:	5'-GCGCCTGCAGCTACCTGTGTTTGATATAAAAT-3'
B11C58Bsp1407I:	5'-GCTATGTACACATGGAGGTGGATCCGCAATTACGA-3'
T7-7VirB11Agro3':	5'-GGCTGCCATGGAGGTGGATCCGCAA-3'

Restriction sites are underscoring and Shine-Dalgarno motifs are in *italics*.

3.2. Site-directed mutagenesis primers

Table 5. Site-directed mutagenesis primers

primer name	sequence
523asiteMut:	P-5'-ATCTCTATCGCTTTGTTAG CTAGCT CTCTAGGGTTGAACAAC-3'
VirB1suisMP:	P-5'-GCAGCAATCGTGCAGGTC GCTAGCGG CTTCAATCCTTATGCA-3'
pTrc1+2-12Mut:	P-5'-GTAGTTGTTTTCTA AGAATTC GCGCAAGGGCGAATTC-3'
B1M5:	5'-GCAGCGATCGCTCAGGTC GCTAGCCG CTTTGATCCGCTTGCT-3'
B1suisM5:	5'-GCAGCAATCGTGCAGGTC GCTAGCGG CTTCAATCCTTATGCA-3'
TraLM5:	5'-GCGTACATCGTCGGCCAT GCTAGCT CAAATGGACCGTACAGG-3'
B1_deltaAA:	P-5'-TACGTGCGAAAAGTTGAAAC G/CAAC AGCTCGTCCCCCGTTA-3'
B1_1.Q>E:	P-5'-AAAGTTGAAACGGCCGCT GAAC AGCTCGTCCCCCGTTAACC-3'
B1_2.Q>E:	P-5'-GTTGAAACGGCCGCTCAAG AGCT CGTCCCCCGTTAACCGCG-3'
B1_QQ>EE:	P-5'-AAAGTTGAAACGGCCGCT GAAGAG CTCGTCCCCCGTTAACC-3'
B1_+1P:	P-5'-CGAAAAGTTGAAACGGCC CCG CAACAGCTCGTCCCCCGTTA-3'
B1_1.A>D:	P-5'-TACGTGCGAAAAGTTGAAACGG ACG CTCAACAGCTCGTCCCC-3'
B1_ET>PW:	P-5'-GGCTACGTGCGAAAAGTT CCGTGG GCCGCTCAACAGCTCGTC-3'

Shine-Dalgarno motifs are in *italics* and nucleotides that encode the mutation are in **bold**.

3.3. Specialized sequencing primers

Table 6. Specialized sequencing primers

name	sequence	application
12280>:	5'-CAGCACCTATTCGG-3'	sequencing of pTrc300VirB2-12 and all derived plasmids
11760>:	5'-CAGGACAAGCTCCTGG-3'	see above
10540>:	5'-CGGTTTCGATGGCACC-3'	see above
10020>:	5'-CTGGTAAACTGTCC-3'	see above
9060>:	5'-CATCGTTCGCATGCG-3'	see above
9600>:	5'-GACCAGCTCGGCCGG-3'	see above
8500>:	5'-CGGGCGCTTCTGGCG-3'	see above
8440>:	5'-CCATGTTCATATTGCCGC-3'	see above
VirB1Check:	5'-ATCAAGGGAAACGGGTGGACGG-3'	sequencing of the <i>B. suis</i> <i>virB1</i> gene start region
T7-7 5':	5'-TAATACGACTCACTATAGGGAGA-3'	sequencing of genes inserted downstream of the T7-promoter

T7-Ter:	5'-GCTAGTTATTGCTCAGCG-3'	sequencing of genes inserted upstream of the T7-terminator (in pET21/24)
Trc5:	5'-GGGGAGATCTGACGCGCCCTGACG-3'	sequencing of genes inserted downstream of the pTrc 200/300 polylinker region
Trc3:	5'-CCCCAGTACTTTAAAAGTGCTCATCATT-3'	sequencing of genes inserted upstream of the pTrc 200/300 polylinker region
uni24:	5'-ACGACGTTGTAAAACGACGGCCAG-3'	sequencing of genes inserted downstream of pCR®2.1-TOPO insertion site
rev24:	5'-TTCACACAGGAAACAGCTATGACC-3'	sequencing of genes inserted upstream of pCR®2.1-TOPO insertion site
Trx3new:	5'-GCATTGGTAACTGTCAGACC-3'	sequencing of genes inserted upstream of the pT7-H ₆ TrxFus polylinker region

4. Growth media, supplements and antibiotics

4.1. Growth media

LB	(Miller, 1972)	1% tryptone; 0.5% yeast extract; 0.5% NaCl
LBON	(Bhandari, 1997)	1% tryptone; 0.5% yeast extract
YEB	(Baron <i>et al.</i> , 1997)	1% tryptone; 0.5% sucrose; 0.1%; 2 mM MgSO ₄
AB	(Winans <i>et al.</i> , 1988)	1% glucose; 0.39% MES; 1 mM Na-K-phosphate pH 5.5; 1 x AB salts (20 x AB salts: 20 g NH ₄ Cl; 6 g MgSO ₄ x 7 H ₂ O; 3 g KCl; 0.2 g CaCl ₂ ; 50 mg FeSO ₄ x 7 H ₂ O per liter; pH 5.5)
TGE	(Olsen, 1973)	1% tryptone; 0.5% yeast extract; 0.85% NaCl; 0.5% glucose; 0.015% CaCl ₂

4.2. Supplements, antibiotics and inhibitors

supplements, antibiotics or inhibitors	stock solution	final concentration:	
		<i>E. coli</i>	<i>A. tumefaciens</i>
carb	100 mg/ml in H ₂ O	100 µg/ml	150 µg/ml
str	50 mg/ml in H ₂ O	50 µg/ml	100 µg/ml
spc	50 mg/ml in H ₂ O	50 µg/ml	300 µg/ml
ery	50 mg/ml in methanol	--	150 µg/ml
kan	50 mg/ml in H ₂ O	50 µg/ml	--
tm	100 mg/ml in DMSO	20 µg/ml	--
cm	50 mg/ml in methanol	20 µg/ml	--
IPTG	0.5 M in H ₂ O	0.5 mM	0.5 mM
AS	0.2 M in DMSO	--	0.2 mM in liquid culture, agar plates; 0.5 mM for conjugation assay
X-Gal	40 mg/ml in dimethylformamide	40 µg/ml	--
MTFPT	10 mM in DMSO	various	various
Oleic acid	10 mM in DMSO	--	various
Linoleic acid	10 mM in DMSO	--	various

5. Buffers and solutions

Crosslink Buffer (CLB)	50 mM MES-KOH; 150 mM NaCl; 0.1 mM EDTA; pH 6.5
StreptII-Buffer (S2B)	300 mM NaCl; 100 mM Tris/HCl; 1 mM EDTA; 2 mM DTT; pH 7.0
PSB	StreptII-Buffer with 50% glycerol
TAE	40 mM Tris/HCl; 20 mM acetic acid; 1 mM EDTA, pH 7.8
TBS	20 mM Tris/HCl; 137 mM NaCl; pH 8.0
TBS-T	20 mM Tris/HCl; 137 mM NaCl; 0.1% Tween-20; pH 8.0
PBS	137 mM NaCl; 2.7 mM KCl; 8 mM Na ₂ HPO ₄ ; 1.7 mM KH ₂ PO ₄

6. Growth conditions

6.1. *Escherichia coli*

For overnight cultures all *E. coli* strains were grown in LB or LBON under aerobic conditions at 37°C using 20 ml tubes in a laboratory shaker (Modell Kühner, B.Braun Melsungen) at 200 rpm. Day cultures were inoculated to an OD₆₀₀ of 0.05 in vessels of appropriate volume with the same media under vigorous shaking at 37°C (Certomat-R, B. Braun Biotech International). The protein over-producing strain GJ1158 was induced at an OD₆₀₀ of 0.4-0.8 by addition of 5 M NaCl stock solution to a final concentration of 0.3 M. Cultivation under aerobic conditions then proceeded at different temperatures for varying amounts of time as given in table 7. Unless otherwise indicated, the total culture volume was 1 l in four 500 ml Erlenmeyer flasks filled with 250 ml LBON.

Table 7. Growth conditions for protein production with GJ1158

protein(s)	optimal temperature	cultivation time
VirB1 (C- or N-terminal tag)	26°C	4 h
VirB1/VirBX (bi-cistron)	26°C	6 h
(StreptII-)VirB4suis	26°C	18 h
H ₆ Trx-HP0523	26°C	6 h
H ₆ Trx -VirB7suis	37°C	6 h
(H ₆ Trx or StreptII)-VirB8suis	37°C	4 h
(H ₆ Trx or StreptII)-VirB9suis	37°C	4 h
(H ₆ Trx or StreptII)-VirB10suis	27°C	6 h
(H ₆ Trx or StreptII)-VirB11suis	27°C	18 h
(StreptII-)VirB11agro	20°C	18 h

StreptII-HP0525	26°C	4 h
StreptII-TrwD	27°C	18 h
StreptII-TraG	27°C	18 h

6.2. *Agrobacterium tumefaciens*

A. tumefaciens overnight cultures were grown in 20 ml tubes with YEB in a laboratory shaker at 26°C. Day cultures were inoculated to an OD₆₀₀ of 0.1 for experiments that aimed at VirB protein analysis and to an OD₆₀₀ of 0.25 for conjugation experiments in 100 ml Erlenmeyer flasks containing AB at 20°C and 140 rpm (Gyrotory waterbath shaker Model G76, New Brunswick Scientific Co., Inc.). For virulence gene induction *A. tumefaciens* cells were either maintained in liquid culture at 20°C or plated on solid agar media as described elsewhere (Schmidt-Eisenlohr *et al.*, 1999a; Hapfelmeier *et al.*, 2000).

7. Photometric methods

7.1. Optical density

The optical density of bacterial cultures was determined turbidometrically at 600 nm wavelength with an U-1500 Spectrophotometer (Hitachi)

7.2. Absorption

Protein concentration was measured according to Bradford at 595 nm wavelength. Protein Assay Dye Reagent Concentrate (Bio-Rad) was used, and samples with 2-10 µg of BSA gave the calibration standard (Bradford, 1976)

8. Molecular biology methods

8.1. PCR

DNA was amplified either with *Pyrococcus furiosus* (Pfu) or *Thermus aquaticus* (Taq) DNA polymerase and appropriate buffer systems from different commercial and non-commercial sources. Generally, 100 µl reactions contained 800 µM of the four dNTPs, 10 pmol of each primer, between 1 mM and 2 mM MgCl₂ and approximately 1 ng of template DNA. A “Gradient Thermocycler” (Biometra) was used to perform a 30 cycles program. Times and temperatures of denaturation, annealing and elongation were moderately varied to meet the special requirements of the polymerase and primer-template pairs used in different experiments.

8.2. DNA isolation

E. coli or *A. tumefaciens* cells from 2 ml of an overnight culture were sedimented by centrifugation and treated as described in the “JETquick Spin Column Technique” manual for

plasmid minipreparations. DNA fragments, which were generated by PCR or excised from agarose gels were purified with the same system using the respective protocols. DNA was precipitated with ethanol after elution from the column (Sambrook *et al.*, 1989)

8.3. DNA *in vitro* modifications

8.3.1. Restriction cleavage and dephosphorylation

DNA was cleaved using restriction enzymes and buffers supplied by MBI Fermentas and New England Biolabs (NEB) following manufacturers protocols. In the case of DNA cleavage close to the end of a fragment, restriction digest proceeded over night. To avoid religation, cleaved vector DNA was treated with Shrimp Alkaline Phosphatase (Roche Diagnostics).

8.3.2. Removal of staggered ends

To create 5'-phosphorylated blunt ended DNA fragments ssDNA overhangs were removed with Mung Bean Nuclease (NEB) according to the manufacturer's protocol.

8.3.3. Ligation

Ligation of DNA fragments was conducted in 20 µl total volumes at room temperature for two to 16 hours using T4 ligase (MBI Fermentas) and T4 ligase buffer (NEB). In most cases linearized vector was incubated with a large excess of insert in order to obtain insert-carrying clones.

8.4. Site-directed mutagenesis

Generation of site-directed mutations in genes was achieved following the protocol of the "Gene editor TM site-directed mutagenesis system" (Promega). Since this requires the presence of the *bla* gene on the respective vector, subcloning of genes into such a vector had to be done in some cases.

8.5. DNA-sequencing

DNA sequences were determined with the chain termination method (Sanger *et al.*, 1977) using the BigDye® Terminator v1.1 cycle sequencing kit (Applied Biosystems), purified vector DNA and 10 pmol of sequencing primer per reaction. The reaction was subsequently processed as suggested by the manufacturer and analyzed by a capillary-sequencer (ABI Prism R310, Applied Biosystems)

8.6. Transformation of plasmid DNA

Transformation of electrocompetent bacteria with plasmid DNA was achieved with a Gene Pulser™-electroporation system (Bio-Rad) at 2000 V, 800 Ω and 25 µFaraday (Fiedler

and Wirth, 1988). When chemically competent *E. coli* JM109, BMH71-18*mutS* (Promega) or TOP10 (Invitrogen) were used, transformation was carried out as described by the supplier.

9. Biochemical methods

9.1. (d)NTPase assay

The standard reaction mixture (20 μ l) consisted of ATPase buffer (50 mM Tris-HCl; 50 mM KCl; 2 mM $MgCl_2$; 1 mM DTT; pH 7.5) and unless otherwise indicated, 1 mM of the respective (d)NTP. For determination of the optimal pH value for the reaction, buffer A (50 mM Tris/HCl; 50 mM KCl; 2 mM $MgCl_2$; 1 mM DTT; pH 7.0) and buffer B (50 mM CHES/NaOH; 50 mM KCl; 2 mM $MgCl_2$; 1 mM DTT; pH 9.5) were mixed in empirically determined ratios to obtain the desired pH values. Two μ l of an 10 x enzyme stock solution (final concentrations of enzymes calculated based on active sites: 500 nM for StrepII-VirB11*B. suis*, His-TrxVirB11*B. suis* and StrepII-HP0525; 5 μ M for StrepII-TrwD and StrepII-TraG; 1 μ M for StrepII-VirB11*A. tumefaciens*) in PSB were pre-incubated with 16 μ l buffer for 5 min, 2 μ l of 10 mM (d)NTP stock solution (in H_2O) were added to start the reaction, which proceeded for 20 or 30 min. The (d)NTPase activity was determined based on P_i liberation with the malachite-green assay (Cogan *et al.*, 1999). The reaction was stopped either by transfer of 20 μ l aliquots of the mixture into vials containing an equal volume of 5 mM EDTA on ice, or by direct detection of the P_i content. To that end H_2O was added to a final volume of 500 μ l followed by addition of 172 μ l Solution I (172 μ l of 2.1 M H_2SO_4 , 28 mM ammoniumheptamolybdate) and 128 μ l Solution II (0.35 % polyvinylalcohol, 0.76 mM malachite green) as described by Cogan *et al.*. The formation of the blue phosphomolybdate-malachite green complex was in linear relation to the amount of released P_i and was determined through spectrophotometric measurement at 610 nm after 20 min incubation at RT. For the standard curve 100 μ M NaH_2PO_4 was prepared freshly from a 10 mM stock solution and 0 to 60 μ l (corresponding to $[P_i]$ between 0 μ M and 12 μ M) were mixed with water to a final volume of 500 μ l. Solution I and Solution II were added and the OD_{610} was determined. Concentration of P_i was plotted against the OD_{610} to determine the slope of the standard curve. The velocity of the enzymatic reaction was either depicted as pmol P_i /min or as the percentage of the maximum value that was observed under ideal conditions. To analyze the impact of other StrepII-tagged VirB proteins from *B. suis* on the ATPase activity of StrepII-VirB11, the standard reaction mix for each data point contained 14 μ l of buffer, 2 μ l of 10 x enzyme stock solution (167 nM, VirB11*suis* hexamer) and 2 μ l of VirB protein (1.67 μ M, monomer). The reaction was started by addition of 2 μ l 10 mM ATP. Negative controls were performed with the potential interacting protein, which had been denatured by incubation at 100°C for 5 min. Increase of the P_i concentration was measured as described during 20 min and samples were taken every two minutes.

9.2. Determination of protein-protein interactions

9.2.1. Strep-Tactin® Sepharose® pull-down assay

10 µl of purified StrepII-tagged proteins (5 pmol/µl in PSB) were incubated with 20 µl Strep-Tactin® Sepharose® (50% suspension in StrepII-buffer, IBA GmbH) for 15 min. 80 µl S2B and 10 µl Trx-fusion protein (5 pmol/µl in PSB) were added next. After 15 min of incubation at RT, the sepharose was sedimented (13.000 rpm, 2 min) and washed three times with 200 µl-500 µl in the same buffer. Bound proteins were eluted with 35 µl 1 mM biotin.

9.2.2. Chemical crosslinking with DSS

10 pmol/µl stock solutions of purified StrepII-tagged proteins in PSB were prepared. 5 µl of protein A was mixed with either 5 µl protein B, or 5 µl PSB as negative control. After 5 min, 90 µl CLB was added and the mixture was incubated for another 30 min. Crosslinking started by addition of 0.025 µl-1.25 µl 10 mM DSS, proceeded for 1 h and was stopped by mixing with an equal volume of 2 x Lämmli SB (Lämmli, 1970). For the crosslinking of StrepII-VirB11 (+/- inhibitor), 5 µl of 10 pmol/µl stock solution in PSB was mixed with 5 µl PSB and 70 µl CLB was added. For the negative control 10 µl DMSO and 10 µl H₂O were added. In order to assay crosslinking with substrate alone, 10 µl DMSO and 10 µl ATP (10 mM in H₂O) was added. 10 µl MTFPT (10 mM in DMSO) and 10 µl ATP (10 mM in H₂O) was added to assess inhibitor effect on multimerization. Incubation and crosslink proceeded as described.

10. Electrophoretic methods

10.1. Electrophoretic separation of DNA

DNA was separated in horizontal TAE agarose gels. The agarose concentration was 0.5% to 1.5%, dependent on the fragment sizes of the sample; the ethidiumbromide concentration in the gels was 0.4 µg/ml. Samples were mixed with 1/10 vol. of DNA SB (50% glycerol, 0.05% bromophenolblue). For visualization of DNA the gel was placed on a UV-screen (Eagle Eye™, Stratagene)

10.2. Protein separation by SDS-PAGE

Depending on the size of the proteins of interest, two different methods were applied. For proteins of a MW of >20 kDa, glycine-SDS-PAGE (10%-15% acrylamide; Lämmli, 1970) was performed. To separate proteins of a MW <20 kDa, tricine-SDS-PAGE was done (12% acrylamide; Schägger and v. Jagow, 1987). Gels were then either subjected to protein transfer for Western-blot or directly stained with 0.2% Coomassie blue solution. Silver

staining (Bloom *et al.*, 1987) was performed when very low amounts of proteins had to be visualized.

10.3. Electroelution

The purification of high quantities of insoluble protein (500 µg-1 mg) for generation of polyclonal antisera required elution from polyacrylamide gels, followed by precipitation and immunization (Biogenes, Berlin). This was done with the “Biotrap”-system (Schleicher & Schüll) according to the manufacturer’s description.

11. Chromatographic methods

Different chromatographic purification steps within one protein purification process were performed in a uniform buffer at 4°C.

11.1. Immobilized metal chelate affinity chromatography (IMAC)

Sedimented bacterial cells were resuspended in 4-8 ml S2B (no DTT; 0.5 mM PMSF) and passed 3 x through a French Pressure Cell (Aminco) at 18,000 psi. The lysate was subjected to centrifugation (SS34 rotor, 25 min, 13,000 rpm at 4°C) and the supernatant applied to an HPLC-system (Äkta Purifier, Amersham Pharmacia Biotech) with a 5 ml Co²⁺-charged IMAC column (Talon™ Superflow, Clontech). Hexa-His-tagged recombinant protein was eluted according to a step-gradient protocol. At a flow rate of 0.5-1.0 ml/min the column was first washed for 5 CV (column volumes). Then a stringent washing step with 20 mM imidazole proceeded for 2.5 CV, before 150 mM imidazole was applied to the column for 2.5 CV. Both the stringent wash fractions and the elution fractions were collected in 2 ml aliquots.

11.2. Strep-Tactin Sepharose chromatography

Cells were lysed in S2B (0.5mM PMSF) as described above. N-terminal StrepII-fusion protein was purified from the supernatant with 1 ml Strep-Tactin® Sepharose® (IBA GmbH) following the instructions given by the manufacturer.

11.3. Gel filtration

Samples generated by affinity chromatography (1 ml maximum) were loaded onto Superdex 200™ or Superdex 75™ gel filtration columns in the same buffer and the flow rate was 0.5 ml/min or 1.0 ml/min. To determine the MW of proteins, the columns were calibrated with the “Gel filtration Calibration Kit” (Amersham Pharmacia Biotech), which uses proteins in the range between 13.7 kDa and 669 kDa.

11.4. Enrichment of proteins and dialysis

In order to concentrate protein samples after intermediate and final purification steps centrifugal filter devices (Amicon® Ultra-15, Millipore) with either 10 kDa or 30 kDa nominal molecular weight limit were used as described in the provided protocol. After concentration, the samples were dialysed for >12 h against 1 l of PSB in a dialysis tubing (Visking, Roth) at 4°C. Samples were stored at –20°C until further use.

12. Bacteriological methods

12.1. Conjugation assay

12.1.1. *A. tumefaciens*

For conjugation experiments *A. tumefaciens* donor and recipient were incubated at 20°C on AB minimal medium plates containing defined quantities of AS or IPTG inducers following standard protocols (Bohne *et al.*, 1998). In conjugation assays focussing on the T4SS of the donor, the recipient strain (UIA143pTi, ery^R) harboured the Ti-plasmid to ensure formation of the receptor structure and efficient DNA-uptake. A donor strain of choice (A348 derivate harbouring pLS1, carb^R) and the recipient strain were cultured under virulence-inducing conditions and then mixed on an agar plate containing AS and for virulence gene induction and IPTG for expression of plasmid-encoded genes. The conjugation then proceeded for 2-3 days and cells were harvested, diluted to 10⁻⁸ in PBS and plated on YEB medium containing ery and carb for selection of the transconjugands (UIA143pTi pLS1, ery^R carb^R). The number of donor cells was determined and the transfer efficiency calculated as number of transconjugand cells (TC) per output donor cells (D). Likewise, the assay was performed to determine the state of the T4SS serving as the receptor structure for IncQ uptake in the recipient. In this case the donor strain was always WT A348 pLS1 and after dilution of the mating mixtures the number of transconjugands (TC) per recipient cells (R) determined the transfer efficiency.

12.1.2. *E. coli*

Overnight cultures of donor and recipient bacteria were sedimented by centrifugation and washed twice in an equal volume of LB to remove antibiotics. The pellet was suspended in 100 µl of LB, the OD₆₀₀ was determined and donor and recipient were plated in a one to one ratio on 0.5 ml solid LB in a 24-well tissue culture plate (Becton Dickinson). Incubation at 37°C proceeded for 1 h. Cells were then washed off with 1 ml LB, subjected to a dilution series from 10⁰ to 10⁻⁶ and plated onto LB agar with selective antibiotics. For inhibitor analysis, the donor was plated 1 h prior to addition of the recipient to permit inhibitor action on T4SS function.

12.2. Virulence assay

The virulence of *A. tumefaciens* was tested by inoculating fresh wound sites on leaves of *Kalanchoë daigremontiana* with 10 µl of bacterial cell suspension $OD_{600} = 0.25$. In addition, ten- and hundredfold dilutions were applied onto the lesions. Tumor formation was analysed after four-six weeks.

12.3. Phage infection assay

Bacteriophage IKe was propagated and used to identify the amount of IncN-determined conjugative pili. In this assay, stationary phase cultures of FM433 pKM101 were mixed with the inhibitor and then preincubated with different titers of the IncN pilus-specific bacteriophage IKe, which infects and lyses cells after binding to proteins of IncN-determined pili. The mixture was subsequently poured into soft agar plates and plaque formation was counted after incubation at 37°C overnight; plaque numbers from the control without MTFPT was set to 100 %. Development of plaques is related to the status of the pilus in the respective strain, because it roughly corresponds to the availability of IncN-pilus components on the cell surface. Bacterial cultures were preincubated with MTFPT concentrations ranging from 1 µM to 1000 µM by adding a 20 µl of a 10x stock solution, thus ensuring constant DMSO content in all samples.

13. Immunological methods

13.1. Protein transfer

For detection of proteins by Western Blot, proteins were transferred onto a PVDF-membrane (Immobilon-P, Millipore) in a vertical blot device (Trans Blot Cell, Bio-Rad; Blot Buffer: 192 mM glycine, 25 mM Tris, 20% methanol) at 90 V for 1 h or 30 V for 16 h. Proteins attached to peptide array membranes were transferred in a semi-dry blot device (Fast-Blot, Biometra) following the protocol suggested by the company (Jerini AG). For each protein transfer, a PVDF membrane, six pieces of Whatman paper of appropriate size and three different transfer buffers were prepared (Cathode Buffer (CB): 25 mM Tris, 40 mM 6-aminohexanoic acid, 20 % methanol, pH 9.4; Anode Buffer I (AB I): 30 mM Tris, 20% methanol, pH 10.4; Anode Buffer II (AB II): 300 mM Tris, 20 % methanol, pH 10.4). The PVDF membrane was prepared by soaking it with methanol and incubation in Anode Buffer I for 10 min. Pieces of Whatman paper were soaked with the different transfer buffers and arranged on the semi-dry blot device in the following order.

- cathode

2 x Whatman paper soaked in CB
peptide array membrane
PVDF membrane

2 x Whatman paper soaked in AB I
2 x Whatman paper soaked in AB II

+ anode

Protein transfer proceeded at 1 mA/cm² for 2 h at 4°C. The PVDF membrane was subjected to Western blot and the peptide array membrane was regenerated by washing it with water (three times for 10 min), Regeneration Buffer I (62.5 mM Tris, 2% SDS, pH 6.7; four times for 30 min), 10x PBS (three times 20 min), TBS-T (three times 20 min) and finally TBS (three times 10 min). In order to remove tightly bound protein, which might disturb subsequent experiments with the peptide array membrane, it was placed in the semi-dry blot device as described above and residual proteins were transferred at 1 mA/cm² for 2 h at 4°C. Between experiments, the membrane was stored in TBS-T at 4°C.

13.2. Western blot

Detection of proteins according to Harlow and Lane (1988) was achieved utilizing “goat anti-rabbit IgG-HRP” (Bio-Rad), a chemiluminescence detection system (Western Lightning, Perkin Elmer Life Sciences Inc. or Lumi Light^{PLUS}, Roche Diagnostics) and blue sensitive photographic film (B+, WicoREX®).

13.3. Overlay assay

Approximately 1 µg of protein in SB was separated in a 12% glycine-SDS-PAGE and transferred onto a PVDF membrane as described; the membrane was incubated in regeneration buffer (10 mM Hepes pH 7.5; 10 mM MgCl₂; 50 mM NaCl; 0.1 mM EDTA; 1 mM DTT; 10% glycerol; Homann *et al.*, 1990) for 24 to 48 h. The membrane was incubated with TBS-T containing 5 % skimmed milk powder for 1 h in order to reduce unspecific adhesion of protein and then incubated with approximately 5 µg/ml of the potentially interacting protein in the same buffer at 4°C for 16 h. After washing the membrane, the protocol proceeded like that of the standard Western-blot utilizing primary antibody to identify the overlaid protein.

13.4. Peptide array experiments

The entire sequence of VirB1 from *B. suis* (Accession: NP_699276, see also Fig. 5) without the signal peptide was displayed on a cellulose membrane as seventy 13-mers, covalently bound at the C-terminus and with N-terminal acetylation, shifting three amino acid positions each time:

```
peptide 1: AAIVQVESGFNPY
peptide 2:  VQVESGFNPYAIG
peptide 3:   ESGFNPYAIGVVG
peptide 4-68: defined by sequence and specification (see above)
peptide 69:                      TDAPPGKDNTDGV
peptide 70:                      PPGKDNTDGVVVF
```

The protocol for “Mapping of discontinuous epitopes” from the supplier’s manual was applied (Jerini AG). The peptide array membrane, which features all possible epitopes of VirB1 was preincubated for 30 min in TBS-T, transferred into blocking solution (Roche Diagnostics) for 1 h, washed again with TBS-T for 10 min and then incubated in blocking solution containing 1-5 µg/ml of different proteins for 12 h at 4°C. Before transfer of the attached proteins onto PVDF membranes with a semi-dry blot device (see 12.1), the peptide array membrane was washed three times in TBS-T for 10 seconds.

13.5. Generation of polyclonal antisera

Soluble StrepII-VirB11 from *B. suis* was purified by affinity chromatography, whereas StrepII-VirB1 was obtained from an inclusion body preparation, separated by SDS-PAGE, excised from the gel and subjected to electroelution. Approximately 0.5 mg of each protein was lyophilized and used for immunization of rabbits (BioGenes).

14. Data processing

14.1. Statistical and graphical data processing

To capture images of polyacrylamide gels, Western blots and plant leaves, an UMAX UTC-6400 scanner was used. After first adjustments with Photoshop 6.0 (Adobe), the final images were created with PowerPoint (Microsoft) or Canvas 7.0 (Deneba Systems). Statistical analysis, curve fitting and imaging was done with Excel 98 and Prism 4 (trial-version, GraphPad), using linear and nonlinear regression algorithms with standard parameters.

14.2. Protein sequence analysis

The ClustalW (version 1.82) algorithm for multiple sequence alignment (Higgins *et al.*, 1994; www.ebi.ac.uk/clustalw) or EMBOSS for alignment of two less conserved amino acid sequences was applied (Smith and Waterman, 1981; Needleman and Wunsch, 1970; www.ebi.ac.uk/emboss/align). Sequence information was processed with NORSp (Liu and Rost, 2003; cubic.bioc.columbia.edu/services/NORSp) in order to discover long regions

without regular secondary structure. Predictions of secondary structure were obtained with the PHD-algorithm (Rost, 1996; www.embl-heidelberg.de/predictprotein). To create a conservation plot of sequence alignment, the alignment data were transferred to the AMAS-server (Barton and Livingstone, 1993; barton.ebi.ac.uk/servers/amas_server.html) using standard default values. All structure images were generated with DINO 0.9.0 (Philippsen, 1998-2003; cobra.mih.unibas.ch/dino/intro.php).

Results

1. Characterization of structural and functional properties of VirB1

1.1. Display of conservation between the VirB1 SLT domain and its orthologs LysG and Slt70

The murolytic enzyme hen egg white lysozyme (*Gallus gallus* LysC or HEWL) was one of the first proteins whose structure was solved, which may be partly due to the availability of large quantities of raw material for purification (Blake *et al.*, 1965). The nomenclature of the well-described enzyme is EC 3.2.1.17 or EC 3.2.1.14, the latter referring to the chitinolytic activity that murolytic enzymes generally possess. Until now, the structures of 18 lysozymes from different organisms have been solved. In addition, the three structures of the lytic transglycosylases (EC 3.2.1.-) LaL from bacteriophage λ , Slt35 and Slt70 (both from *E. coli*) are also available. The enzymatic action of lysozymes and soluble lytic transglycosylases (SLT) differs, but the protein fold is highly conserved (Mushegian *et al.*, 1996).

Sequence comparison of *B. suis* VirB1 with two murolytic enzymes, whose X-ray structure was known, yielded interesting results. The SLT portion of the large donut-shaped Slt70 from *E. coli* ranges from amino acid P494 to A620 and has a significant degree of sequence similarity to *B. suis* VirB1 (ID: 23.1%; SIM: 38.1%; Gaps: 35.6%). Other proteins like LysG from *Anser anser* (GEWL) (ID: 18.0% Sim: 33.1%; Gaps: 23.8%) and *G. gallus* Lys C are less similar, although they were previously chosen to model the structure of a VirB1 ortholog (Mushegian *et al.*, 1996). Structural superposition shows that despite an almost identical tertiary structure of LysG and Slt70 (G. Koraimann, unpublished), their sequence similarity (ID: 22.0%; SIM: 36.3%; Gaps: 32.7%) is less than that between Slt70 and VirB1. It is therefore appropriate to use the surface model of Slt70 to visualize regions of VirB1-interaction with other VirB proteins.

The AMAS algorithm was used to assign values expressing the degree of conservation to all AA-positions in a multiple sequence alignment, ranging from A (identical) to 8 (weakly conserved). One of the sequences in this alignment was a protein with known tertiary structure (here: *E. coli* Slt70) and the other one was *B. suis* VirB1. The software DINO was next applied to create a map of conserved residues on the surface of the known 3-dimensional model (Fig. 4). It is assumed that conserved patches on the surface are likely to interact either with partner proteins or substrate(s).

Following the modeling we found that many of the amino acids conserved between VirB1 and Slt70 or LysG and Slt70 were not exposed on the surface but rather seem to stabilize the structurally conserved lysozyme fold. The most prominent conserved surface patch was the active site cleft with the catalytic E (Glu), which is ubiquitously found throughout all lysozyme-like enzymes (Fig. 4). This model of the *B. suis* VirB1 structure was instrumental for the analysis of its protein-protein interactions as outlined below.

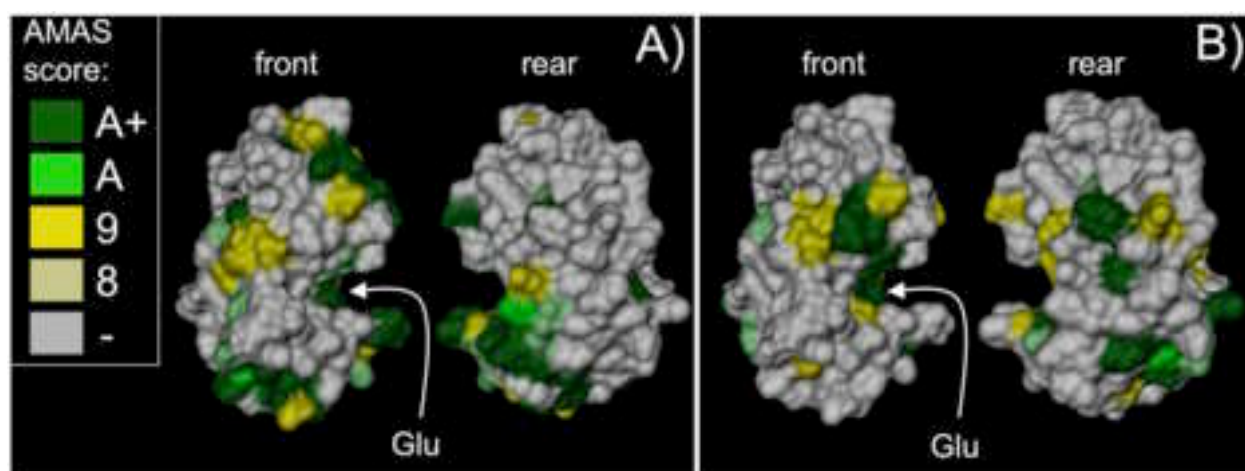


Fig. 4. Prediction of conserved surface residues in different murein transglycosylases. Conserved amino acids between the SLT domain of *B. suis* VirB1 and *E. coli* Slt70 (A) or *A. anser* LysG and *E. coli* Slt70 (B) are displayed on the surface of the Slt70 soluble lytic transglycosylase domain. The results from an EMBOSS alignment were processed and submitted to the AMAS server to validate the degrees of conservation. Identical residues in each of the two pairs are shown in dark green (A+), high similarity (A) in green and lower similarity is in yellow (9) and light yellow (8). The figure was prepared with DINO.

1.2. An *in silico* analysis of VirB1 ortholog conservation

VirB1 orthologs show significant similarity to the SLT domain of Slt70, and our modeling suggests that the structure of these SLTs is also conserved. Nevertheless, we noted differences, which may have interesting implications for the biology of these proteins. One sequence stretch, that can be found in *B. suis* VirB1, *A. tumefaciens* VirB1 and also TraL from pKM101, cannot be aligned to the sequences of Slt70, LysG or LysC whose structures are known. According to the alignment and secondary structure prediction, this stretch may form an α -helical region of about 17 AA N-terminal to the highly conserved GLMQ motif, and this region could contribute to the distinct enzymatic features or the regulation of specialized lytic transglycosylases. The respective region N-terminal to amino acid 517 in the *E. coli* Slt70 (Fig. 5) sequence localizes within a loop region adjacent to the active site cleft. Apart from this difference, many but not all SLT-like proteins from T4SS have long C-terminal domain-like regions with interesting properties.

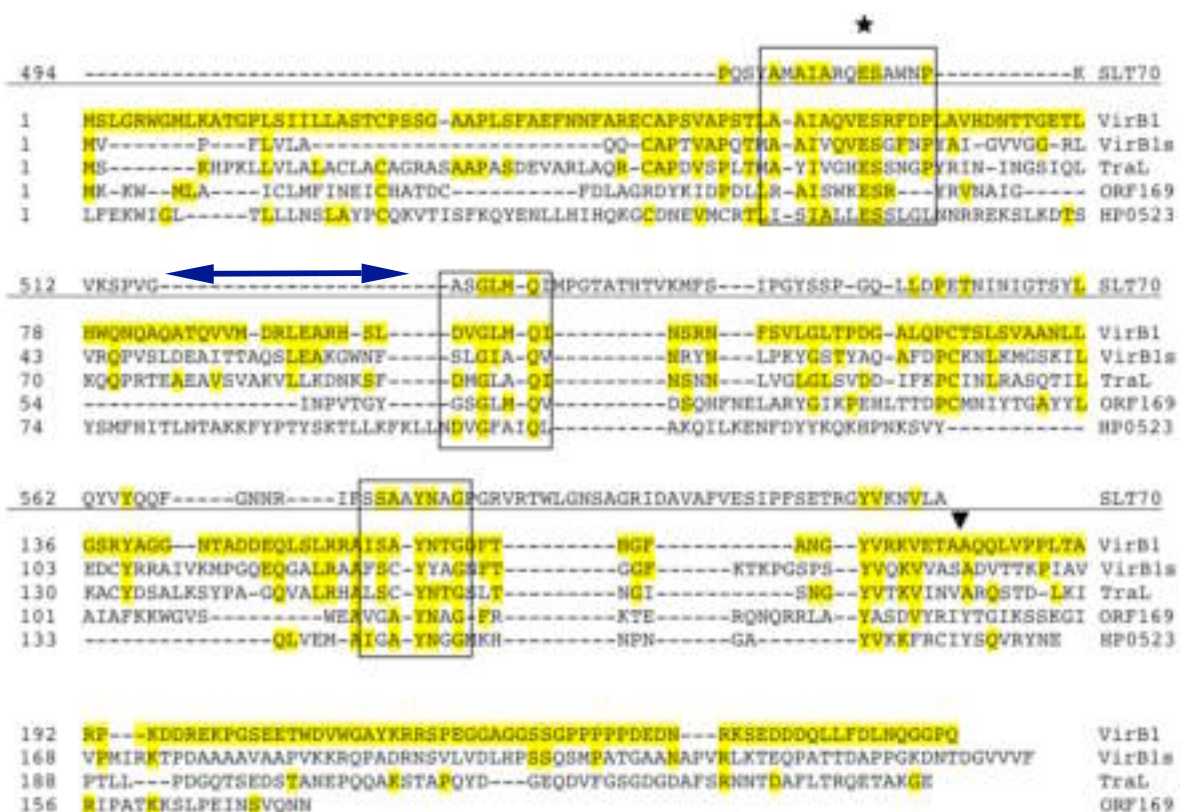


Fig. 5. Alignment of the VirB1 orthologs investigated in this study. Residues identical to *A. tumefaciens* VirB1 are shaded, conserved residues implicated in the enzymatic activity are indicated by black frames. The putative active site Glu is labeled with a star, the cleavage site of *A. tumefaciens* VirB1 is indicated with a black arrowhead. The alignment of the VirB1 orthologs was generated with the MegAlign program, the SLT domain of *E. coli* Slt70 was aligned to *B. suis* VirB1 with EMBOSS (Needle algorithm) and fit into the alignment. A dark blue arrow indicates the 17 amino acid stretch characterizing VirB1 orthologs.

1.3. Secondary structure prediction of the VirB1 C-terminus

It has been shown earlier that VirB1 from *A. tumefaciens* undergoes posttranslational processing and that the C-terminal part, denominated VirB1*, is released by proteolytic processing (Baron *et al.*, 1997). Although the SLT domain of VirB1 from *A. tumefaciens* is completely located in the N-terminal half, both parts of the protein independently contribute to tumorigenesis (Llosa *et al.*, 2000). Since VirB1 from *A. tumefaciens* was found to interact with other T4SS components in a yeast two-hybrid assay (Ward *et al.*, 2002), it was speculated that full-length VirB1 might undergo protein-protein interactions with other T4SS components. This notion was strongly supported by the finding that VirB1* could be co-immunoprecipitated with VirB9 following chemical crosslinking. VirB1* accumulated in extracellular fractions, and it is possible that it exerts additional (non SLT-related) functions for virulence, e.g. modification of the host membrane or participation in pilus formation. It was also proposed that VirB1* could act as a chaperone, facilitating the correct folding of the main pilus component VirB2. Alternatively, processing of VirB1 could be the first step of an accelerated degradation process of the lytic protein in order to maintain the integrity of the

cell wall. The fact that only full-length VirB1 or VirB1*, but not the N-terminus were detected in Western blots after expression from the same promoter (C. Höppner and C. Baron, unpublished data) also hints at a quick degradation of the SLT domain, whereas VirB1* was stable and thus accumulated inside and outside of the cell.

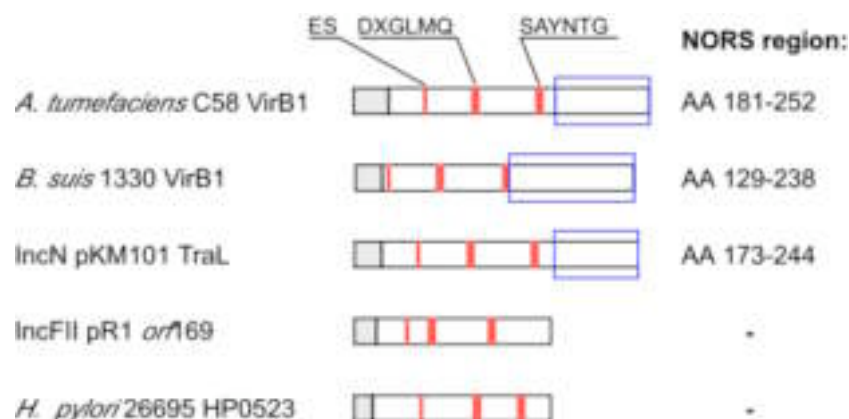


Fig. 6. Features of the sequence of VirB1 orthologs. Predicted signal peptides are in grey and the active site signature sequence of the orthologs is highlighted (Höppner *et al.*, 2004; modified). The NORS regions as predicted by NORSp are boxed, and their lengths are shown on the right.

Sequence analyses of a number of VirB1 orthologs demonstrated special properties of the C-terminal part. The sequences of VirB1* and also of the C-termini of *B. suis* VirB1 and pKM101 TraL were classified as NORS-regions (Fig. 6). These are regions of more than 70 AA length that show less than 12% secondary structure elements and an amino acid composition different from loop regions. It was demonstrated that these very flexible regions show similar degrees of conservation as other domains in similar proteins, and that they are more abundant in proteins with functions as regulators or transcription factors than in those with functions in biosynthesis or energy metabolism-related proteins (Liu *et al.*, 2002). This implicates important functional roles, most likely for transient protein-protein interactions with different partners. Only 4% of all procaryotic proteins contain NORS regions, and within the *virB*-operon of *A. tumefaciens* and *B. suis*, channel component VirB10, which is supposedly involved in a high number of interactions (Cascales and Christie, 2003), is the only other protein that possesses such a region.

1.4. Biochemical analysis of *B. suis* VirB1 interactions

1.4.1. Coproduction of VirB1 and other VirB proteins in bi-cistronic expression vectors

Recombinant proteins produced in *E. coli* are often insoluble or improperly folded and one reason for this is that their natural binding partners are absent. One method to circumvent this problem of heterologous gene expression is the co-expression of the genes encoding such proteins together with genes coding for potential interaction partners

(Lutzmann *et al.*, 2002). If the two proteins subsequently co-purify this constitutes strong evidence for their interaction.

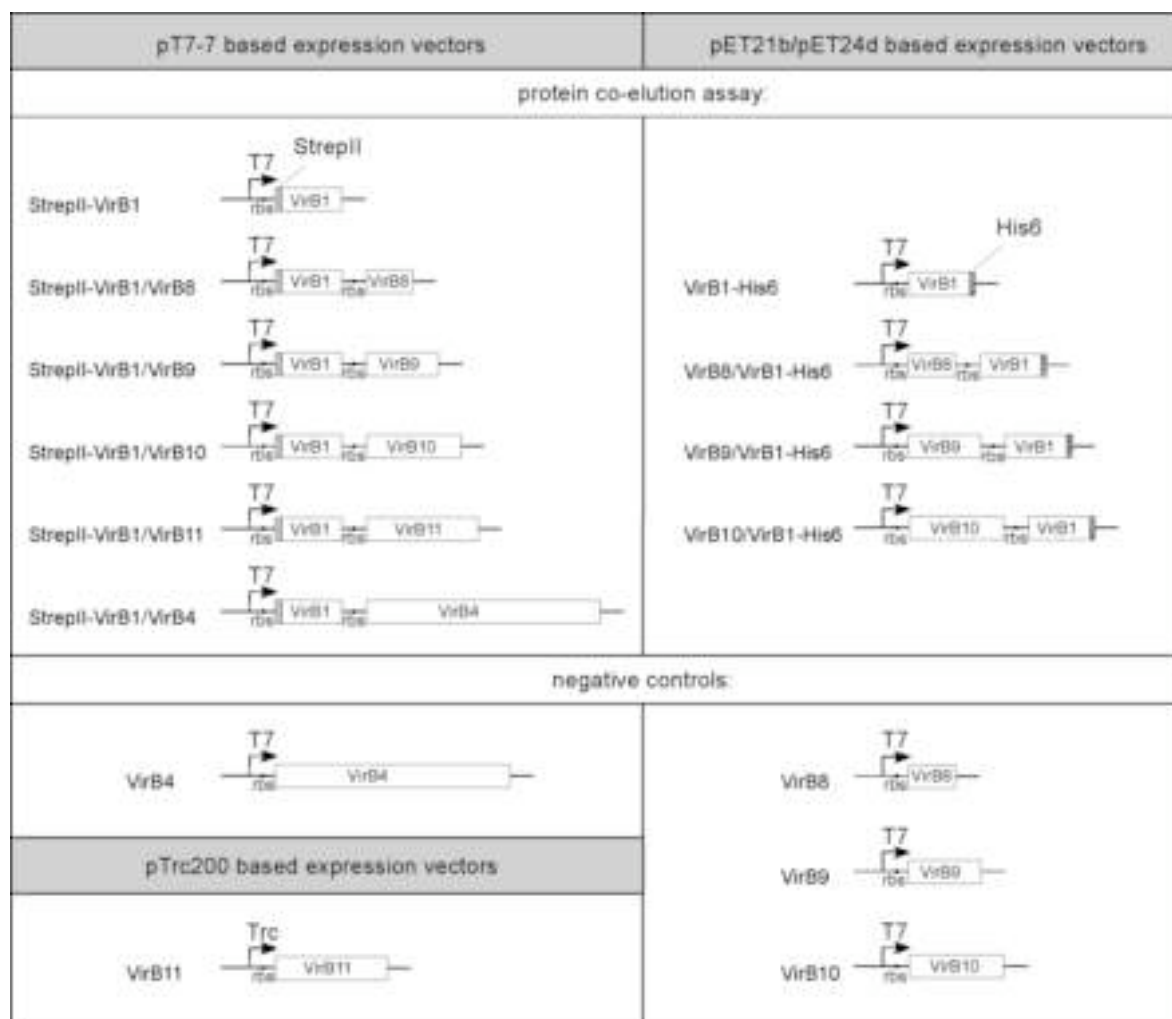
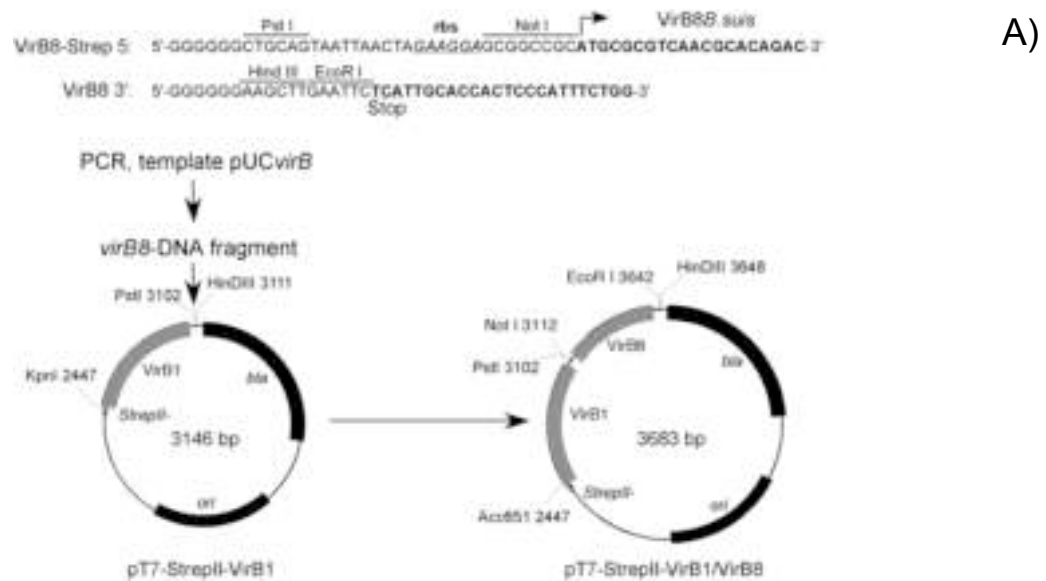


Fig. 7 (preceding page). Graphical representation of the mono- and bi-cistronic vector constructs used in this study. The first bi-cistronic vector based on pT7-StrepII was created by inserting a *virB8* fragment as defined by the primers VirB8-Strep 5' and VirB8 3' (Fig. 7A and table 4) creating T7-StrepII-VirB1/VirB8 (A). Substitution of *virB8* with other *vir* genes utilizing *NotI/EcoRI*-sites to remove *virB8* and to introduce the other genes via the same sites yielded all of the pT7-based bi-cistronic constructs. Another lineage of bi-cistron vectors producing VirB1-His was created with pET21b/pET24d. The depicted mono-cistronic vectors served as negative control in the experiments. rbs: ribosomal binding site, Trc: Trc promoter, T7: T7 promoter

The potential interactions of VirB1 with other components of the *B. suis* T4SS were tested by expression from vectors encoding either N- or C-terminally tagged VirB1 fusion proteins and their putative interaction partners VirB8, VirB9, VirB10, VirB11 or VirB4. To this end, a *virB8* fragment with a ribosomal binding site was prepared with *PstI/HindIII* and inserted into pT7-StrepII-VirB1 cleaved with the same enzymes. The insert was designed to permit substitution of the *virB8* fragment by excising it from the resulting vector pT7-StrepII-VirB1/VirB8 with *NotI/EcoRI* and inserting fragments of *virB9*, *virB10*, *virB11* and *virB4* as defined by the respective oligonucleotide primers (Table 4). Following this procedure, bi-cistron constructs based on the T7-7 vector and co-expression of N-terminally StrepII-tagged VirB1 and a putative interaction partner were created (Fig. 7).

In order to co-produce C-terminally His₆-tagged VirB1 with putative interaction partners, a vector based on pET21b/pET24d was modified to permit expression of bi-cistronic mRNA (as in Lutzmann *et al.*, 2002; vectors created by S. Höppner). The first *orf* of the pET21b-based vector series encodes the putative interaction partner and was created by cleavage of the vector with *NcoI/NotI* and insertion of fragments of *virB8*, *virB9* and *virB10* treated with the same restriction endonucleases. Subsequently, *virB1* was inserted by cleavage and insertion with *NheI/EcoRI*, which placed *virB1* in frame with the vector sequence encoding the C-terminal His₆-tag.

A series of constructs for the expression of non-tagged proteins was generated to serve as controls, as these proteins did not bind avidly to affinity columns. Based on the pET21b-based bicistron vectors, three constructs that served as negative controls were created by excision of *virB1* with *Sall/XhoI* and religation of the vector. Untagged VirB8, VirB9 or VirB10 were produced upon induction of expression from these vectors. The full-length *virB4* gene was inserted into pT7-7, that had been cleaved with *NotI/EcoRI*, in order to obtain a vector for mono-cistronic production of VirB4. Insertion of the full-length *virB11* gene into pTrc200 cleaved with *BspHI/XbaI* created a vector for mono-cistronic production of non-tagged VirB11.

I decided to work with two different tags since the interactions of VirB1 with other T4SS components might depend on regions of VirB1 that include either the C- or the N-terminus. If expression from both vector types and subsequent analysis did not give any

evidence for an interaction, this was not likely due to interference by the tags. It became apparent, however, that in most cases low amounts of either C- or N-terminally tagged VirB1 and the co-produced putative interaction partner were retrieved from the affinity column, which made it necessary to further analyse the interaction by gel filtration. In spite of the two-step separation procedure, the untagged VirB proteins from both monocistronic and bicistronic expression were detected in gel filtration eluates. As a consequence, if VirB1 and the putative interaction partner are found in the same fractions after co-elution from the gel filtration column, this does not automatically prove interaction. The two proteins might possess a similar apparent MW that could not be resolved in the Superdex 200 column. In order to decide between co-elution due to a similar MW and co-elution as an effect of interaction, the elution of these putative interaction partners after expression from a bicistronic expression vector was compared with the elution after expression from a monocistronic expression vector. If no difference in elution of the untagged protein is observed in the two cases, it indicates that there is no interaction between VirB1 and the second protein. Monocistronic expression of the untagged putative interaction partner was therefore carried out as a negative control in all experiments.

1.4.1.1. Purification of C- and N-terminally affinity-tagged VirB1

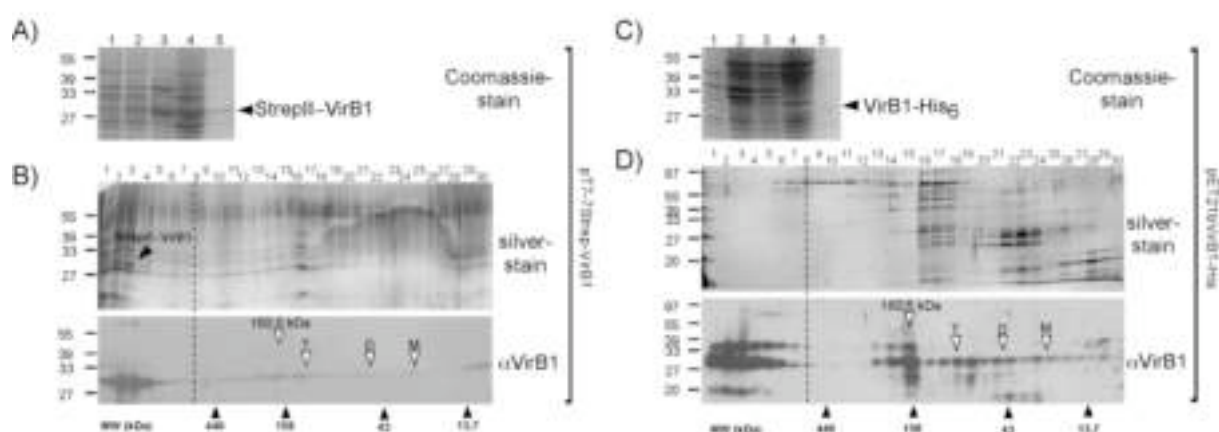


Fig. 8. Overproduction and purification of StrepII-VirB1 and VirB1-His₆. Different steps of the overproduction and purification from *E. coli* cells producing either StrepII-VirB1 (A) or VirB1-His₆ (C) were analyzed by Coomassie staining of SDS gels. Lanes as follows, 1: pre-induction, 2: harvest, 3: insoluble fraction, 4: soluble fraction, 5: post-affinity chromatography. Samples from affinity chromatography containing StrepII-VirB1 (B) and VirB1-His₆ (D) were applied to a Superdex 200 gel filtration column. Silverstain (B, D Top) or Western blot analysis (B, D Bottom) was performed to detect recombinant VirB1. Fraction numbers are indicated, starting with 1 (at 38 ml elution volume) and they represent 2 ml fractions each. White arrowheads point to the expected size of monomeric (M), dimeric (D) and tetrameric (T) protein. A dashed line marks the Superdex 200 void volume at >600 kDa. Numbers on the left indicate reference proteins for SDS-PAGE. The names of the respective expression vectors are given on the right. Black arrowheads indicate the elution of gel filtration reference proteins with their associated MW from the Superdex 200 column.

StreptII-VirB1 (Fig. 8 A, B): After expression at 27°C, the protein was purified from lysed *E. coli* cells by affinity chromatography (Fig. 8 A). Gel filtration using a Superdex 200 column was performed with the aim to further purify the protein. Analysis by silver staining and Western blotting detected the major portion of StreptII-VirB1 in the void volume, corresponding to a MW above 600 kDa. Faint VirB1-specific signals were detected only by Western blotting in fractions 25, 22 and 16, which correspond to the monomeric, dimeric and tetrameric form of StreptII-VirB1 (Fig. 8 B).

VirB1-His₆ (Fig. 8 C, D): Purification with IMAC did not yield sufficient protein for detection in a Coomassie-stained polyacrylamide gel (Fig. 8 C). The sample was subjected to gel filtration and VirB1-His₆ was detected in many elution fractions. Similar to the results described above, a major portion of VirB1-His₆ eluted in the void volume of the Superdex 200 column, but VirB1-specific signals were also found in fractions 24, 21 and 18, corresponding to mono-, di-, and tetrameric assemblies (Fig. 8 D). An additional VirB1-specific signal was detected in fractions 14 and 15 during the analysis of both N- and C-terminally tagged VirB1 proteins, which corresponds to a 160.5 kDa putative hexamer (Fig. 8 B, D).

The C-terminus of VirB1-His₆ appeared to be inaccessible for binding to the affinity column since only small amounts of this protein were purified by IMAC. Comparison of the samples from affinity chromatography (Fig. 8 A and C, lanes 5) shows the lower amount of His₆-VirB1 that was retrieved as compared to StreptII-VirB1. In analogy to the process observed in case of *A. tumefaciens* VirB1 (Baron *et al.*, 1997), the C-terminus may have been proteolytically removed after production in *E. coli*. Since no notable signals indicating such a processing product were detected (Fig. 8 B, D), cleavage of the C-terminal part is probably not a good explanation for the low amounts of VirB1-His₆. In spite of its presence in strongly reduced amounts, the Western blot signal of VirB1-His₆ (Fig. 8 D) appears stronger than for StreptII-VirB1 (Fig. 8 B), but this is due to the fact that the chemoluminogram was exposed to X-ray film twenty times longer.

Unpublished results from G. Koraimann's laboratory (Graz, Austria) showed the association of *E. coli* chaperone GroEL with the C-terminus of some VirB1 orthologs. The possibility that GroEL binds to VirB1 was therefore assessed by Western blot analysis of the samples eluted from the gel filtration column using VirB1- and GroEL-specific antisera.

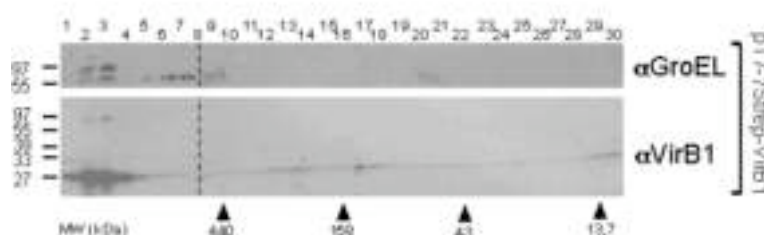
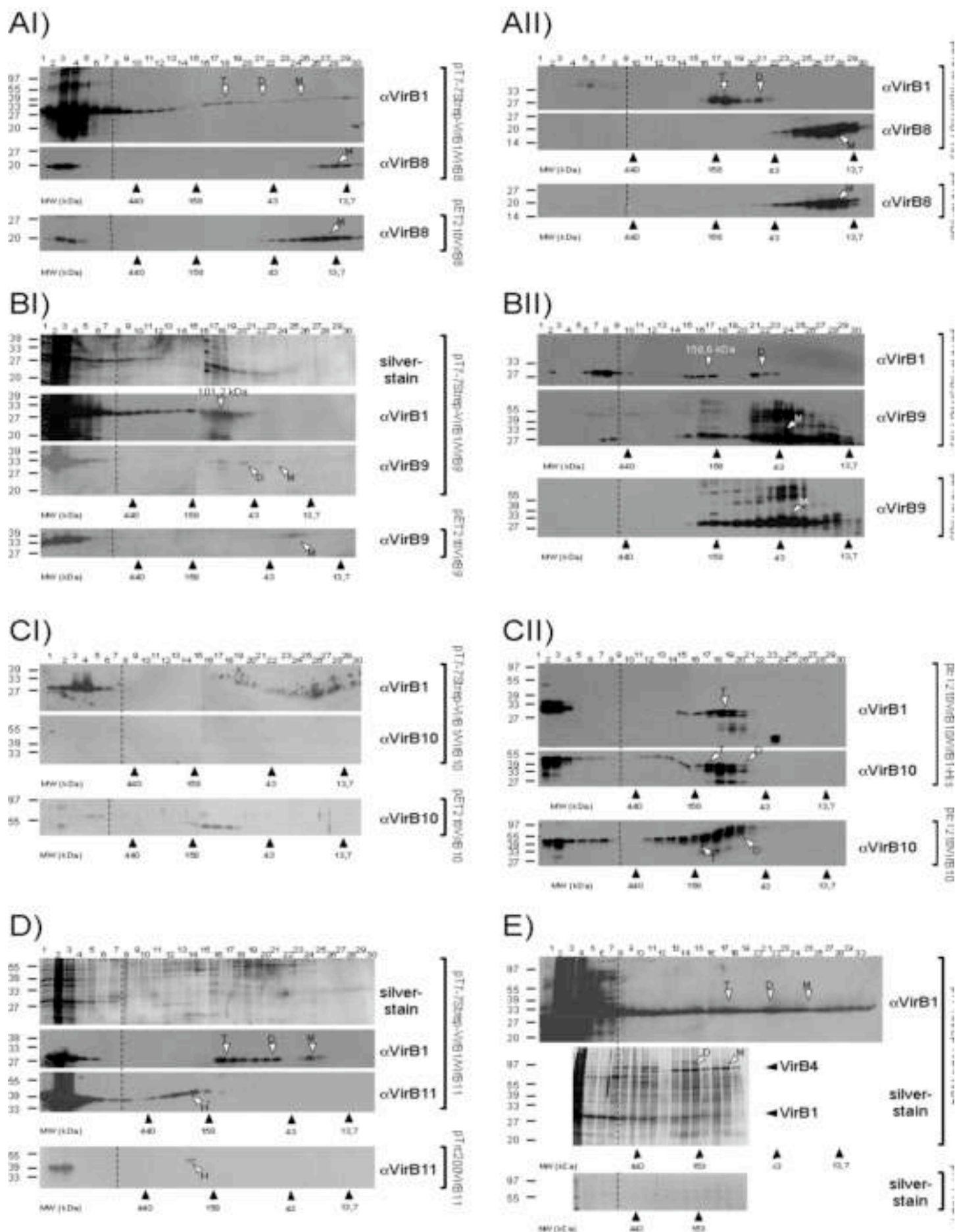


Fig. 9. Elution of *B. suis* VirB1 and *E. coli* GroEL. Samples of StrepII-VirB1 purified by affinity chromatography were separated with a Superdex 200 gel filtration column. SDS-PAGE and Western blot analysis with VirB1- and GroEL-specific antisera was performed. Fraction numbers are indicated, starting with 1 (38 ml elution volume) and representing 2 ml fractions. A dashed line marks Superdex 200 void volume at >600 kDa. Numbers on the left indicate reference proteins for SDS-PAGE. Name of the vector used for expression is given on the right. Black arrowheads indicate elution of reference proteins and the associated numbers show the MW.

This analysis revealed that GroEL co-eluted from the gel filtration column with StrepII-VirB1 (Fig. 9). GroEL may bind to VirB1, which would explain the detection of VirB1 predominantly in high MW complexes. GroEL and VirB1 were both detected in fraction 2 and 3, and in addition GroEL was present in fractions 6 to 8, as indicated by the signal appearing at approximately 60 kDa.

Subsequent experiments aimed at elucidating the influence of other T4SS components on the molecular mass of VirB1, as determined by co-purification during affinity chromatography followed by analytical gel filtration. The amounts of VirB1 and its interaction partners obtained from 1 l of *E. coli* overproduction cultures did not permit the detection of the proteins by Coomassie or silver staining, and it was therefore necessary to use specific antisera. One additional concern during these studies was that small amounts of untagged VirB proteins also bound to and eluted from the affinity columns. In order to establish interactions it was therefore necessary to verify the interaction by gel filtration. The results of the separation co-expressed proteins were compared with the elution of untagged VirB proteins expressed from mono-cistronic vectors. If they differed from those obtained with co-expressed proteins, it was taken as evidence for an interaction.

Fig. 10. (next page) Coelution of VirB1 with other T4SS components. Samples containing StrepII-VirB1 + VirB8 (AI) and VirB1-His₆ + VirB8 (AII), StrepII-VirB1 + VirB9 (BI) and VirB1-His₆ + VirB9 (BII), StrepII-VirB1 + VirB10 (CI) and VirB1-His₆ + VirB10 (CII), StrepII-VirB1 + VirB11 (D) and StrepII-VirB1 + VirB4 (E) were separated with a Superdex 200 gel filtration column. Silver staining or Western blot analyses were performed to detect recombinant VirB proteins. Fraction numbers are indicated, starting with 1 (38 ml elution volume) and representing 2 ml of elution volume each. White arrowheads point to the expected size of monomeric (M), dimeric (D) and tetrameric (T) protein. The dashed line marks the column void volume at >600 kDa. Numbers on the left indicate reference proteins for SDS-PAGE. Black arrowheads indicate the elution of gel filtration reference proteins with the associated MW from the Superdex 200 column. Name of the vector used for expression is on the right of each panel; single *virB* genes were expressed from mono-cistronic vectors as negative controls (bottom of each panel). All experiments were performed up to three times and gave similar results.



1.4.1.2. Analysis of VirB1-VirB8 bicistron products

StreptII-VirB1+VirB8 (Fig. 10 AI): StreptII-VirB1 forms high MW complexes that elute from the gel filtration column in the void volume. In addition, small amounts of StreptII-VirB1 were detected in fractions 24, 20 and 16 to 18 corresponding to the mono-, di- and tetrameric form. Irrespective of the expression of *virB8* from mono- or bicistronic vectors, the protein predominantly eluted in fractions 24 to 28, indicating monomeric protein and co-expression had no effect on the elution of VirB1. Some VirB8 eluted in the void volume indicating aggregate formation.

VirB1-His₆+VirB8 (Fig. 10 AII): VirB8 eluted as a monomer in fractions 24 to 28, but the elution of VirB1-His₆ differed from that of StreptII-VirB1. The relative amount of high MW complexes was strongly reduced and the protein eluted in fractions 17 to 21, supposedly the tetrameric and dimeric form. Co-expression with *virB8* had no apparent effect on the elution of VirB1-His₆.

1.4.1.3. Analysis of VirB1-VirB9 bicistron products

StreptII-VirB1+VirB9 (Fig. 10 BI): StreptII-VirB1 eluted as a high MW complex in the void volume and in fractions 17 and 18, indicating a MW of about 100 kDa. In contrast to other bicistron expression experiments, the presence of VirB9 in the void fraction could even be visualized in a silver-stained polyacrylamide gel, indicating relatively high amounts of the protein. VirB9 was detected predominantly in the void volume, but minor amounts were detected in fractions corresponding to the monomer, dimer and, like StreptII-VirB1, in fraction 17 and 18. When VirB9 was produced from a mono-cistronic vector, the protein could be detected by Western blot only in the void volume and in the fraction corresponding to the monomer.

VirB1-His₆+VirB9 (Fig. 10 BII): VirB1-His₆ eluted from the column in three different forms. First, in fractions 6, 7, 8 and 9, representing a high MW complex that had a lower MW than that of VirB1-His₆ when it was expressed from a mono-cistronic vector (Fig. 8). Second, in fractions 15, 16 and 17, corresponding to a MW of approximately 160 kDa and third, in fractions number 21, 22 and 23, corresponding to a size intermediate to the dimer and tetramer. VirB9 eluted in fractions 6 to 9 and 15 to 17 but the largest portion of the protein was monomeric. In contrast, when VirB9 was expressed from a mono-cistronic vector, it predominantly eluted in fractions 22 to 25, which corresponds to the supposed monomer.

1.4.1.4. Analysis of VirB1-VirB10 bicistron products

StreptII-VirB1+VirB10 (Fig. 10 CI): StreptII-VirB1 formed high MW complexes that eluted from the gel filtration column in the void volume, and VirB10 was not detected in these experiments. VirB10 produced from a mono-cistronic vector eluted in the void volume and in fractions 16 to 18, indicating a MW intermediate to dimeric and tetrameric VirB10.

VirB1-His₆+VirB10 (Fig. 10 CII): VirB1-His₆ eluted in the void volume and in fractions 17, 18 and 19, which corresponds to a MW expected for the VirB1-His₆-tetramer. VirB10 produced in a strain carrying the mono-cistronic vector eluted in the void volume and in fractions 17 to 19, indicating a MW between the dimeric and tetrameric form. The elution of VirB10 co-expressed with VirB1-His₆ and VirB10 produced from mono-cistronic mRNA was indistinguishable, and therefore gave no indication of an interaction.

1.4.1.5. Analysis of VirB1-VirB11 bicistron products

StreptII-VirB1+VirB11 (Fig. 10 D): StreptII-VirB1 formed high MW complexes that eluted from the gel filtration column in the void volume and it was also detected in fractions 24, 20, 19, 17 and 16, corresponding to the mono-, di- and tetrameric form. VirB11 was detected in the void volume and in fractions 12 to 14, corresponding to the hexameric form of the protein (see chapter 2.2.1). VirB11 produced from a mono-cistronic vector eluted in similar fractions from the gel filtration column. However, the amount of proteins produced in the cells was reduced indicating that VirB1 may interact with VirB11 and thereby stabilize it.

1.4.1.6. Analysis of VirB1-VirB4 bicistron products

StreptII-VirB1+VirB4 (Fig. 10 E): StreptII-VirB1 formed high MW complexes that eluted from the gel filtration column in the void volume, but small amounts of the protein were detected across all the analyzed fractions. As a *B. suis* VirB4-specific antiserum was not available, the protein was visualized in a silver-stained gel in fractions 16 and 17 (monomer) and 13 and 14 (dimer). Co-elution of StreptII-VirB1 and VirB4 was apparent in these fractions. VirB4 was also expressed from a mono-cistron vector and it may unspecifically attach to the Strept-Tactin Sepharose affinity column. However, it could not be visualized by silver staining in the eluates from the subsequent gel filtration column, suggesting that binding of the non-tagged protein to the column can not account for the results observed after co-expression of StreptII-VirB1 and VirB4. The co-elution therefore indicates an interaction.

1.4.2. Strept-Tactin® Sepharose® pull-down assay

An alternative way to demonstrate protein-protein interactions is a pull-down assay that exploits the affinity of the StreptII-tag to the Strept-Tactin Sepharose affinity matrix. The VirB proteins that were tested for their capacity to bind VirB1 were affinity purified as His₆-tagged thioredoxin-fusions (here: His-Trx-) to achieve high solubility and their co-precipitation with StreptII-tagged VirB1 bound to the affinity matrix was determined. The results are shown in Fig. 11.

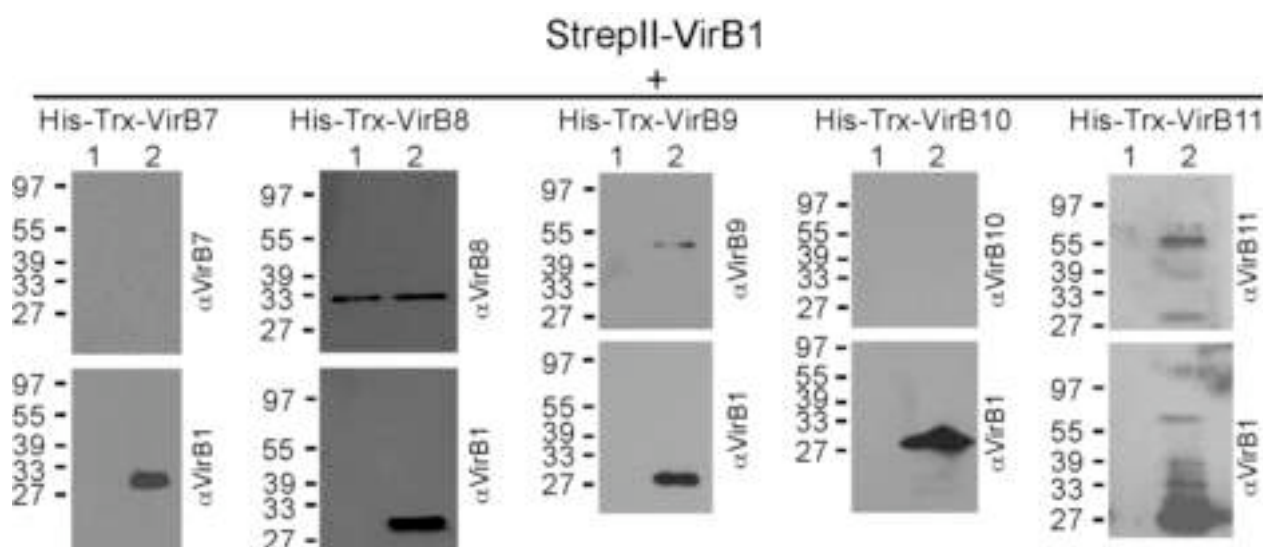


Fig. 11. Strep-Tactin Sepharose pull down assay with StrepII-VirB1. StrepII-VirB1 was preincubated with the Strep-Tactin matrix before addition of the indicated His-Trx-VirB proteins. After three times washing with S2B, proteins were eluted from the matrix with 1 mM biotin, and analysed by SDS-Page and subsequent Western blot. Lanes 1 show the negative control where only His-Trx-VirB was incubated with the matrix, lanes 2 show the pull-down assay. Experiments were repeated five times and representative results are shown here.

His-Trx-**VirB7** and also His-Trx-**VirB10** did not co-precipitate with StrepII-VirB1, showing that they do not interact in this assay. This result also demonstrates that the His₆-thioredoxin *per se* has no affinity for the matrix utilized here, which is an important negative control. A very different observation was made in case of His-Trx-**VirB8**, which bound to the matrix irrespective of the presence of StrepII-VirB1. Since even extensive washing could not remove the protein from the Strep-Tactin matrix, it was impossible to use this method to assess the VirB8-VirB1 interaction. Co-fractionation (=likely interactions) with StrepII-VirB1 were demonstrated in case of His-Trx-**VirB9** and His-Trx-**VirB11**. Observations from the bi-cistronic expression experiments had already provided some evidence for an interaction between VirB1 and VirB9 and VirB1 and VirB11 (1.4.1.5), and those were further substantiated here.

1.4.3. Crosslinking of purified VirB1 to other VirB proteins

The reagent DSS was used to crosslink potentially interacting proteins in solution as described in chapter 9.2.2 of the Materials and Methods section. The samples were subsequently separated by SDS-PAGE and subjected to Western blotting.

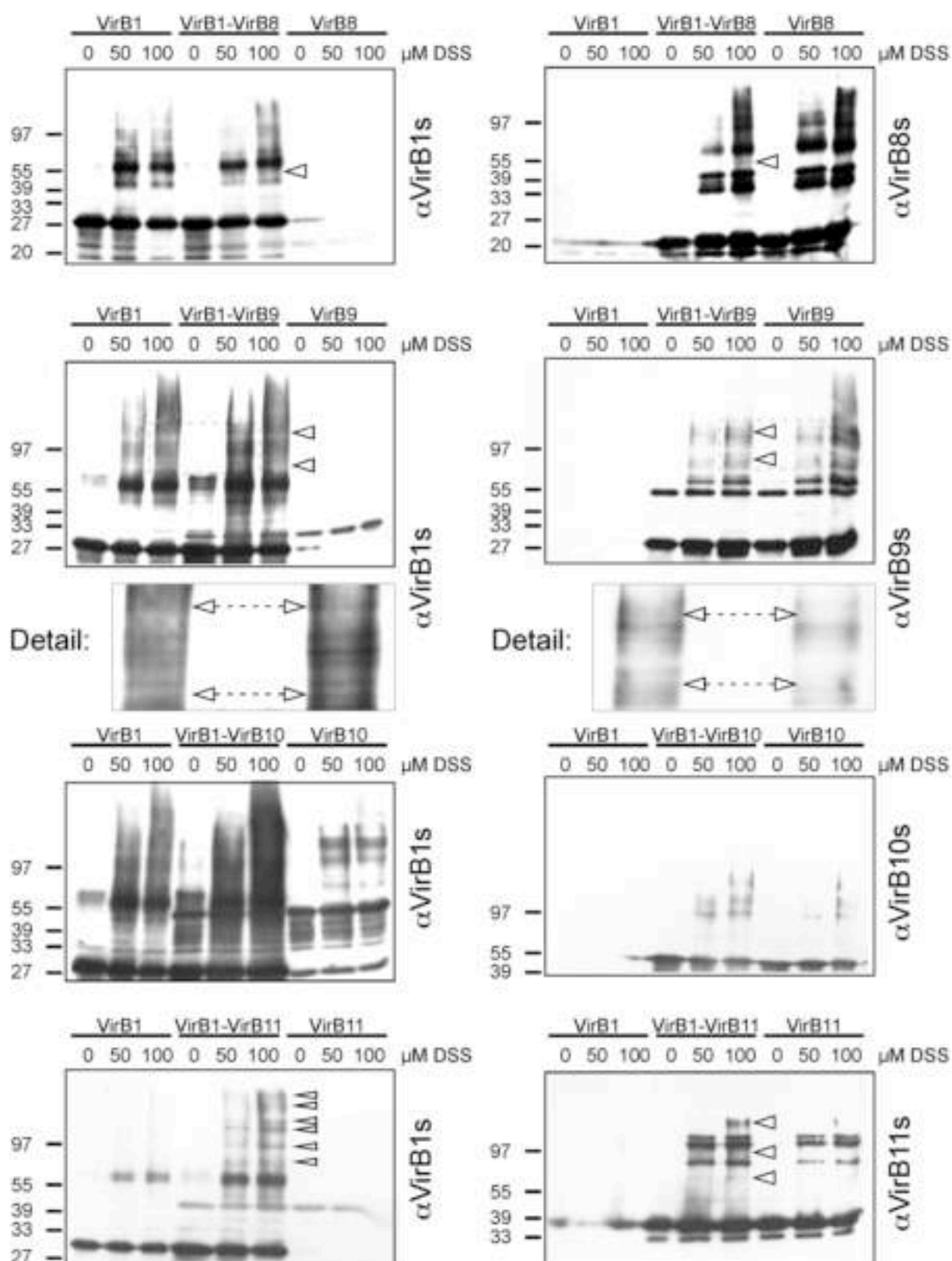


Fig. 12. Crosslinking of Streptococcus pneumoniae VirB1 with other Streptococcus pneumoniae VirB proteins. The panels have a uniform organization. Streptococcus pneumoniae VirB1 alone (left), a mixture of Streptococcus pneumoniae VirB1 and the indicated Streptococcus pneumoniae VirB protein (center) or Streptococcus pneumoniae VirB protein alone (right) were incubated with concentrations of DSS ranging from 0 μM to 100 μM. The specific antisera used for detection are shown on the right side of each panel. Numbers on the left indicate reference proteins. Arrows point to signals that appeared exclusively after crosslinking of the protein mixture. A box in the panels with the results from the Streptococcus pneumoniae VirB1/Streptococcus pneumoniae VirB9 crosslink shows the part of panel that has been magnified in order to show more detail (below).

VirB1: Upon treatment of StreptII-VirB1 with increasing concentrations of the crosslinking reagent, a VirB1-specific signal appeared in the Western blot that corresponds to a StreptII-VirB1-dimer (Fig. 12, left column, left panel-side). More diffuse signals were observed at approximately 100 kDa and larger, indicating the formation of StreptII-VirB1 tetramers and of even higher molecular mass oligomeric states. The signal patterns of other StreptII-VirB proteins on Western blots detected with specific antisera were also altered by the addition of DSS (Fig. 12, right column, right panel-side). **VirB8:** VirB8-specific signals appeared at molecular masses corresponding to the mono-, di-, tri-, and tetramer of the protein. **VirB9:** Similarly, StreptII-VirB9 may form monomers, dimers and tetramers in solution since specific signals corresponding to the respective molecular masses were detected in the experiment after inclusion of DSS. **VirB10:** A weak VirB10-crossreactive signal was detected at approximately 100 kDa after addition of DSS, which may indicate the formation of StreptII-VirB10 dimers. **VirB11:** The VirB11-specific signals that appeared on a Western blot featuring StreptII-VirB11 incubated with DSS confirm the formation of many clearly defined oligomeric states of the protein, with the hexamer being the signal with the highest MW.

The analysis of crosslinking products formed after incubation of mixtures of the StreptII-tagged T4SS components in the presence of DSS led in some cases to the identification of new products identified with both antisera. This was taken as evidence for an interaction of the co-incubated proteins. (Fig. 12, both columns, center-panel). **VirB1/VirB8:** When StreptII-VirB1 and StreptII-VirB8 were incubated together with DSS a new product was detected both with the VirB1- and VirB8- specific antisera. The MW of this product is 55 kDa, which matches precisely the sum of the two individual proteins. **VirB1/VirB9:** Two faint new signals were observed on a chemoluminogram analyzing crosslink formation of a mix of StreptII-VirB1 and StreptII-VirB9 in the presence of DSS. These two distinct signals at 70 kDa and 140 kDa were detected with VirB1- and VirB9-specific antisera, and they were not detected when the proteins alone were incubated with DSS. **VirB1/VirB10:** In contrast to the other protein combinations, there was no evidence for the formation of unique crosslink products between StreptII-VirB1 and StreptII-VirB10. **VirB1/VirB11:** In contrast, a large number of novel VirB1-specific signals appeared on a Western blot following co-incubation of a mix of StreptII-VirB1 and StreptII-VirB11 in the presence of DSS. In contrast, VirB11-specific antisera did not detect all of these products, but signals likely corresponding to crosslink products were detected at 70 kDa and 97 kDa with both antisera.

It is apparent that StreptII-VirB1 interacts with VirB9 and VirB11, as suggested by the formation of detectable crosslinked products after addition of DSS. In contrast to the previous

experiments there is also a clear indication that VirB8 and StreptII-VirB1 interact. Since different approaches pursued here gave evidence for interactions of VirB1 with VirB9 and VirB11, and VirB8 may also interact with VirB1, the putative interaction partners were subjected to peptide array experiments with a VirB1 membrane (Material and Methods, 13.4) to identify the binding site(s).

1.4.4. Peptide-array analysis of VirB1 interactions

Peptide array experiments were conducted in order to assess the interactions of VirB1 that were suggested by the experiments outlined above and to narrow down the binding site on VirB1. Proteins StreptII-VirB8, StreptII-VirB9 and StreptII-VirB11 of *B. suis* were assayed for interaction with VirB1 peptides displayed on a membrane, which represents the entire sequence of the processed form of VirB1. Three identical membranes were used to analyze parallel experiments, and the membranes retained VirB protein in every case.

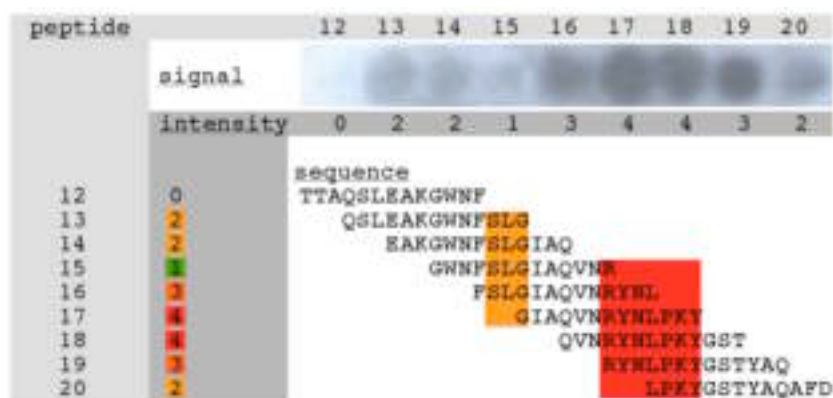


Fig. 13. Method of peptide array evaluation. Signals from the Western blot (here: detail from the VirB1 membrane incubated with VirB9) are categorized by eye, the intensity value (1=weak, 2=intermediate, 3=strong, 4=very strong) corresponds to a certain peptide number and color. By alignment, a sequence stretch responsible for the observed signal pattern can be identified. In the case of “RYNLFPKY” the most intense signal is categorized as 4 (very strong), so this value and the corresponding color (red) are assigned to the whole sequence stretch.

Western blots from five independent experiments, which determined the binding of an interaction partner to specific peptides, were graphically superimposed to obtain a representative mean result. The intensity of the signal for each spot was categorized from 1 (weak) to 4 (very strong) by eye. By aligning the sequences of the binding peptides, it was possible to identify domains of VirB1 that bind the respective VirB protein. When more than one spot defined an interacting domain in the sequence, the highest value of signal intensity present was assigned to the entire domain (Fig. 13).

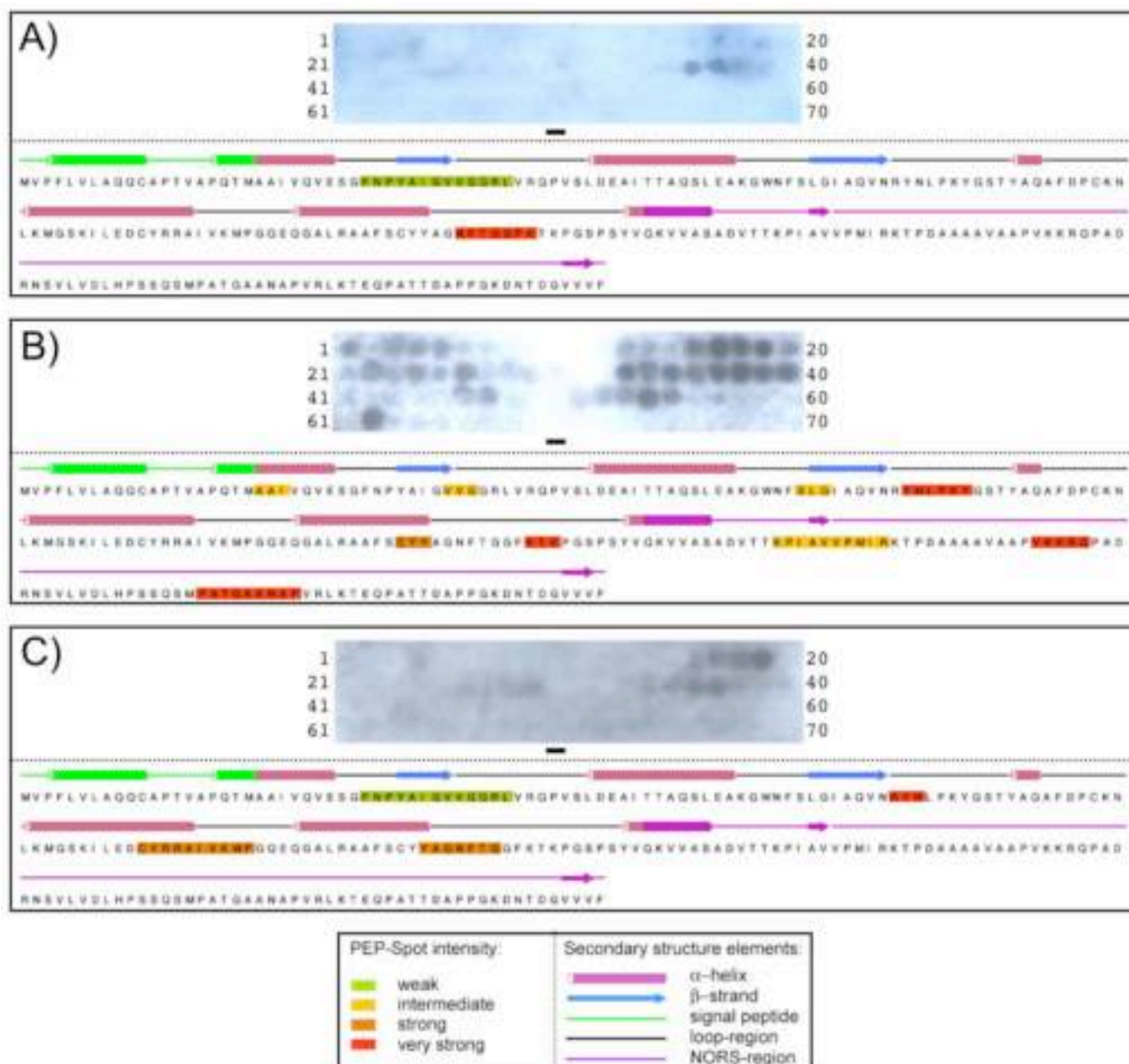


Fig. 14. Patterns of VirB8-, VirB9- and VirB11-specific signals on the VirB1 peptide array membranes. The signal patterns for the interactions of VirB8 (A), VirB9 (B) and VirB11 (C) with the VirB1 membrane represents the results of five independent experiments, which were graphically superimposed. A color code is used to indicate the intensity of VirB protein binding (= interaction) for every stretch of the VirB1 sequence. Secondary structure elements and the proposed signal peptide of VirB1 as predicted by the Ph.D.-algorithm (Rost, 1996) are shown.

The three assessed proteins StrepII-VirB8, StrepII-VirB9 and StrepII-VirB11 bound to different regions of VirB1 and the binding strengths were different. StrepII-VirB9 bound to the highest number of VirB1 peptides, but StrepII-VirB8 and StrepII-VirB11 also bond to a defined set of VirB1 peptides. Since interacting amino acids are often found in external loop regions, a prediction of the VirB1 secondary structure was done with the Ph.D algorithm and the proposed secondary structure is also shown in Fig. 14.

Weak binding of VirB8 occurred to a region C-terminal of the catalytic E27, which is predicted to be a loop/ β -sheet region. VirB8 strongly interacted with another loop region N-terminal to the predicted NORS region (Fig. 14 A).

StreptII-VirB9 bound different amino acid stretches throughout the entire sequence of VirB1. Interactions of intermediate strength occurred with three parts of the VirB1 sequence that are only three amino acids long. StreptII-VirB9 bound to the first three amino acids following the predicted signal peptide of VirB1, a loop region C-terminal to a short β -sheet and N-terminal to the conserved GIAQ motif, which is characteristic to all SLTs. An extended domain bound with intermediate strength by StreptII-VirB9 was localized to in the part of VirB1 classified as NORS region. Strong interactions to the amino acids CYY were observed, which are predicted to participate in the formation of an α -helix N-terminal to the NORS region. Very strong binding to a loop region shortly after the GIAQ motif and N-terminal to the start of the NORS region was detected. In addition, two long amino acid sequence stretches in the NORS region were strongly recognized by StreptII-VirB9 (Fig. 14 B).

Similar to StreptII-VirB8, StreptII-VirB11 bound only to a limited set of peptides on the VirB11 array membrane. A weak interaction of StreptII-VirB11 with the VirB1 sequence is apparent in a loop/ β -sheet region C-terminal to the catalytic E27. Strong binding to an α -helix/loop region and a loop region in the amino acid sequence constituting the second half of the SLT domain were detected. A Very strong interaction of StreptII-VirB11 was observed with a short loop region C-terminal from the GIAQ motif (Fig. 14 C).

The interactions of VirB1 with VirB8, VirB9 and VirB11, which had been suggested by previous experiments, were further substantiated with this method. Most interacting amino acids stretches identified here constitute loop or NORS regions, which are especially suited for establishing transient protein-protein interactions, suggesting that the interaction sites may be biologically relevant.

1.5. Heterologous expression of the *B. suis* *virB* operon in *A. tumefaciens*

A multitude of studies on the T4SS of *A. tumefaciens* have provided information about VirB1. By analyzing the VirB1 ortholog from *B. suis* in the context of its native T4SS it should be possible to assess, whether the characteristic properties defined for VirB1 also apply to the ortholog in *B. suis*. Since experiments with the biosafety level 3 (BL 3) pathogen *B. suis* require specialized resource- and time-consuming safety measures, an alternative approach to analyze the significance of VirB1 in the *B. suis* T4SS was pursued here.

It was demonstrated before that the *A. tumefaciens* T4SS is not only able to transfer T-DNA into plant cells but also to effect transfer of non-self transmissible IncQ plasmids into other *A. tumefaciens* cells in a VirB-dependent manner (Stahl *et al.*, 1998). The transfer efficiency of IncQ plasmids like pLS1 (carb^R) was significantly increased when the recipient

strain displayed a T4SS that probably served as a receptor structure for the donor (Bohne *et al.*, 1998). This assay permits to assess the requirement of VirB proteins for efficient plasmid transfer in the recipient or in the donor strain. It was demonstrated that other T4SS like the ComB system from *H. pylori* serve as natural competence systems and mediate DNA-uptake (Hofreuter *et al.*, 2001). The ComB system only consists of orthologs to a subset of the VirB proteins, similar to *A. tumefaciens*, in which expression of a subset of the *virB* operon in the recipient already enhanced IncQ plasmid uptake (Binns *et al.*, 1998; Liu and Binns, 2003). According to this, the requirements for the formation of a transfer-promoting receptor structure seem to be less stringent than for formation of a functional T4SS on the donor side, as not all VirB proteins are essential for a the T4SS receptor. Recipient strains devoid of VirB3, VirB4 or one the putative transmembrane channel components (VirB7-VirB10) are more severely attenuated than other VirB mutants. Expression of various *virB* operon subsets demonstrated that expression of *virB1-virB5* or *virB6-virB11* on the recipient side results in strains attenuated between 100- and 1000-fold. In contrast to that there is a stringent requirement for VirB2 through VirB11 on the donor side, and VirB1 mutants are strongly attenuated. Therefore, functional assembly of the *B. suis* T4SS was tested on the recipient side using an IncQ plasmid conjugation assay. Functional assembly of the *B. suis* T4SS in the *A. tumefaciens* membrane was tested after expression of the *B. suis virB* genes in the recipient strain.

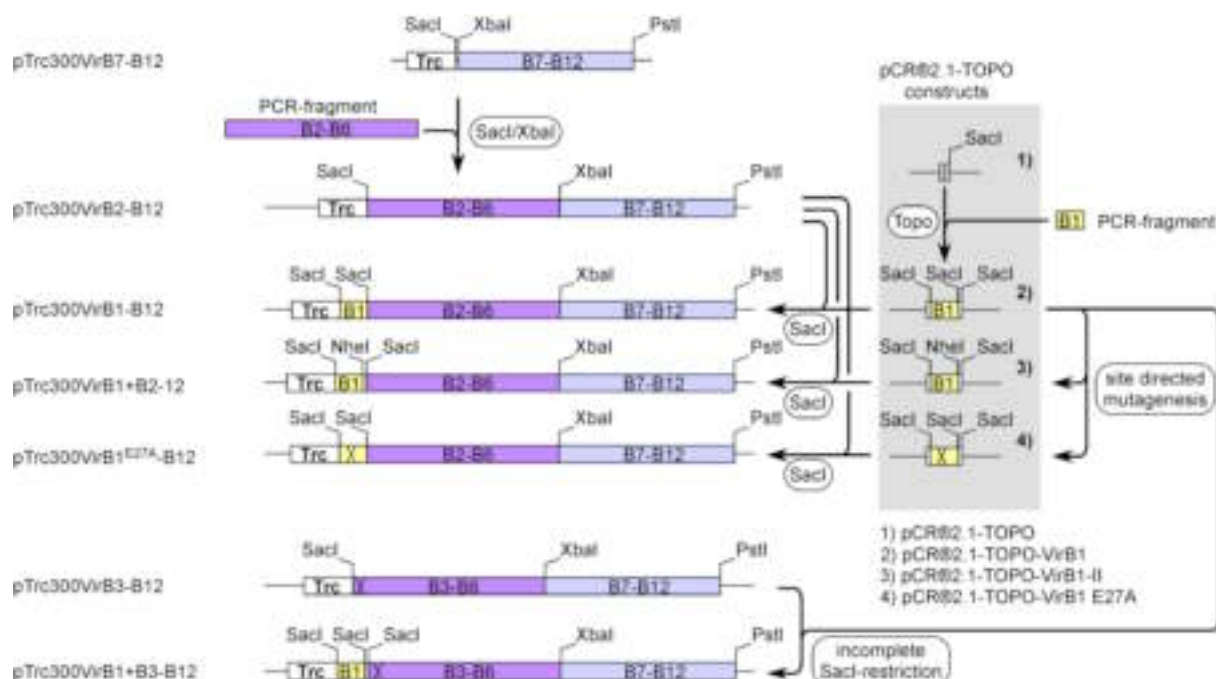


Fig. 15. Construction of the pTrc300VirBX-B12 vectors. The organization the *virB* operon in the created vector family is shown here. Different parts of the *virB* operon together with their restriction sites are shown in yellow (*virB1*), purple (*virB2-virB6*) and light blue (*virB7-virB12*). Arrows show the operations and the rounded boxes show the molecular biology techniques that were used to obtain the new constructs. All sites that feature a directed or spontaneous mutation are marked with an X. (Topo) refers to Topoisomerase-directed insertion of a Taq-generated PCR product into vector pCR@2.1-TOPO (Topo-Cloning, Invitrogen). pCR@2.1-TOPO-VirB1: *virB1* fragment with rbs inserted into the vector, pCR@2.1-TOPO-VirB1-II: pCR@2.1-TOPO-VirB1 with its *SacI* site was mutated to *NheI* by site directed mutagenesis, pCR@2.1-TOPO-VirB1 E27A: pCR@2.1-TOPO-VirB1 with the catalytic E27 changed to A by site directed mutagenesis.

Previous experiments indicated that pTrc300VirB2-B12 created by Q. Yuan could indeed raise the transfer efficiency in a conjugation assay when the vector was present in the recipient, and it was suspected that VirB1 could further improve this. In the course of the analysis of the role of VirB1 in the *B. suis* T4SS, several vectors encoding different subsets of the *virB* operon were created. The most promising experiment was to analyze properties of a vector that expressed *virB1* in addition to *virB2-virB12*, and this vector was constructed by insertion of a *virB1* fragment excised with *SacI* pCR@2.1-TOPO-VirB1 (Fig. 15, 2) into pTrc300VirB2-12. Routine sequencing of this vector yielded two unanticipated findings. First, the original vectors pTrc300VirB2-12 and pTrc300VirB2-6 were found to have a missense mutation in the start codon of the *virB2* gene, which had previously not been noticed although the *virB* operon sequence was determined. Tests for *virB2* expression in strains harbouring these vectors showed absence of the protein from cell lysates, but this had been explained previously with the low amount of VirB2 in the cells or a low sensitivity of the VirB2-specific antiserum. The vectors pTrc300VirB2-B12 and pTrc300VirB2-B6 were accordingly renamed to pTrc300VirB3-B6 and pTrc300VirB3-B12. Second, it was found that during the insertion of *virB1* into pTrc300VirB3-B12, a 56 bp fragment had been accidentally

inserted between *virB1* and the mutated *virB2* gene. The fragment derived from pCR®2.1-TOPO-VirB1 was inserted most likely due to an incomplete *SacI* excision of *virB1*. The resulting vector was hence named pTrc300VirB1+B3-B12. To assess whether production of VirB2 increased the efficiency of pLS1 transfer into the recipient UIA143 the vector pTrc300VirB2-12 was created by cleavage of the *virB2-B6* fragment from a new PCR amplification with *SacI/XbaI* and insertion into pTrc300VirB7-B12 linearized with the same two enzymes. Subsequently pTrc300VirB2-12 was cleaved with *SacI* and the *virB1* fragment excised from pCR®2.1-TOPO-VirB1 with *SacI* was inserted, creating pTrc300VirB1-B12 (Fig. 15). Initial tests demonstrated that UIA143 pTrc300VirB1+B3-B12 was a better recipient than UIA143 pTrc300VirB1-B12. To rule out that the difference between the transfer efficiencies was related to the “extra” 56 bp fragment inserted after *virB1*, another vector for expression of *virB1-12* including the extra 56 bp named pTrc300VirB1+B2-B12 was created. To this end, the *virB1* gene encoded on pCR®2.1-TOPO-VirB1 was subjected to site-directed mutagenesis. The aim was to change the *SacI* site of pCR®2.1-TOPO-VirB1 that was accidentally left uncleaved during the creation of pTrc300VirB1+B3-B12 into *NheI* (creating pCR®2.1-TOPO-VirB1-II; Fig. 15.3). This permitted controlled *SacI*-excision and insertion of *virB1*+56bp into pTrc300VirB2-B12 and hence creation of pTrc300VirB1+B2-B12 (Fig. 15). Similar, pCR®2.1-TOPO-VirB1 was subjected to site directed mutagenesis creating pCR®2.1-TOPO-VirB1^{E27A} (Fig. 15, 4), encoding *virB1* with a mutation of the catalytic E27. This fragment was subsequently excised from pCR®2.1-TOPO-VirB1^{E27A} with *SacI* and inserted into pTrc300VirB2-B12, creating pTrc300VirB1^{E27A}-B12 (Fig. 15). The newly created vectors were transferred into UIA143 and their ability to stimulate pLS1 transfer was tested and compared to that of the original vector pTrc300VirB3-B12 with the mutation in *virB2*.

1.5.1. Heterologous expression of different subsets of the *virB* operon

To reproduce the observation that pTrc300VirB3-12 causes an increased transfer efficiency in a conjugation assay, the experiment was repeated focussing on different subsets of the *virB* operon from *B. suis*. Moreover, it was interesting to learn whether this effect is also caused by the *tra* region of pKM101, which encodes a structurally related T4SS.

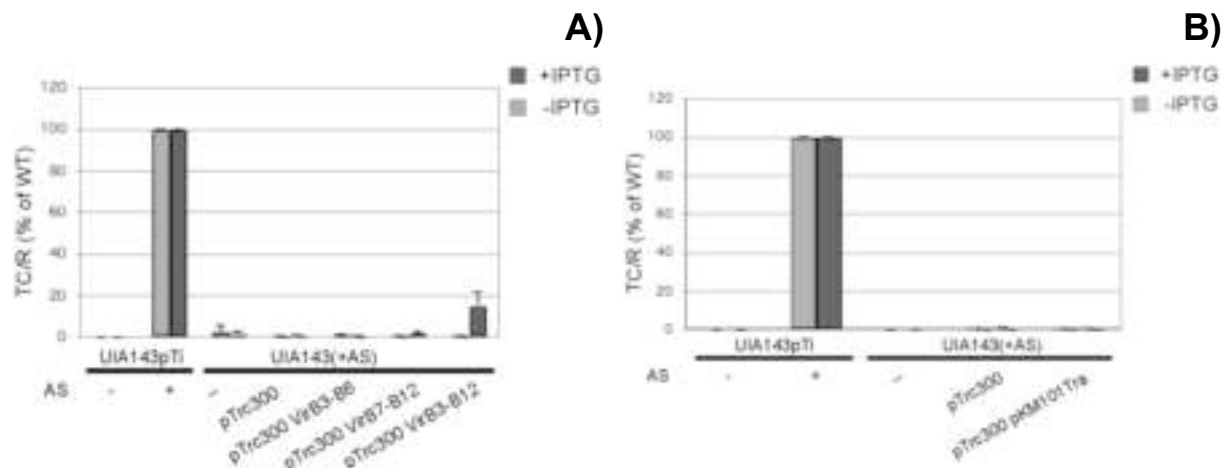


Fig. 16. Conjugation assay with recipient strains expressing subsets of either the *B. suis virB* operon (A) or the pKM101 *tra* operon (B). The indicated strains were used as recipients in conjugation assays to measure the efficiency of pLS1 transfer from donor strain A348 pLS1. The experiments were conducted either under virulence inducing (+AS) or non-inducing (-AS) conditions. To test the effect of heterologous gene expression in recipient cells, the experiments were carried out in the presence or absence of IPTG, which is required to induce expression of pTrc300-encoded genes. Standard deviation of three independent experiments is shown.

A. tumefaciens conjugation assays with a recipient (UIA143, ery^R) expressing subsets of the *B. suis virB* genes demonstrated that expression of the *virB3-virB12* genes led to a significant increase of pLS1 uptake, whereas expression of *virB3-virB6* or *virB7-virB12* did not elevate transfer efficiency as compared to the negative controls UIA143 and UIA143 pTrc300 (Fig. 16 A). Similarly, expression of the *tra* region from IncN-plasmid pKM101 did not impact pLS1 uptake efficiency (Fig. 16 B). After the confirmation of previous results with pTrc300VirB3-B12, the other strains expressing subsets of the *virB* operon were analyzed in conjugation assays.

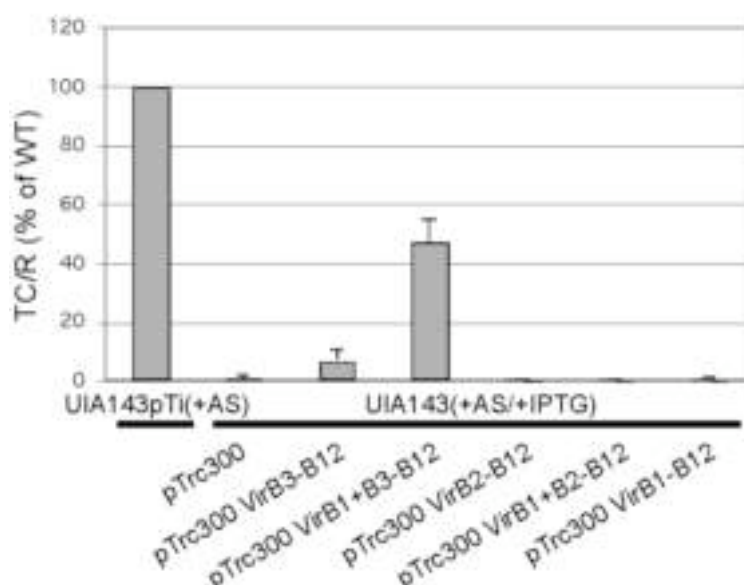


Fig. 17. Conjugation assay with recipients expressing the *virB* operon +/- the *virB1*- and/or *virB2* gene. The indicated *A. tumefaciens* strains were used as recipient in a conjugation assay measuring the efficiency of pLS1 transfer by donor strain A348 pLS1 under virulence-inducing (+AS) conditions and in the presence of IPTG. Transfer efficiency (transconjugand per recipient; TC/R) into induced UIA143pTi (WT) was set to 100 %. Standard deviation of three independent experiments is shown.

Transfer of pLS1 into the recipient strain bearing pTrc300VirB1+B3-B12 had the highest efficiency of almost 50% of the level of acetosyringone-induced *A. tumefaciens* wild type, whereas transfer into UIA143 pTrc300VirB3-B12 had 10% efficiency as compared to the wild type (Fig. 17). Transfer of pLS1 into recipients carrying pTrc300VirB1-B12 and pTrc300VirB2-B12 was not detected. To rule out that the difference between the transfer efficiencies into UIA143 carrying pTrc300VirB1+B3-B12 and pTrc300VirB1-B12 was related to the “extra” 56 bp fragment inserted after *virB1*, another vector for expression of *virB1-B12* including the “extra” 56 bp named pTrc300VirB1+B2-B12 was created as described (Fig. 15). However, pLS1 transfer into UIA143 pTrc300VirB1+B2-B12 was not detected showing that the presence of an intact *virB2* gene had a strong negative effect on the transfer (Fig. 17). To study the molecular basis for these surprising findings, we next studies VirB protein levels in UIA143 carrying the different constructs.

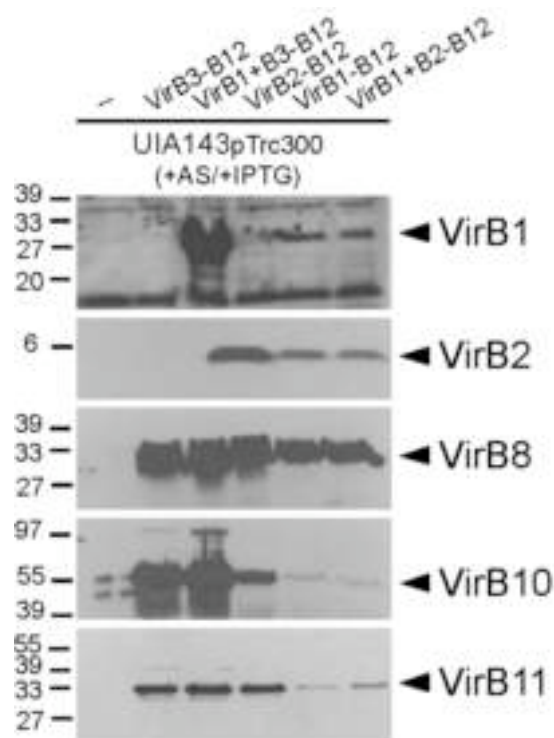


Fig. 18. VirB protein levels in pTrc300VirBX-B12-bearing strains. Production of virulence proteins in *A. tumefaciens* strain UIA143 harbouring pTrc300-constructs was monitored after culture of the indicated strains under virulence-inducing (+AS) conditions as described (Baron *et al.*, 1997). IPTG was added to induce gene expression from the *trc* promoter. Cell lysates were subjected to SDS-PAGE, followed by Western blot analysis with *B. suis* VirB-specific antisera. The experiments were performed twice with consistent results. The black arrowheads point to the VirB-specific signals and numbers on the left indicate reference proteins.

VirB-specific antisera were used to analyze the VirB protein levels of UIA143 cells harbouring pTrc300, pTrc300VirB3-B12, pTrc300VirB1+B3-B12, pTrc300VirB2-B12, pTrc300VirB1-B12 and pTrc300VirB1+B2-B12. These strains were cultivated for 16 h at 20°C (see Materials and Methods 6.2), harvested, lysed and the cell lysates were separated with polyacrylamide gels. Western blot analysis demonstrated that the cellular levels of many VirB proteins differed significantly between the different strains, depending on the organization of the *virB* operon (Fig. 18). The VirB1 levels in strains UIA143 pTrc300VirB1-B12 and UIA143 pTrc300VirB1+B2-B12 were drastically reduced as compared to UIA143 pTrc300VirB1+B3-B12. This observation was unanticipated since the sequences of pTrc300VirB1+B3-B12 and pTrc300VirB1+B2-B12 only differ by one nucleotide in the *virB2* start codon. Similar observations were made in case of other VirB-proteins. The VirB2 level in UIA143 pTrc300VirB2-B12 was higher than in UIA143 carrying pTrc300VirB1-B12 or in UIA143 pTrc300VirB1+B2-B12. The VirB8 and VirB10 levels in UIA143 expressing *virB3-virB12*, *virB1+B3-virB12* or *virB2-virB12* were higher than in UIA143 carrying pTrc300VirB1-B12 or UIA143 pTrc300VirB1+B2-B12. Thus, the expression of the *virB1* gene negatively impacted VirB2 protein levels and expression of *virB2* reduced the amount of detectable VirB1. Whereas the expression of *virB1* did not have an apparent impact on the steady state

level of other T4SS components, the simultaneous expression of *virB1* and *virB2* had a negative effect on the steady state levels of VirB8, VirB10 and VirB11. Finally, *virB2* alone exerted no negative influence on the steady state levels of other VirB-proteins, and only the level of VirB10 was slightly reduced in UIA143 carrying pTrc300VirB2-B12 as compared to UIA143 carrying pTrc300VirB3-B12. Since differences in the vector sequences are very minor, it is presently not clear what leads to the substantial differences in the accumulation of different VirB proteins.

Western blot analysis with VirB1-specific antiserum revealed another interesting detail. In addition to VirB1 (27 KDa) cell lysates from UIA143 pTrc300VirB1+B3-B12 featured another cross-reactive protein at 20 KDa. This putative cleavage or degradation product of VirB1 may also have been present in the other *virB1*-expressing strains but was not detected due to the lower level of VirB1 protein. VirB1 may therefore undergo cleavage similar to its ortholog from *A. tumefaciens*.

Taken together, These results suggest that VirB2 exerted a negative influence both on transfer efficiency, as determined by conjugation assays and, together with VirB1, on the levels of VirB proteins inside *A. tumefaciens* cells. Production of VirB1 in UIA143 pTrc300VirB1+B3-B12 apparently was an important factor for functional assembly of the heterologously expressed T4SS, as it strongly increased plasmid transfer into the recipient as compared to UIA143 pTrc300VirB3-B12

1.5.2. Heterologous expression of the *virB* operon encoding a VirB1 protein variant

Since it is known that introduction of a non-polar *virB1* deletion into the *A. tumefaciens virB* operon causes a drastic reduction of the incorporation of the major pilus-component VirB2 into T-pili, it is reasonable to assume that a likewise effect might be observed for the *B. suis virB* operon. In order to analyze the importance of VirB1 and of its active site for the incorporation of VirB2 and VirB5 into exocellular high molecular mass structures, a mutation was introduced into the *virB1* gene by site-directed mutagenesis, changing the putative catalytic E residue into A (VirB1^{E27A}). The levels of VirB proteins in cell lysates and in fractions of exocellular high molecular mass appendages were determined for strain UIA143 pTrc300, UIA143 pTrc300VirB2-B12, UIA143 pTrc300VirB1-B12 and UIA143 pTrc300VirB1^{E27A}-B12 after 24 h incubation under *virB*-inducing conditions. Exocellular high molecular weight structures were removed from the cell by shearing and ultracentrifugation as described previously and analyzed by SDS-PAGE and a subsequent Western blot (Schmidt-Eisenlohr *et al.*, 1999b).

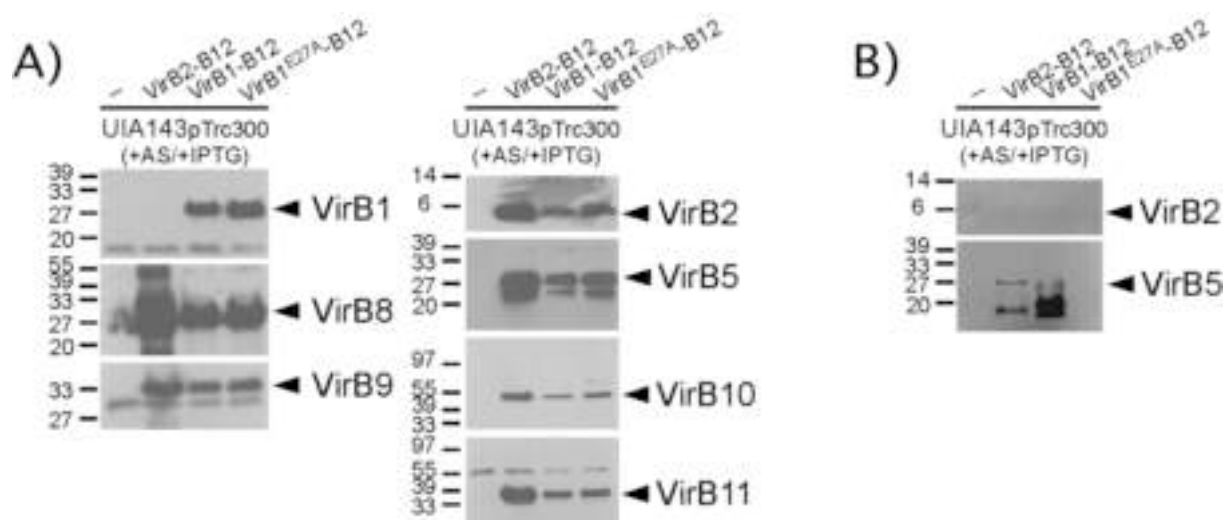


Fig. 19. Levels of VirB proteins in cells and exocellular high molecular weight structures from UIA143 carrying pTrc300VirB2-B12, pTrc300VirB1-B12 and pTrc300VirB1^{E27A}-B12. Production of VirB proteins was monitored after cultivation under virulence-inducing (+AS) conditions (Baron *et al.*, 1997) and IPTG was added to effect gene expression from the *trc* promoter. Cell lysates (A) and exocellular high MW appendages (B) were subjected to SDS-PAGE, followed by Western blotting with *B. suis* VirB-specific antisera. Experiments were performed twice with consistent results. The black arrowheads point to the VirB-specific signals and numbers on the left indicate reference proteins.

Whereas the levels of VirB proteins in cell lysates did not differ between strains expressing the full *virB* operons with or without the active-site mutation (VirB1 and VirB1^{E27A}), the level of some VirB proteins in cell lysates was significantly higher in UIA143 pTrc300VirB2-B12, (see also 1.5.1). No VirB protein was detected in lysates from the negative control strain UIA143 pTrc300 (Fig. 19 A). Western blot analysis confirmed that the amount of the putative minor pilus component VirB5 found in fractions of exocellular appendages was comparable between strains carrying either pTrc300VirB2-B12 or pTrc300VirB1-B12. Interestingly, no VirB5-specific signal was detected in the sample from strain UIA143 pTrc300VirB1^{E27A}-B12, indicating the absence of a *virB* gene-determined pilus-like structure (Fig. 19 B). This result suggests that the active site of VirB1 contributes to the functionality of the *B. suis* T4SS in *A. tumefaciens*. The putative major pilus component VirB2 was never detected in fractions of exocellular appendages, confirming the observations made in a more detailed analysis of this particular topic (Carle, 2004).

1.6. Genetic analysis of *A. tumefaciens* VirB1

1.6.1. Heterologous complementation of the *virB1* deletion mutant PC1001

VirB1 orthologs in T4SS share limited sequence similarity and were identified due to their conserved localization in the *virB*-like operons and their active site signatures. To test the hypothesis that these proteins are interchangeable between different T4SS, a selection of VirB1 orthologs was used (VirB1 from *A. tumefaciens* C58, VirB1s from *B. suis*, TraL from the IncN plasmid pKM101, the protein encoded by the F-plasmid *orf169* gene (F169) and HP0523 from *H. pylori*). A schematic representation of these proteins and their active site

signatures is shown in Fig. 6. The sequence identity to *A. tumefaciens* C58 VirB1 is 27% for *B. suis* VirB1s, 31% for TraL, 19% for *H. pylori* HP0523 and only 17% for the F169 protein. The genes were PCR-amplified with specific oligonucleotide primers (Table 4), the overhanging ends were cleaved with *NcoI/Scal* and cloned into similarly restricted broad host range expression vector pTrc200. In addition to these constructs, the regions in the genes encoding the conserved G residues from the active sites of *A. tumefaciens* VirB1, *B. suis* VirB1 and TraL were changed to A with the aim to distinguish between enzymatic functions and other tasks that VirB1 orthologs fulfill in T4SS. This required subcloning of the respective genes into pT7-7, since the site-directed mutagenesis system (Promega) requires presence of a β -lactamase resistance gene.

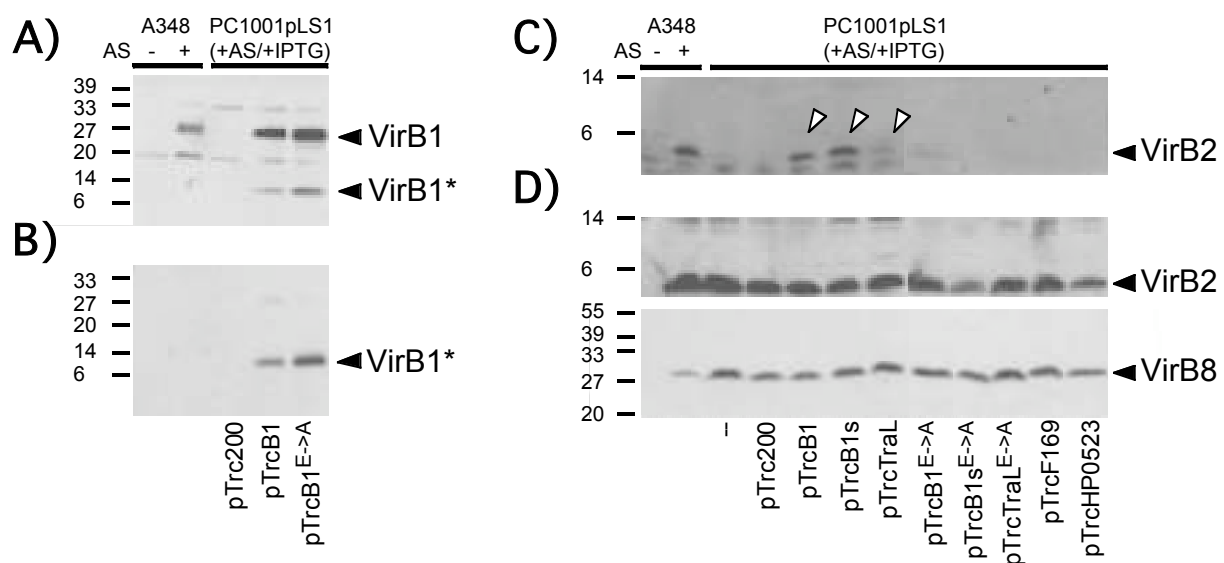


Fig. 20. Cleavage of the active site mutation and complementation of T-pilus formation by strain PC1001 expressing *virB1* orthologs. Processing of VirB1 (A) and secretion of VirB1* (B) was monitored by culturing the indicated strains under virulence inducing (+AS) or non-inducing (-AS) conditions as described (Baron *et al.*, 1997). IPTG was added to effect gene expression from the *trc* promoter. Cell lysates (A) and precipitated supernatant (B) were subjected to SDS-PAGE. Subsequently, a Western blotting and detection with C58 VirB1-specific antiserum was done. Exocellular high-molecular mass T-pilus fractions (C) and cell lysates (D) were separated by SDS-PAGE followed by Western blotting with VirB2 and VirB8-specific antisera. Experiments were performed three times, the arrows point to signals of VirB2 in exocellular fractions that were detected in at least two out of three experiments. Numbers on the left indicate reference proteins.

The plasmids were transformed into *A. tumefaciens* A348 *virB1* deletion strain PC1001, followed by growth under virulence gene-inducing conditions and analysis of VirB protein content in subcellular fractions (cell lysate, supernatant and pilus fraction). Whereas in the induced wildtype A348 the VirB1 cleavage product VirB1* was neither detected in the cell lysate nor in the supernatant fraction, it was clearly visible in PC1001 producing VirB1 and VirB1^{E→A} (Fig. 20 A, B). This can likely be explained by the specificity of the antisera for strain C58 VirB1. Processing of VirB1 and export of VirB1* into the extra-cellular space was not affected by the active site mutation since equal levels of full length VirB1 in cell lysates

(Fig. 20 A), and secreted VirB1* (Fig. 20 B) were detected in samples from PC1001 carrying either pTrcB1 or pTrcB1^{E→A}.

VirB1 is known to be required for pilus formation in A348 (Schmidt-Eisenlohr *et al.*, 1999b), which emphasizes its necessity for T4SS assembly. To test for complementation, the A348 WT and PC1001 carrying pTrc200 with or without VirB1 ortholog-encoding genes were grown on AB plates under virulence gene inducing conditions, followed by subcellular fractionation (cell lysate and pilus fraction) and analysis of VirB8 and VirB2 content with specific antisera.

Cellular VirB2 and VirB8 protein levels of the analyzed strains grown under virulence-inducing conditions were similar. The presence or absence of VirB1 did not affect the cellular accumulation of T-pilus component VirB2 or T4SS core component VirB8 (Fig. 20 D). Surface-exposed high molecular mass structures were removed from the cell by shearing and ultracentrifugation as described (Schmidt-Eisenlohr *et al.*, 1999b). No significant amounts of VirB2 could be detected in exocellular fractions of PC1001, but T-pilus formation was restored to near wildtype levels by introduction of pTrcB1 and pTrcB1s. A weak restoration of extracellular VirB2 levels was observed in PC1001 pTrcTraL only in two of three experiments, but pTrcF169 and pTrcHP0523 repeatedly failed to complement pilus formation. The active site variants of VirB1, VirB1s and TraL did not complement T-pilus formation, proving the requirement of the active site E residue (Fig. 20 C).

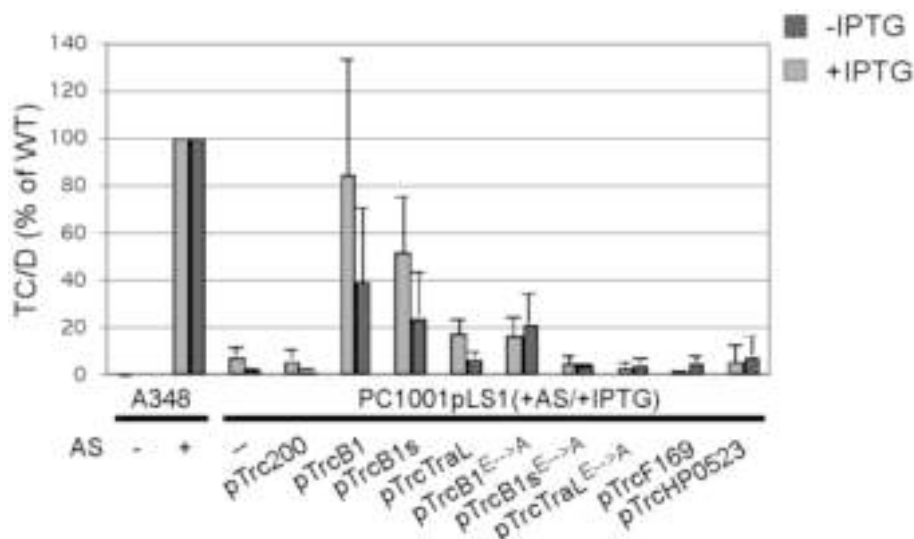


Fig. 21. Complementation of pLS1 donor activity of strain PC1001. The indicated strains were used in a conjugation assay to measure the efficiency of pLS1 transfer. The experiment was done either under virulence inducing (+AS) or non-inducing (-AS) conditions. Bars indicate transfer efficiency (in % of induced A348pLS1). To test the effect of VirB1 ortholog production the experiments were carried out in the presence (grey bars) or absence (dark grey bars) of IPTG. Standard deviation of three independent experiments is shown (black lines).

Since pilus isolation efficacy is inherently difficult to quantify and would probably not permit the detection of a very low degree of complementation, conjugation assays were conducted in order to analyze the transfer capabilities of pLS1-carrying strains. IncQ plasmid pLS1 can be transferred to recipient *A. tumefaciens* cells in a VirB-dependent manner, relying on the recognition of relaxosome complexes by the *A. tumefaciens* T4SS (Stahl *et al.*, 1998). Since this plasmid confers carbenicillin-resistance, the transfer efficiency can be easily quantified. Plasmid pLS1 was introduced in A348 and PC1001 harbouring pTrc200 with or without genes encoding *virB1* orthologous proteins. After incubation of these strains with UIA143 pTiA6, the transfer efficiency was quantified by assessing the number of output donor (D) and transconjugants (TC) on selective media. As expected from previous observations (Bohne *et al.*, 1998), the transfer efficiency of PC1001 was only 10% of the WT value. The introduction of pTrcB1 almost completely restored transfer, pTrcB1s bearing donor obtained transfer efficiency of 50% and a small increase could also be assigned to the presence of pTrcTraL. Interestingly, pTrcB1^{E→A} also conferred the ability to modestly raise the transfer efficiency of PC1001 to almost 20% of the WT. The other donor strains were unable to transfer pLS1 to recipient cells (Fig. 21).

When the experiment was conducted without addition of IPTG to the conjugation assay, similar but reduced effects of the different constructs were observed, showing that the *trc* promoter determined a significant level of expression even under non-inducing conditions (Fig. 21). This observation was confirmed by Western blot analysis of *trc*-controlled proteins, showing that low levels were produced even in the absence of IPTG (not shown).

An additional set of experiments was carried by Dr. A. Binns and Dr. Z. Liu from the University of Pennsylvania (Philadelphia, USA) in the context of this collaborative work. The effects of VirB1-orthologs on the complementation of tumor formation by *A. tumefaciens* PC1001 on *N. tabacum* leaf discs and transfer efficiency upon expression of *virB1* genes on the recipient side of conjugation experiments yielded results, which were consistent with our findings and therefore supported the findings presented here (Höppner *et al.*, 2004). VirB1 orthologs that have a C-terminal NORS region like VirB1s and TraL are therefore able to complement VirB1, whereas “short” VirB1 orthologs like HP0523 and F169 are unable to do so. The fact that VirB1^{E→A} has residual complementing ability suggests two different contributions of VirB1 to virulence.

1.6.2. Mutational analysis of the VirB1 processing-site

The importance of the C-terminal domain-like region of VirB1 for its biological activity has been stressed before (Llosa *et al.*, 1998; Baron *et al.*, 1998). However, it is still unknown what importance correct and efficient cleavage of VirB1 and subsequent secretion of VirB1* has for the T4SS.

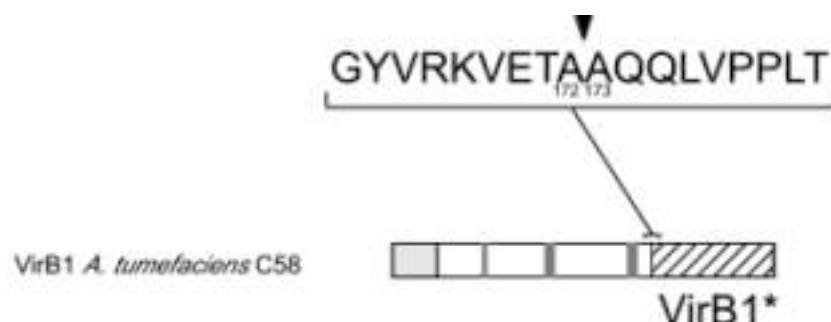


Fig. 22. The VirB1 cleavage site sequence. The following AA-substitutions and deletions surrounding the cleavage site (arrow) of VirB1* were created by site-directed mutagenesis 1: VirB1 Δ AA172 2: VirB1 A172D 3: VirB1 Q174E 4: VirB1 Q175E 5: VirB1Q174E/Q175E 6: VirB1 A173P 7: VirB1 E170P/T171W

To shed light on this particular question, directed mutations were introduced in the region encoding the vicinity of the *A. tumefaciens* C58 VirB1 cleavage site (Fig. 22). By introduction of amino acid substitutions and deletions (deletion of A172 and A173; substitution of A172 with D; substitution of Q174, Q175 or both residues with E; substitution of A173 with P; substitution of E170 with P and T171 with W) it was attempted to affect cleavage of VirB1. In order to do that, the *virB1* gene from pTrcB1 was subcloned into pT7-7 and a site-directed mutagenesis system (Promega) was used according to manufacturer's protocol, utilizing the site-directed mutagenesis primers listed in Table 5. After confirmation of the correct sequence, mutagenized *virB1* fragments were re-inserted into pTrc200 with *Nco*I/*Sal*I and the vector-based production and processing of VirB1 and the secretion of VirB1* in *A. tumefaciens* strain PC1001 was analyzed by cultivation of the cells under virulence gene-inducing conditions and subsequent analysis of VirB protein content in subcellular fractions (cell lysate, supernatant and pilus fraction).

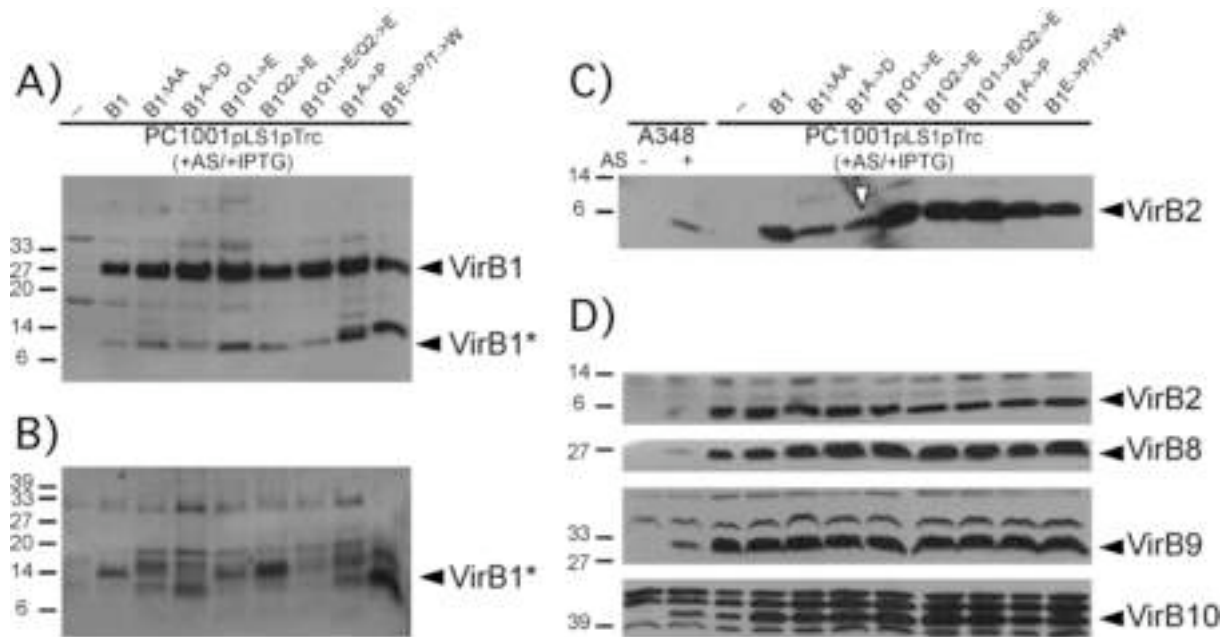


Fig. 23. Effects of cleavage site alterations on VirB1 processing, VirB1* export and assembly of the pilus. The production and processing of VirB1 and secretion of VirB1* were monitored by cultivation of the indicated strains under virulence-inducing conditions in the presence of IPTG. Cell lysates (A) and precipitated supernatant (B) were subjected to SDS-PAGE. Subsequently Western blotting with C58 VirB1-specific antiserum was performed. Exocellular high-molecular mass T-pilus fractions (C) and cell lysates (D) were separated by SDS-PAGE followed by Western blotting with VirB2-, VirB8-, VirB9- and VirB10-specific antisera. The white arrowhead points to the signal of VirB2 in the exocellular fraction of PC1001pTrcB1^{A→D}. Numbers on the left indicate reference proteins. Experiments were repeated five times with consistent results.

Some of the *virB1*-mutants were affected in VirB1 processing and VirB1* secretion. Although the cellular levels of VirB1 did not notably differ between all the analysed strains, changes affecting the amount and MW of VirB1* in cell lysates (Fig. 23 A) and culture supernatants (Fig. 23 B) were observed. While the VirB1 proteins carrying mutations of Q174 or Q175 (Fig. 23 A, B; lane 3,4) were processed similar to the WT, the changes affecting the A172 or A173 (Fig. 23 A, B; lane 1,2,6) had different phenotypes. Processing products of VirB1^{ΔAA} and VirB1^{A→D} were detectable in the cell lysate, though the latter only at a reduced level. More strikingly, there was no signal indicating the presence of VirB1* of WT MW in culture supernatants of PC1001 producing these two variants. Instead, the molecular masses of signals indicate the generation of one or more aberrant VirB1 processing products. VirB1^{A→P} was not processed to a product different from VirB1*, and high amounts of it were detected in the cell lysate (Fig. 23 A; lane 6), while aberrant signals were detected in culture supernatants (Fig. 23 B; lane 6). The absence of VirB1* from cell supernatants was also observed in PC1001 producing VirB1^{Q1→E/Q2→E} although its cellular level was normal. VirB1^{E→P/T→W} was processed to yield aberrantly sized VirB1*, and relatively large amounts of this cleavage product were detected in the supernatant (Fig. 23 A, B; lane 7).

Exocellular high MW T-pilus fractions were isolated to analyze effects of the VirB1 protein variants on T-pilus formation. While cellular accumulation of T4SS components VirB2 and VirB8 was equal in PC1001 producing either VirB1 or VirB1 variants (Fig. 23 D), the level of VirB2 in the pilus fractions from strain PC1001 pTrcB1^{ΔAA} and PC1001 pTrcB1^{A→D} was notably reduced (Fig. 23 C).

It is apparent that some of the amino acid substitutions inserted into the vicinity of the VirB1 cleavage site had effects on the processing of VirB1, and a modest effect on T-pilus formation was observed in two cases. This leads to the question if aberrant cleavage of VirB1 is associated with a reduction of T4SS function. To assess whether non-wildtype-like processing and secretion of VirB1 has an effect on the plasmid donor efficiency, conjugation assays were performed. After incubation of PC1001 pLS1 (carb^R) expressing *virB1* and its mutants with the recipient strain UIA143 pTiA6 (ery^R), the transfer efficiency was quantified on selective media.

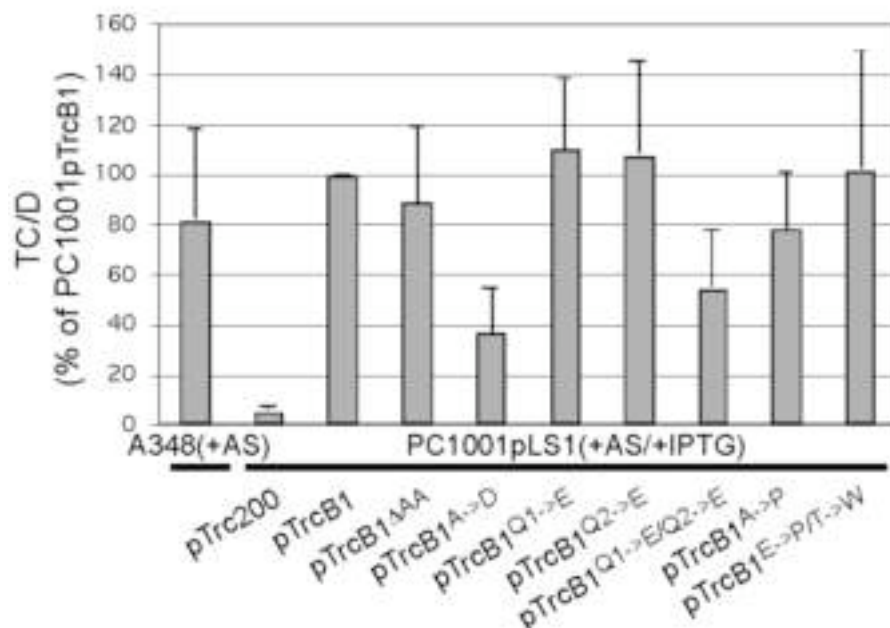


Fig. 24. Complementation of pLS1 donor activity of strain PC1001 with cleavage site variants of VirB1. The indicated strains carrying pTrc200 expressing *virB1* active site variant constructs were used in a conjugation assay to measure the efficiency of pLS1 transfer. The experiment was conducted under virulence inducing (+AS) conditions and in the presence of IPTG. Grey bars indicate transfer efficiency (in % of PC1001 pTrcB1) and the standard deviation of four independent experiments is shown for each value (black lines).

The pLS1 transfer efficiency of strains PC1001 pTrcB1^{A→D} and PC1001 pTrcB1^{Q1→E/Q2→E} moderately differed from the WT (Fig. 24). Dr. A. Binns and G. Nair from the University of Pennsylvania (Philadelphia, USA) performed a different functional assay of these two strains, determining tumor formation on *N. tabacum* leaf discs. The reduced efficiency of PC1001pTrcB1^{A→D} was confirmed, but PC1001pTrcB1^{Q1→E/Q2→E} was indistinguishable from

the WT. To reveal possible differences in the production, processing and accumulation of VirB1* in cell lysates, time-course studies were conducted next.

After 6-8 hours of pre-incubation in AB medium, virulence protein production in the strains A348, PC1001 pTrc200, PC1001 pTrcB1 and PC1001 pTrcB1^{A->D} was induced with AS and IPTG. Samples were taken at 1, 3, 5 and 20 h in order to observe the production and processing of VirB1 in cell lysates by Western blot analysis.

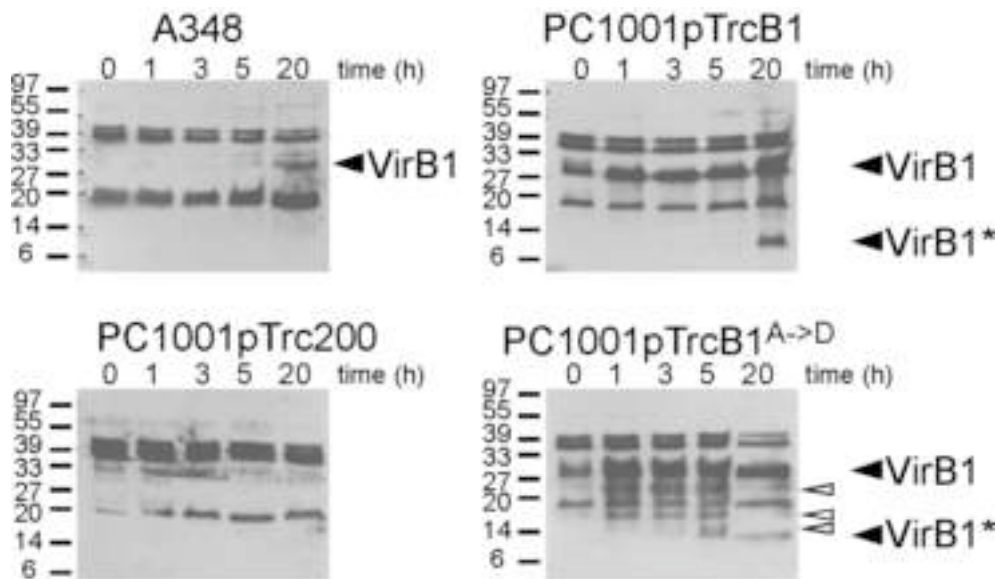


Fig. 25. Time course of VirB1 production and processing in *A. tumefaciens* strains under virulence-inducing conditions. White arrowheads point to VirB1-specific signals that only appear in the Western blot with samples from PC1001pTrcVirB1^{A->D}. Black arrowheads point to signals of VirB1 and VirB1*. Numbers on the left indicate reference proteins.

In A348 only weak signals of its native VirB1 and no VirB1* were detected after 20 h of induction. This is likely due to the VirB1-specific antiserum used in these studies, which had been raised against VirB1 of *A. tumefaciens* C58 (Höppner *et al.*, 2004). As expected, the Western blot with samples from PC1001 pTrc200 was devoid of inducible VirB1-specific signals. Strong VirB1-specific signals were detected in PC1001 expressing *virB1* or *virB1*^{A->D} before induction with IPTG and the protein levels increased after addition of IPTG. Analysis of the lower molecular mass processing products showed that in contrast to PC1001 pTrcB1 additional VirB1-specific signals were detected after induction of strain PC1001 pTrcB1^{A->D}. These signals appeared 1 h post-induction and their number and intensity increased, and a ladder of decreasing molecular masses was apparent. After 20 h, however, the VirB1-specific signals in cell lysates of PC1001 pTrcB1^{A->D} were almost indistinguishable from those in PC1001 pTrc200VirB1 (Fig. 25).

Taken together, mutants of the VirB1 cleavage site were created and cellular processing of the mutant proteins differed from the WT-protein in some cases. The cleavage site variation of VirB1^{A→D} obviously affected the kinetics and specificity of VirB1 processing and it was secreted with reduced efficiency, but a VirB1*-like product was still formed in PC1001 pTrcB1^{A→D}.

1.6.3. Effect of the heterologous production of an HP0523-VirB1*-hybrid in PC1001.

Heterologous complementation of a *virB1* mutant either with different VirB1 orthologs or mutant VirB1 protein showed that the VirB1 C-terminus fulfills an important though not essential function for the *A. tumefaciens* T4SS. Some VirB1-orthologs such as F169 and HP0523 could not complement the lack of VirB1. This might be an effect of a missing C-terminal appendage (NORS region), since all orthologs that functionally complemented the *virB1* defect possessed this characteristic region. The following experiment was conducted with the aim to obtain direct evidence for the role of HP0523 as a lytic transglycosylase and to shed light on the importance of the VirB1 C-terminus. A number of hybrid proteins consisting of parts of HP0523 and VirB1 were created and tested for processing and their ability to complement pLS1 transfer and pilus formation in PC1001.

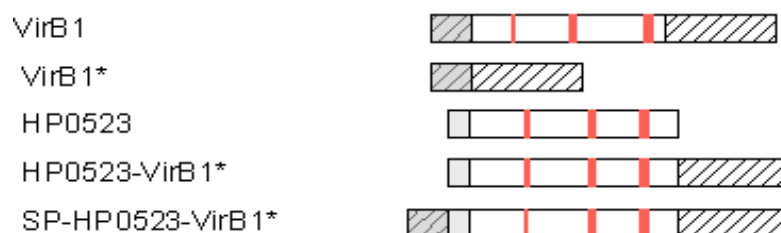


Fig. 26. Domain organization of hybrid VirB1 protein used for complementation of PC1001. The predicted signal peptide of *A. tumefaciens* VirB1 is in hatched grey, of that of HP0523 in grey. The active site signature sequences of the two orthologous SLT domains (Bayer *et al.*, 1995) are highlighted in red. The hatched box indicates VirB1*. Genes encoding all these protein variants were inserted into pTrc200.

pTrc200 constructs expressing genes for VirB1, VirB1* and HP0523 were already available from previous studies, and vectors producing hybrid proteins HP0523-VirB1* and SP-HP0523-VirB1* were created next. To this end, *hp0523* and *virB1** fragments were produced by PCR amplification from *H. pylori* genomic DNA and pGK217 (Material and Methods, 2) using specific primers (Tab. 4). The ends of the *hp0523* fragment were cleaved with *EcoRI* and *NcoI*, of those of *virB1** with *NcoI* and *Acc65I*. The processed fragments were mixed in a ratio 1:1 and added in excess to pTrc200 cleaved with *EcoRI* and *Acc65I* and then ligated to create pTrcHP0523-B1*. As the predicted signal peptide of HP0523 did not correspond to the consensus sequence, it was a possibility that the *A. tumefaciens*

protein export machinery may not recognize it. To ensure proper subcellular localization of the hybrid protein, a vector for production of the HP0523-B1* fusion protein with the VirB1 SP was created next. pTrcHP0523-B1* was used to create pTrcSP-HP0523-B1* by insertion of the fragment encoding the *virB1* signal peptide (annealed oligos SPVirB1-5' and SPVirB1-3', Tab. 4) into the *EcoRI* site. Vectors producing the VirB1 constructs listed in Fig. 26 were transformed into *A. tumefaciens* A348 *virB1* deletion strain PC1001, followed by growth under virulence gene-inducing conditions and analysis of VirB protein content in subcellular fractions (cell lysate and pilus fraction).

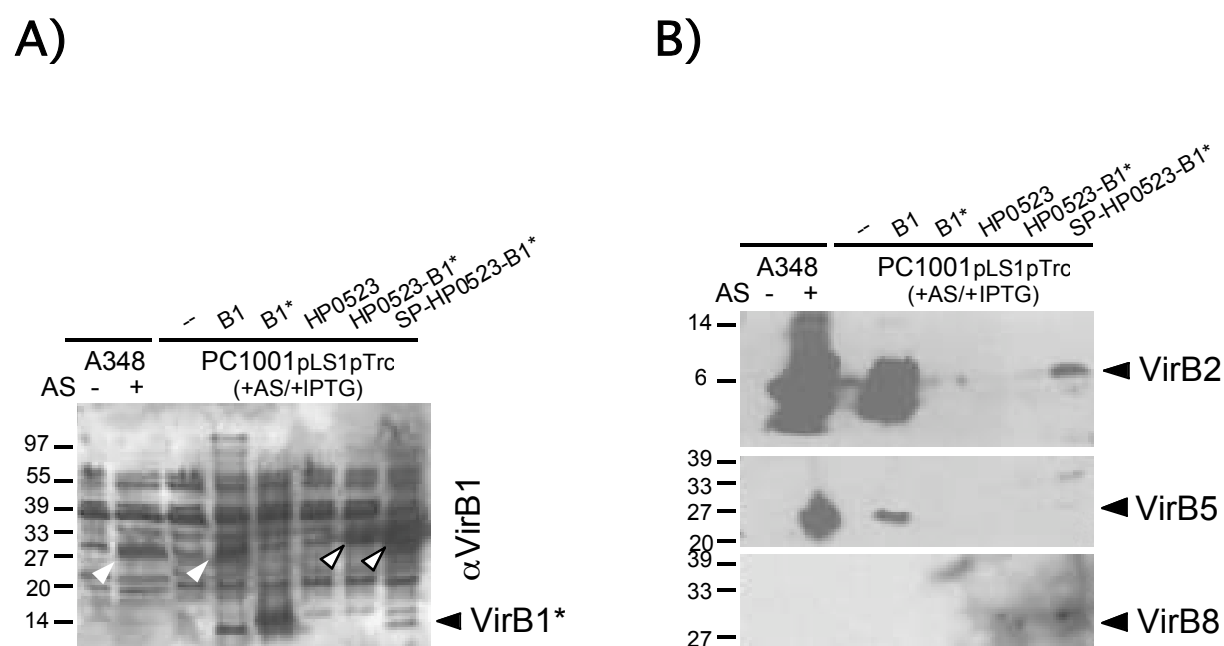


Fig. 27. Production and processing of HP0523-VirB1*-hybrid protein with and without the VirB1 signal peptide and the effect on pilus production. Processing of VirB1 or HP0523-VirB1*-hybrid protein and secretion of VirB1* was monitored by culture of the indicated strains under virulence inducing (+AS) or non-inducing (-AS) conditions as described (Baron *et al.*, 1997). IPTG was added to effect gene expression from the *trc* promoter. Cell lysates were subjected to SDS-PAGE and Western blotting, followed by detection with VirB1-specific antiserum (A). White arrowheads point to the VirB1-specific signal, framed white arrowheads point to signals of the HP0523-VirB1 hybrid protein, black arrowhead indicates VirB1*. To analyse the complementation of T-pilus formation, the WT strain A348 and PC1001 ($\Delta virB1$) carrying the indicated constructs were cultured under virulence-inducing or non-inducing conditions with IPTG. Exocellular high-molecular mass T-pilus fractions (B) were separated by SDS-PAGE followed by Western blotting with VirB2-, VirB5- and VirB8-specific antisera. Experiments were performed twice and gave consistent results. The arrowheads point to signals of VirB2, VirB5 and VirB8 detected in exocellular fractions. Numbers on the left indicate reference proteins.

VirB1 and VirB1* were heterologously produced in PC1001 and processing of the proteins yielded VirB1*, which was detected in a Western blot with VirB1-specific antiserum. No signal was detected in the lane with a sample from strain PC1001 producing HP0523, and a specific antiserum was not available. A signal at the expected MW of 27 kDa was detected in the lane with samples from PC1001 producing HP0523-VirB1* and was even

stronger when SP-HP0523-VirB1* was produced. The signals were probably due to the recognition of the VirB1* C-terminus by the *A. tumefaciens* VirB1-specific antiserum. Interestingly, no processing of the hybrid-protein without the VirB1 signal peptide was observed, but a low amount of VirB1* was detected in cells producing SP-HP0523-VirB1*. This indicates that VirB1* is produced in dependence of a functional signal peptide (Fig. 27 A).

Surface-exposed high molecular mass structures were isolated from the cell by shearing and subsequent ultracentrifugation as described (Schmidt-Eisenlohr *et al.*, 1999b). No significant amounts of VirB2 pilin were detected in exocellular fractions of PC1001 but T-pilus formation was restored to near-wildtype levels by the introduction of pTrcB1. pTrcB1*, pTrcHP0523 and pTrcHP0523-B1* failed to complement pilus formation. However, heterologous production of the hybrid protein SP-HP0523-VirB1* resulted in partial complementation of T-pilus formation as monitored by the detection of VirB2 in exocellular high molecular mass fractions. The minor pilus component VirB5 was only detected in samples from induced A348 WT, PC1001 expressing *virB1* and PC1001 pTrcSP-HP0523-B1* (Fig. 27 B). These results lead to the conclusion that HP0523 can functionally substitute for the SLT domain of VirB1, but the observation that trace amounts of VirB8 were repeatedly detected in the exocellular high MW fractions from PC1001 pTrcSP-HP0523-B1* contests this notion. Since VirB8 was only detected in exocellular high molecular mass fractions from this strain, the effect may be due to a toxic effect of the *H. pylori* VirB1 ortholog on PC1001, which led to limited cell lysis.

To quantify the complementation of plasmids producing HP0523 fusions, conjugation assays with donor strain PC1001 pLS1 (carb^R) carrying the constructs pTrc200, pTrcB1, pTrcB1*, pTrcHP0523, pTrcHP0523-B1* and pTrcSP-HP0523-B1* and the recipient strain UIA143pTiA6 (ery^R) were performed as described in 1.5 and 1.6.1.

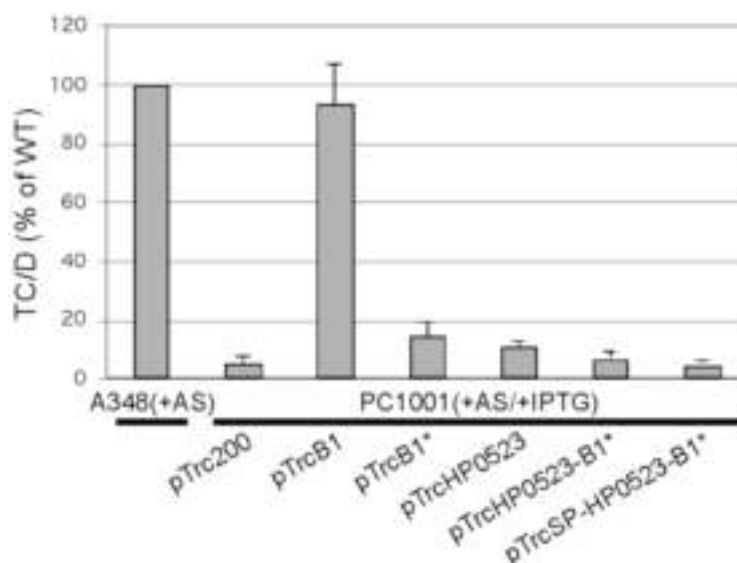


Fig. 28. Complementation of pLS1 donor activity of strain PC1001 expressing different parts of *virB1* and *hp0523*. The indicated strains carrying pTrc200 and *virB1*-*hp0523*-hybrid constructs were used in conjugation assays to measure the efficiency of pLS1 transfer. Bars indicate transfer efficiency (in % of induced A348pLS1). The experiment was done under virulence-inducing (+AS) conditions and in the presence of IPTG. Standard deviation of three independent experiments is shown.

Expression of *virB1* in PC1001 restored pLS1 transfer efficiency to WT-level. In contrast, neither production of VirB1* nor that of any of the HP0523-hybrid proteins led to an increase of pLS1 transfer beyond background levels (Fig. 28). This result is in contrast to observations from the analysis of T-pilus formation, where the hybrid protein SP-HP0523-VirB1* partially complemented pilus formation. Production of SP-HP0523-B1* in PC1001 led to detection of VirB2 protein in the exocellular fraction but complementation of IncQ transfer was not observed. Moreover, PC1001 pTrcSP-HP0523-VirB1* was unable to incite tumor formation on leaves of *K. daigremontiana* (not shown). The complementation of pLS1 transfer by SP-HP0523-VirB1* may be too low to be detected in the conjugation assay. Alternatively, the production of the hybrid protein may complement certain functions of VirB1, creating a phenotype where pilus biogenesis and T-DNA/IncQ transfer ability are uncoupled.

2. *In silico*, *in vitro* and *in vivo* analysis of T4SS traffic-(d)NTPase orthologs

Orthologs of the traffic-(d)NTPase VirB11 are essential components of T4SS in a number of different proteobacteria. They not only are an interesting subject for functional studies but also potential targets for anti-infective drugs, that might affect cessation of (d)NTP hydrolysis. We tried to assess general properties of some VirB11 orthologs with *in silico*, *in vitro* and *in vivo* methods. This task was supported by the use of a compound with a specific inhibitory effect on HP0525, the VirB11 ortholog from *H. pylori*. While an *in silico* analysis helps to discover conserved features of this enzyme family, *in vitro* assays were necessary to determine enzyme properties and the effect of inhibitors. Finally, *in vivo* assays were conducted in order to analyze whether inhibition of VirB11 is reflected by a decreased efficiency of T4SS functions.

2.1. Sequence conservation among the studied VirB11 orthologs

The VirB11 ATPases are a subclass of the VirB11-PuIE family of (d)NTPases, which are required for the functionality of T4SS and T2SS. These (d)NTPases are indispensable for substrate secretion and assembly of the secretion system, and several amino acids are conserved, most of them involved in enzymatic activity. To further dissect common features of some representative members of this protein family, the full-length sequence of protein TrwD from IncW-plasmid pR388, TraG from IncN-plasmid pKM101, VirB11 of *A. tumefaciens*, VirB11 of *B. suis* and HP0525 from *H. pylori*, were subjected to a multiple sequence alignment using the ClustalW server.



Fig. 29. Sequence conservation of the VirB11 orthologs. A sequence alignment of *B. suis* VirB11, pKM101 TraG, pR388 TrwD, VirB11 from *A. tumefaciens* C58 and *H. pylori* HP0525 was calculated with the ClustalW-algorithm. Labels as follows: (*) identical AA in all five sequences, (:) marks a high and (.) a lower degree of AA conservation at the respective aligned position. Protein names are given on the left side, last AA-position in the respective line on the right side. Red boxes indicate all AAs involved in the active site pocket and catalytic activity in HP0525 (Savvides *et al.*, 2003); shaded box indicates the linker region between the N- and C-terminus; A: Walker A nucleotide binding motif.

The analysis aligns amino acid residues that are implied in the catalytic activity like the Walker A box and the two conserved E residues at HP0525 position 209 and 248 (Savvides *et al.*, 2003). Other amino acids throughout the sequence are also highly conserved (Fig. 29). The amino acid sequence identities for pairs of VirB11 orthologs were as follows: HP0525/VirB11suis: 30%; HP0525/VirB11Agro: 22%; HP0525/TraG: 16%; HP0525/TrwD: 24%; VirB11suis/VirB11Agro: 33%; VirB11Agro/TraG: 37%; VirB11Agro/TraG: 30%; TrwD/TraG: 38%. As structural data are available for the ADP-bound form of HP0525 it was possible to display the information from the VirB11 sequence alignment as a conservation map on the surface structure of HP0525. The results from the ClustalW-alignment (Fig. 29) were processed and submitted to the AMAS-server to further validate the degrees of amino acid conservation. These data were displayed on the surface of the HP0525 structure (see also Results, 1.1).

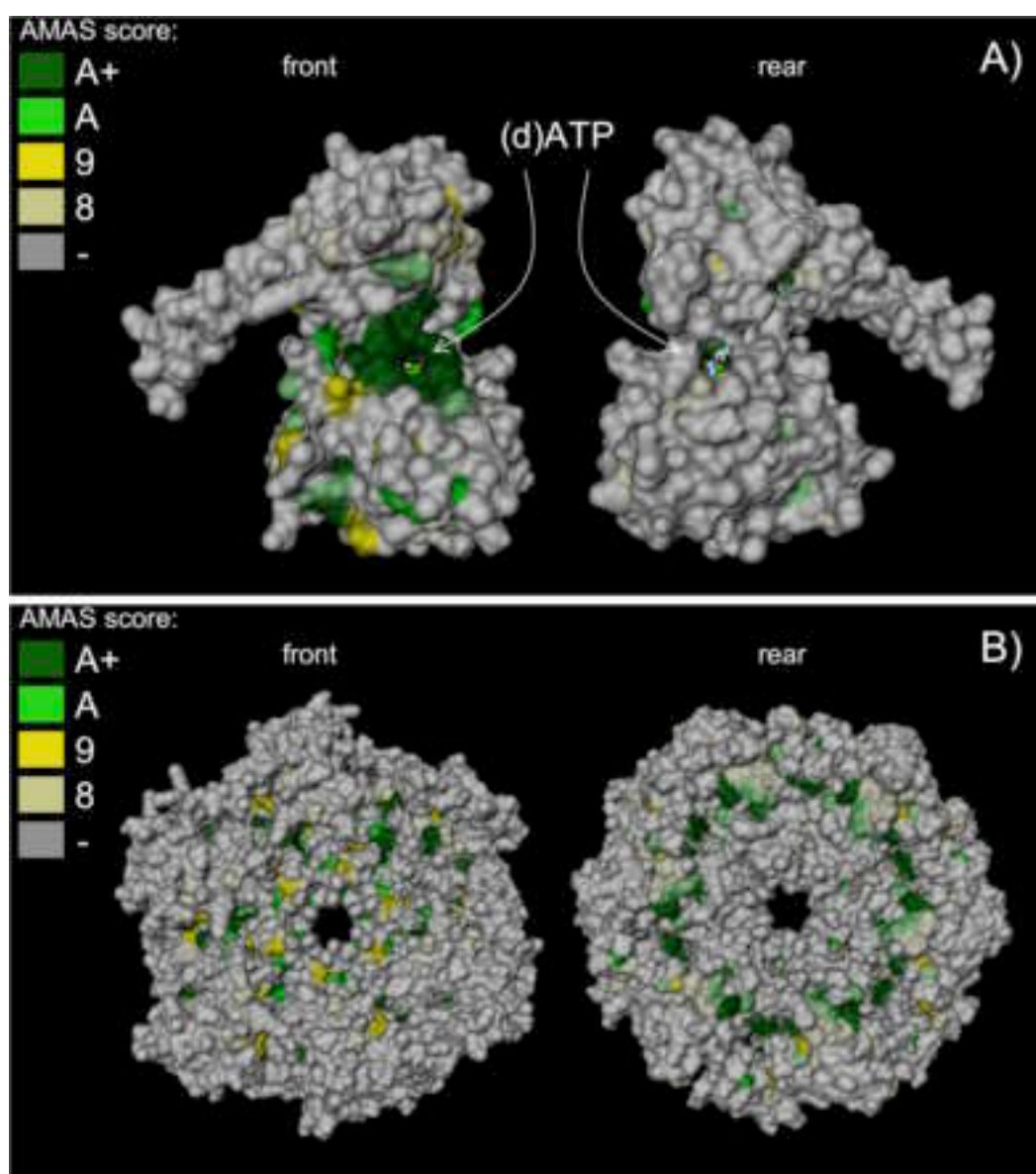


Fig. 30. Structural conservation among VirB11 orthologs displayed on the surface of HP0525. Predicted surface of the monomer (A) and, in a different orientation, the holoenzyme (B) of HP0525. In (A) the NTD is on top, the larger CTD on the bottom of the panel. In the “front” image of the holoenzyme NTDs are facing the observer, in the “rear” image the CTDs. Identical residues in all five proteins are marked in dark green (A+), high similarity in green (A) and lower similarities are in yellow (9) and light yellow (8). The figure was prepared with DINO (cobra.mih.unibas.ch/dino).

Many of the conserved amino acid residues in the N-terminal domains (NTD) and C-terminal domain (CTD) of HP0525 are not exposed to the surface, implying a highly conserved tertiary structure fold. Surface-exposed conserved amino acids are of special interest in the context of this work, as they may be binding sites for inhibitors. The surface area with the largest coherent area of identical AA-residues in all five proteins was formed by amino acids of the active site pocket and in close vicinity to the (d)NTPs γ -phosphate (Fig. 30 A, front). The residues located close to the nucleotide purine/pyrimidine were not conserved, which may be explained by different substrate preferences (Fig. 30 A, rear). The region of

highly conserved AA-residues in the active site was not visible in images of the hexameric protein, because it is located in a solvent-accessible position buried inside the hexameric structure of VirB11 (Fig. 30 B). Apart from this region, the surfaces of the studied VirB11 orthologs did not exhibit further conserved patches. The hexameric holoprotein could be viewed either from the putative periplasmatic side (Fig. 30 B, front), showing conservation of the NTD, or from the opposite side (Fig. 30 B, rear) displaying the CTD part of the HP0525 hexamer, which is supposedly inserted into the inner membrane (Yeo and Waksman, 2004).

2.2. Purification and characterization of VirB11 orthologs from different T4SS

2.2.1. Purification of VirB11 orthologs

After analysis of the structure of HP0525 (Yeo *et al.*, 2000), a purification strategy for the VirB11 orthologs was developed. The N-terminus of the HP0525 monomer was not in close contact with parts of the protein that are involved in hexamer formation or catalytic activity. Based on this observation, N-terminal modifications should not affect protein structure and function, and a number of N-terminal StrepII-fusions of VirB11 orthologs were generated accordingly.

Plasmids for recombinant over-expression of VirB11 orthologs were created by PCR amplification of DNA fragments using templates pUC18VirB (*B. suis virB11*), *H. pylori* genomic DNA, pR388 (*trwD*), pKM101 (*traG*) and pGK217 (*A. tumefaciens virB11*). Specific primers are listed in Table 4. Ends of the fragments were treated with restriction endonucleases (specified in Table 3) and inserted into similarly treated vector pT7-StrepII or pT7-H₆TrxFus. The vectors were transformed into *E. coli* GJ1158 cells and protein production was performed as described (Materials and Methods, 6.1 and Table 7). After recombinant expression of the *virB11* genes, the cleared cell lysates were subjected to Strep-Tactin® Sepharose® affinity purification. The eluates from this step were applied to a protein solution concentration device with 30 kDa molecular mass cutoff, to remove low molecular mass cellular proteins, and they were then loaded onto a Superdex 200 gel filtration column to isolate the enzymatically active hexameric proteins. The fractions were subsequently concentrated and dialysed in PSB for long-term storage.

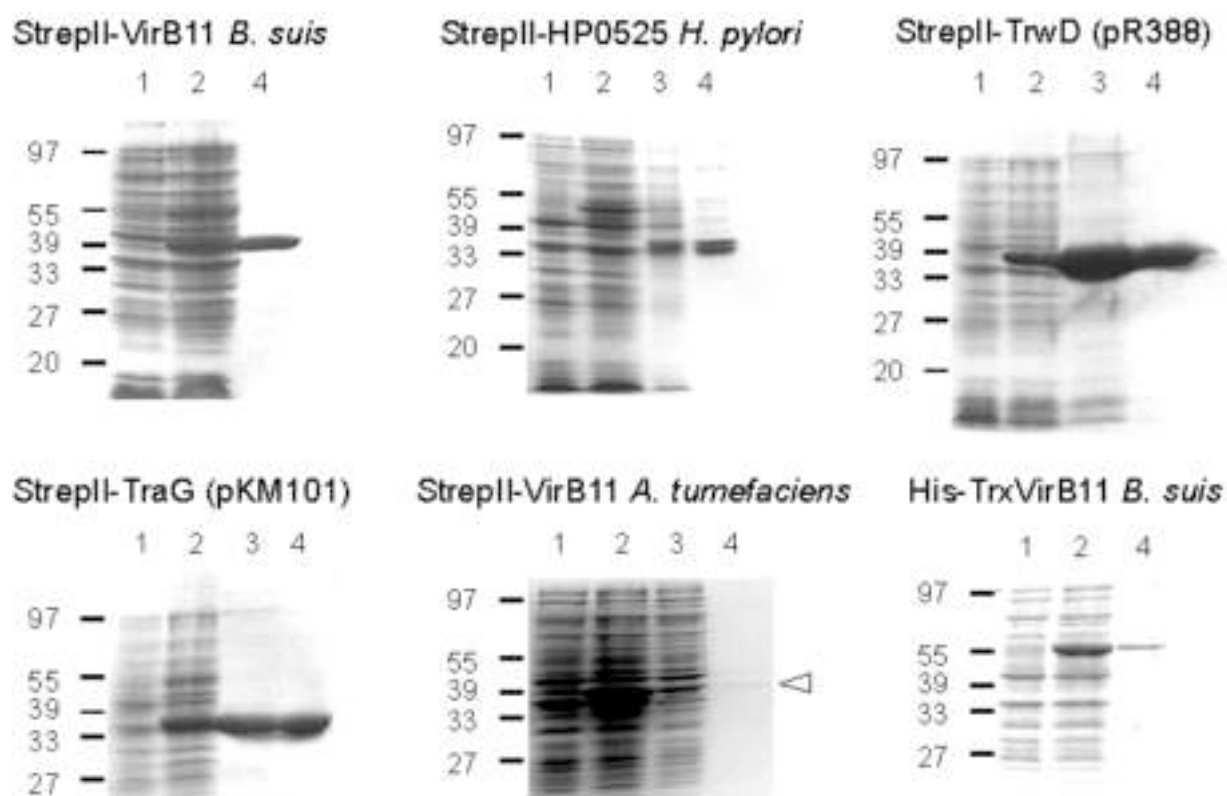


Fig. 31. Coomassie-stained polyacrylamide gels monitoring the purification of VirB11 orthologs. The N-terminally StreptII-tagged VirB11 orthologs were purified from *E. coli* strain GJ1158. Samples were loaded onto a 12% glycine-SDS polyacrylamide gel. Lanes represent: 1:pre-induction, 2:harvest, 3:Eluate I (post-affinity chromatography), 4:Eluate II (post-gel filtration, hexamer). White arrowhead points to purified *A. tumefaciens* StreptII-VirB11. Numbers on the left indicate reference proteins.

SDS-PAGE monitoring the different steps of the purification procedures (cell lysates from pre-induction and harvest, affinity chromatography eluate, gel filtration eluate) of all VirB11 orthologs was performed and the polyacrylamide gels were stained with Coomassie to analyze the purity of the proteins (Fig. 31). The purification of most VirB11 orthologs was efficient, and only the amount of *A. tumefaciens* StreptII-VirB11 was relatively low. Protein concentrations were determined with the Bradford assay (StreptII-VirB11suis: 467 µg/ml; StreptII-HP0525: 1234 µg/ml; StreptII-TrwD: 7100 µg/ml; StreptII-TraG: 3462 µg/ml; StreptII-VirB11Agro: 1238 µg/ml; HisTrxVirB11suis: 3310 µg/ml). A stock solution for the (d)NTPase assay was prepared for each protein by dilution with PSB.

2.2.2. General Properties of the (d)NTPases

To set up NTPase enzyme assays for inhibitor studies, the general properties of the five purified VirB11 orthologs were characterized first. The pH-dependency of enzymatic activity was analyzed at different values (pH 9.2, 8.6, 8.2, 7.9, 7.5 and 7.0), with ATP as substrate and Pi release was determined with the malachite green test in 20 μ l total volume (Materials and Methods, 9.1).

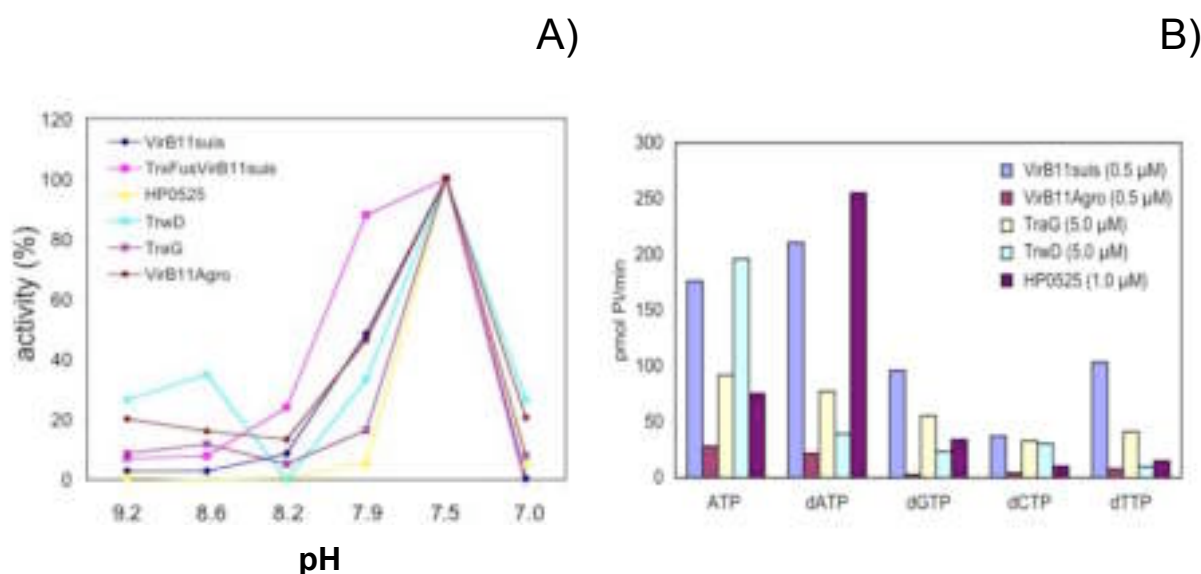


Fig. 32. pH-optimum and substrate preferences of Streptococcus-tagged VirB11 orthologs. The purified enzymes were tested for their optimal pH value and preferred substrate. The pH-value was tested in the range between 7.0 and 9.2, the activities are given as the percentage of the maximal activity observed (A). Substrate preferences were assayed with ATP and the four dNTPs, applying the indicated enzyme concentrations.

All the tested Streptococcus-tagged VirB11 orthologs had their highest enzyme activity at pH 7.5, and the activities were much lower under more acidic or basic conditions (Fig. 32 A). The only exception was TrwD, which had a second activity maximum at more basic conditions of pH 8.6. The substrate preferences were assessed with ATP or one of the four (d)NTPs at a pH value of 7.2 for 20 min. Almost all proteins had high enzymatic activities with ATP, and only HP0525 preferred dATP as a substrate. Limited hydrolysis of all the dNTPs was also observed, although with generally reduced velocities (Fig. 32 B). For all ATPase assays conducted in the following, standard parameters were pH 7.5 with the substrate ATP (dATP in the case of HP0525).

The kinetics of ATP and dATP hydrolysis by the VirB11 orthologs were analyzed in a series of parallel experiments with different substrate concentrations. For analysis, the substrate concentration was plotted against the velocity of P_i -liberation.

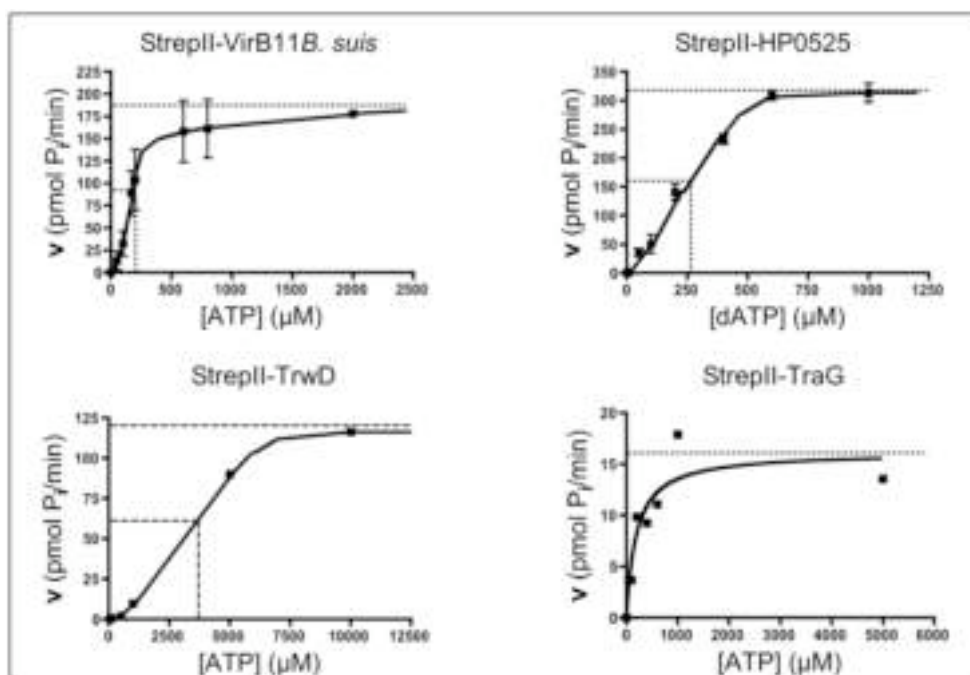


Fig. 33. Enzyme kinetic analysis NTP hydrolysis by VirB11 orthologs. In order to determine the $K_{0.5}$ and $V_{MAX}/2$, a set of different ATP or dATP concentrations was used in the (d)NTPase assay. The enzyme concentration was 0.5 μM for StreptII-VirB11 *B. suis*, 1.0 μM for StreptII-HP0525 and 5.0 μM for StreptII-TrwD and StreptII-TraG. In the case of StreptII-VirB11suis and StreptII-HP0525 experiments were repeated at least three times.

The sigmoidal shape of the curves depicting (d)ATPase velocities in relation to substrate concentration indicated cooperativity in case of the enzymes from *B. suis* and *H. pylori*. As a consequence of the cooperativity, no K_M -value could be assigned to those two enzymes. Instead, the substrate concentration corresponding to the $V_{MAX}/2$ -value was denominated $K_{0.5}$. A similar observation was made in case of StreptII-TrwD, but those experiments were repeated only twice and therefore it was impossible to make a definite statement. StreptII-TraG had very low enzymatic activity and a sigmoidal shape of the course was not observed (Fig. 33).

The enzymatic properties of the analyzed StreptII-tagged VirB11 orthologs are summarized in Table 8.

Table 8. Enzymatic properties of N-terminally StreptII-tagged VirB11 orthologs

Protein	c (μM)	optimal pH	substrate	$K_{0.5}$ (μM)	V_{MAX} (pmol P_i/min)
StreptII-VirB11 <i>B. suis</i>	0.5	7.5	ATP	200	185
StreptII-HP0525 <i>H. pylori</i>	1.0	7.5	dATP	250	320
StreptII-TrwD pR388	5.0	7.5	ATP	3750	120
StreptII-TraG pKM101	5.0	7.5	ATP	200	16
StreptII-VirB11 <i>A. tumefaciens</i>	0.5	7.5	ATP	ND	ND

ND: not determined

2.2.3. *B. suis* StreptII-VirB11 ATPase activity in the presence of other VirB proteins

The role and mode of action of VirB11-like proteins is still largely speculative, but some data suggest the importance of at least transient interactions of this protein with other T4SS components (Ward *et al.*, 2002). Due to the higher solubility of *B. suis* virB-encoded proteins, as compared to those from *A. tumefaciens*, it was possible to directly analyze the impact of putative channel and pilus components on the velocity of VirB11-mediated ATP hydrolysis. Equal volumes of StreptII-tagged VirB5, VirB8 and VirB9 in PSB (provided by A. Carle and L. Krall) were added to the standard ATPase-assay in ten-fold excess respective to the VirB11 hexamer.

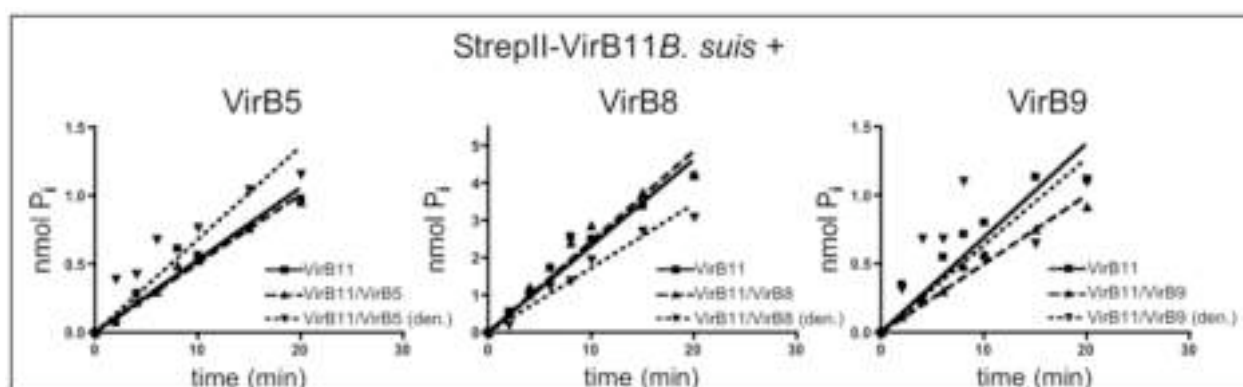


Fig. 34. Impact of StreptII-VirB5, StreptII-VirB8 and StreptII-VirB9 on the ATPase activity of *B. suis* StreptII-VirB11. Liberation of P_i was measured over 20 min in different reactions with either only VirB11, VirB11 + other StreptII-VirB-protein or VirB11 + other denatured StreptII-VirB-protein. The concentration of the ATPase hexamer was 16.7 nM and the concentration of the interacting monomeric proteins was 167 nM. A linear regression algorithm was applied to interpret the data points (Prism4).

The addition of other T4SS components did not cause notable changes of the initial rates of ATP hydrolysis by *B. suis* StreptII-VirB11 (Fig. 34).

VirB11 acts within a T4SS that is localized in the bacterial membrane (2-dimensional matrix) and composed of VirB proteins that form a network of interactions among each other. This ensures a high local concentration of potential interaction partners of VirB11, which may increase its enzyme activity. The assays performed here were conducted with soluble proteins (3-dimensional matrix) and this may decrease the likelihood VirB11 protein-protein interactions so that we could not mimick the *in vivo* situation.

2.3. Studies with VirB11-specific inhibitors

2.3.1. *In vitro* studies of the effect of MTFPT

The company CHIRON, one of the collaborators in the EU frame program 5, which funded this project, applied the native VirB11 ortholog HP0525 from *H. pylori* to a high-throughput screen for inhibitors of the ATPase activity in a combinatorial library. The high-throughput screen using a malachite-green based assay for P_i liberation identified three compounds that drastically reduced ATPase activity, and one of them was commercially available (Maybridge Inc.). Since the identity of the other two novel compounds remained proprietary by the company, those could not be characterized further. I tested the substance 4-methyl-2-[4-(trifluoromethoxy)phenyl]-1,2,4-thiadiazolane-3,5-dione (MTFPT), which was originally named CHIR-1 (Fig. 35), has a molecular mass of 292.23 g/mol and is insoluble in water. Initial tests showed not only inhibition of HP0525, but also an inhibitory effect on *H. pylori* virulence (CHIRON, unpublished data).

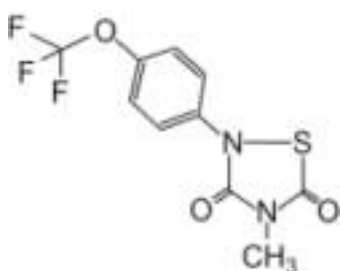


Fig. 35. 4-methyl-2-[4-(trifluoromethoxy)-phenyl]-1,2,4-thiadiazolane-3,5-dione (MTFPT)

As a first step to analyze MTFPT with respect to its effect on a set of purified VirB11-orthologs, *in vitro* ATPase assays were performed. The N-terminally StrepII-tagged VirB11 orthologs were incubated with increasing concentrations of the potential inhibitor and the velocities of the enzyme-catalyzed ATP hydrolysis was measured as described. The standard reaction mixes contained 14 μ l of buffer, 2 μ l of enzyme stock solutions and 2 μ l of DMSO with different MTFPT concentrations

ranging from 1 μ M to 1 mM. The mixtures were preincubated for 5 min on ice and the reaction was started by addition of the respective substrates and continued for 20 min. In order to determine the mode of inhibition, parallel experiments were conducted with different substrate concentrations.

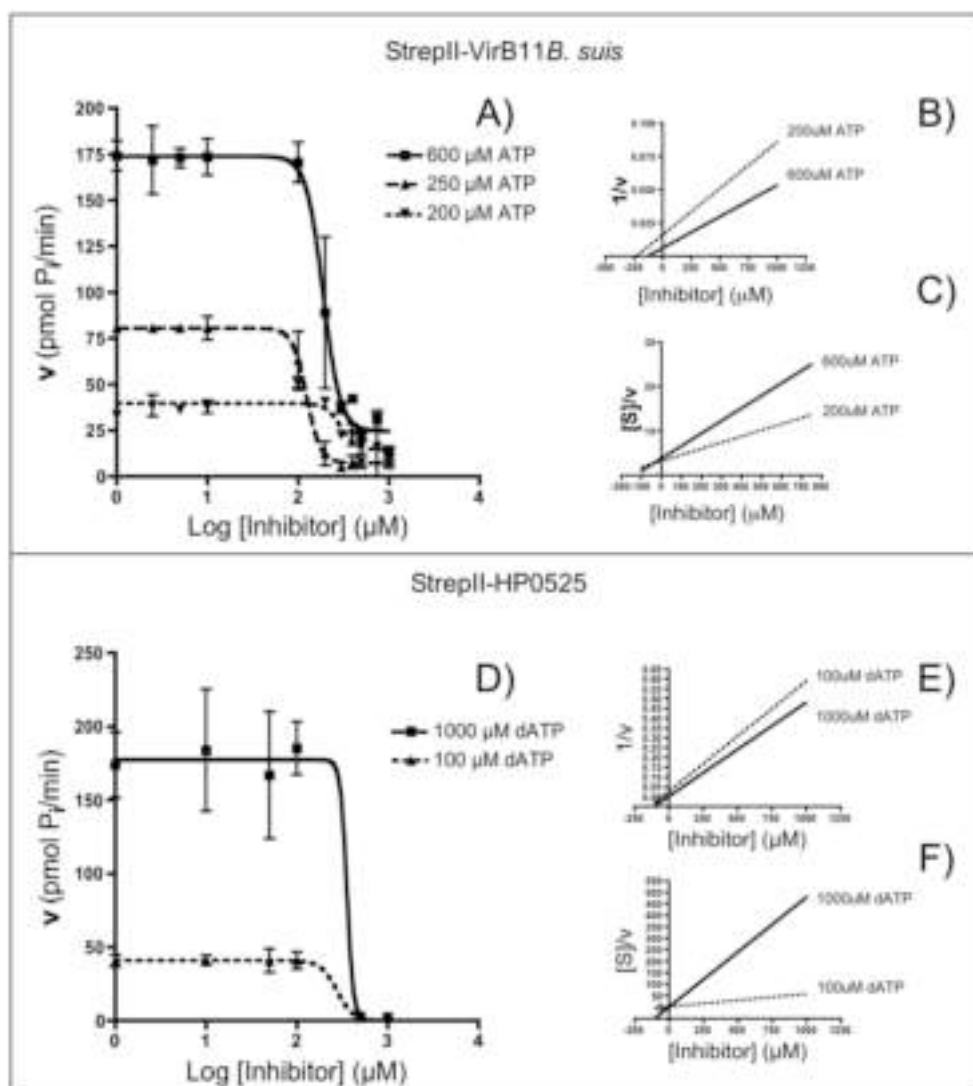


Fig. 36. Effect of MTFPT on Streptococcus VirB11B suis and Streptococcus HP0525. The inhibitor concentration in log-scale is plotted against the velocity of NTP hydrolysis (A, D) using nonlinear regression (sigmoidal dose-response, variable slope). The plots of inhibitor concentration against $1/v$ (B, E) and of inhibitor concentration against S/v (C, F) are calculated for the same data points as shown in A and D. Linear regression was applied in B, C, E and F. Lines represent substrate concentrations of 600 μM (A) or 1000 μM (D); dashed lines represent 200 μM and 250 μM (A) or 100 μM (D). The results from three independent experiments are shown.

The data for Streptococcus VirB11 from *B. suis* indicated a clear reduction of enzyme velocity at increasing inhibitor concentrations and the IC_{50} value was determined to be 242 μM (inhibitor concentration causing a 50% reduction of velocity, also known as $i_{0.5}$). Parallel experiments showed that the IC_{50} value was not impacted by changes of the ATP substrate concentration (Fig. 36 A), which permitted conclusions on the mode of inhibition. In the case of competitive inhibition, substrate and inhibitor compete for the same binding site of the enzyme, and increases of the substrate concentration increase the IC_{50} value. This was not observed here, and therefore competitive inhibition was ruled out. However, it still remained unclear whether the mode of inhibition was non- or un-competitive. To address this question the data were plotted in a different way, applying the *Dixon plot* of $1/v$ against [Inhibitor] (Fig. 36 B, E) and the *Cornish-Bowden plot* of $[S]/v$ against [Inhibitor] (Fig. 36 C, F). If a plot of

$[S]/v$ or $1/v$ against $[Inhibitor]$ gives a straight line, and IC_{50} is the value of $[Inhibitor]$ that gives a value of $[S]/v$ or $1/v$ that is double the value of $[S]/v$ or $1/v$ at $[Inhibitor] = 0$ (i.e. $v = 0.5 v_{MAX}$), then the intercept of the line on the abscissa is equal to $-IC_{50}$. This follows from elementary principles of geometry. In pure non-competitive inhibition, the IC_{50} is independent of $[S]$, so the common intersection point of lines depicting different substrate concentrations lies on the abscissa axis in both plots. This case is the least commonly observed in studies with natural enzymes (Cortés *et al.*, 2001). Here, the slopes of lines and the position of a common intersection point in Fig. 36 B and C suggests mixed-uncompetitive inhibition in the case of MTFPT-action on StreptII-VirB11, a type of inhibition that has features of both non-competitive and un-competitive inhibition.

In order to understand this finding, it is important to know that in **Competitive Inhibition** substrate and inhibitor compete for the free form of an enzyme. Therefore the inhibitory effect decreases upon increase of the substrate concentration. At low substrate concentrations the IC_{50} is therefore low. In **Un-competitive Inhibition** the inhibitor exclusively binds to the enzyme-substrate complex. At low substrate concentrations there is little formation of the enzyme-substrate complex, causing a high IC_{50} . **Non-competitive Inhibition** describes a situation where an inhibitor either binds to the free form of the enzyme or the enzyme-substrate complex. Dependent on the substrate concentration, such an inhibitor either acts competitive or un-competitiv, and the inhibitory effect is independent from the substrate concentration. The three modes of inhibition explained here possess an infinite number of intermediate forms that will commonly be observed in kinetic measurements (reviewed by Burlingham and Widlanski, 2003).

The same experimental setup and data processing was done with StreptII-HP0525. Again, the enzyme reaction velocity decreased with increasing MTFPT concentrations ($IC_{50}=189 \mu M$), and the inhibition was not impacted by the variation of substrate concentration (Fig. 36 D). Similar to *B. suis* VirB11 this suggested non-competitive or mixed-uncompetitive inhibition of StreptII-HP0525 by the compound. Since the inhibitor was discovered through its effect on HP0525 activity, the effect of MTFPT was not surprising, still IC_{50} was considerably lower in the initial tests with the native enzyme (Chiron, unpublished).

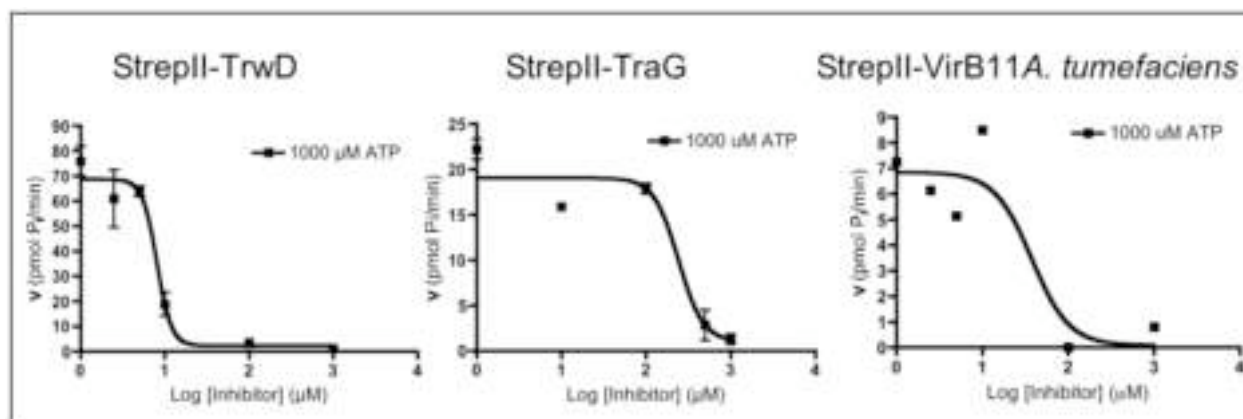


Fig. 37. Effect of MTFPT on StreptII-TrwD, StreptII-TraG and *A. tumefaciens* StreptII-VirB11. The inhibitor concentration in log-scale is plotted against the velocity using nonlinear regression (sigmoidal dose-response, variable slope). For StreptII-TrwD the experiment was performed three times, for StreptII-TraG and *A. tumefaciens* VirB11 two times with similar results.

The same experimental setup was used to analyse the effect of MTFPT on the other StreptII-tagged VirB11-like proteins. Due to their lower enzymatic activity and limited amounts of the proteins, inhibitor tests were performed with only one substrate concentration. The results indicate an inhibitory effect MTFPT on all orthologs with IC_{50} values of 8.1 μ M for StreptII-TrwD, 176 μ M for StreptII-TraG and 38 μ M for StreptII-VirB11Agro (Fig. 37). The results from all inhibitor studies are summarized up in Table 9.

Obviously, the inhibitor MTFPT did not compete for the active site with the substrate, suggesting that the compound bound to the VirB11 orthologs at different sites. Although (d)ATPase activity and hexamer formation can be dissociated in HP0525, it was a possibility that MTFPT bound to a region of the protein which is important for the formation of the hexameric scaffold or the allosteric interaction between its subunits. To analyze this possibility, a chemical crosslinking experiment of StreptII-VirB11 *B. suis* alone and together either with substrate or substrate plus inhibitor was performed. The samples were analyzed by separation with a polyacrylamide gel followed by Western blotting with VirB11-specific antisera.

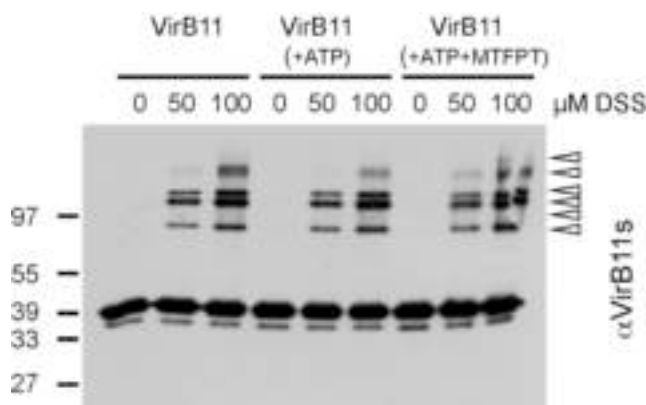


Fig. 38. Crosslinking of Streptococcus suis VirB11 in the presence of substrate and inhibitor. Streptococcus suis VirB11 was incubated with concentrations of DSS ranging from 0 μ M to 100 μ M. The concentration of the substrate ATP and the inhibitor MTFPT was 1000 μ M each. The samples were separated by SDS-PAGE followed by Western blotting with VirB11-specific antiserum. Numbers on the left indicate reference proteins. Arrowheads point to signals appearing exclusively after crosslinking the protein sample.

When Streptococcus suis VirB11 was incubated with DSS, higher molecular mass complexes of different sizes were formed, which is in line with the homo-oligomeric nature of the protein. The analysis revealed no differences between the samples, which had been crosslinked with or without ATP and MTFPT, suggesting that the inhibitor did not cause major conformational changes of the hexameric ATPase (Fig. 38).

Taken together, the results suggest that MTFPT exerted an effect on all five tested (d)ATPases. In the case of *B. suis* Streptococcus suis VirB11 and Streptococcus suis HP0525, MTFPT likely bound to the enzyme and the enzyme-substrate complex as defined for non-competitive inhibition. Since the mixed-uncompetitive inhibition observed here is an intermediate between non-competitive and uncompetitive inhibition, it can be assumed that the inhibitor bound both the free enzyme and the enzyme-substrate complex (as it is the case in non-competitive inhibition), but has a slight preference for the latter. This suggests binding of MTFPT to a conserved region close to, but not at the active site. The inhibitor did not interfere with hexamer formation, which further supports this idea.

2.3.2. *In vivo* studies of the MTFPT inhibitory effect

An inhibitory effect of MTFPT on a number of VirB11-like proteins was established *in vitro*, and in the context of future drug development, it was necessary to assess whether it also inhibits VirB11 activities *in vivo*.

2.3.2.1. Effect of MTFPT on the *A. tumefaciens* T4SS

As first assay, we determined its effect on the *A. tumefaciens* T4SS. Inhibition of *A. tumefaciens* VirB11 should decrease transfer of IncQ plasmid pLS1 to recipient cells (UIA143 pTiA6), since (d)NTP-hydrolysis of VirB11 is essential for this process. To address this question, an *A. tumefaciens* conjugation assay with donor strain A348 pLS1 and UIA143 pTiA6 as recipient was conducted in the presence of MTFPT in concentrations ranging from 1 μ M to 1 mM.

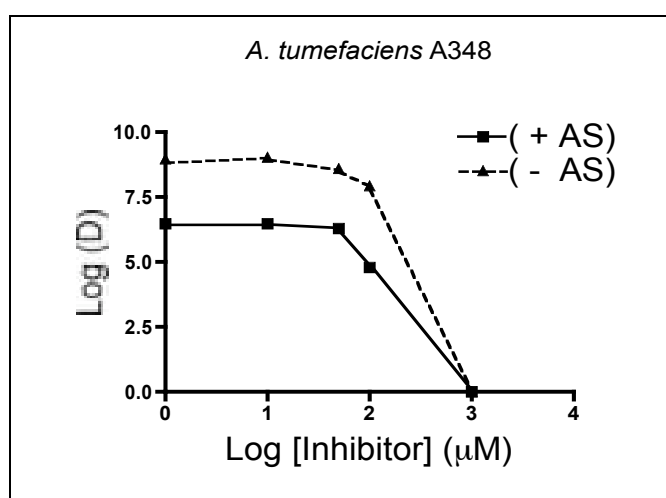


Fig. 39. A348 output donor numbers at different MTFPT concentrations. The inhibitor concentration (Log[Inhibitor]) in μ M is plotted against the output donor number (Log (D)) from the conjugation assay (both in log-scale). Black triangles and the interconnecting dashed lines correspond to cells cultured in the absence of AS (- AS), black squares and interconnecting lines correspond to cells cultured in the presence of AS (+AS).

A. tumefaciens donor and recipient were co-incubated for two days, followed by quantification of the numbers of exconjugants, donors and recipients. This quantification revealed a negative effect of MTFPT on bacterial growth or survival, beginning at 100 μ M MTFPT, and no output donor A348 pLS1 was recovered at 1 mM MTFPT (Fig. 39). The number of transconjugants was almost constant independent of the MTFPT concentration, but due to the toxic effect on the donor, it was not possible to use this assay to quantify plasmid transfer. This toxic effect was also apparent when donor and recipient were cultured under non-inducing conditions (Fig.39, -AS), although the number of output donors was generally higher.

When the capacity of A348 to incite tumor formation in the presence of different MTFPT concentrations was analyzed, it was found that the presence of DMSO in an infected plant wound inhibited the development of tumors (not shown). Since both the inhibitor MTFPT and its solvent DMSO unspecifically interfered with the assays of T4SS functionality described above, the impact of MTFPT on the cellular levels of T4SS components and on pilus formation was determined next.

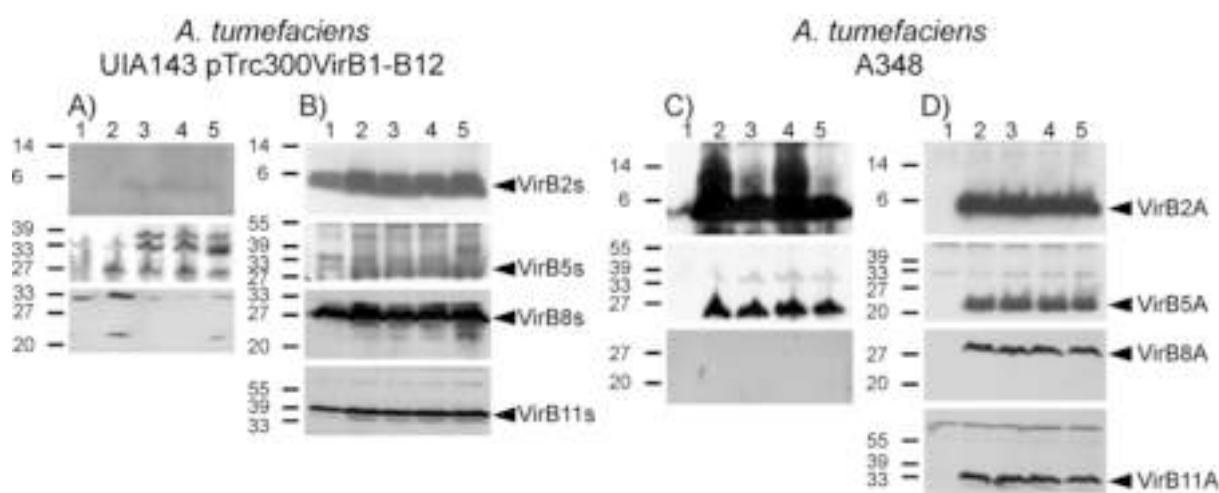


Fig. 40. Effect of MTFPT on the cellular levels of T4SS components and pilus. T4SS components from high MW fractions (A, C) and cell lysates (B, D) of the indicated strains were separated on 15% tricine-SDS-polyacrylamide gels, subjected to Western blotting and analyzed with specific antisera. Black arrowheads point at signals of the indicated proteins. VirBX_A refers to proteins from *A. tumefaciens* and VirBX_S to the orthologs from *B. suis*. Unless otherwise indicated, UIA143 pTrc300VirB1-B12 was induced with 0.5 μ M IPTG and A348 pTiA6 with 200 μ M AS. Lanes are: 1: uninduced, no MTFPT; 2: no MTFPT; 3: 100 nM MTFPT; 4: 1 μ M MTFPT; 5: 10 μ M MTFPT. Numbers on the left indicate reference proteins.

Production of the pTiA6-encoded *A. tumefaciens* T4SS and of the recombinant *B. suis* T4SS as determined by pTrc300VirB1-B12 were induced and exocellular high MW structures were isolated and analysed as described (Schmidt-Eisenlohr *et al.*, 1999b). DMSO in a concentration of 10%, which was required to dissolve MTFPT, neither affected growth of strain A348 pTiA6 nor of UIA143 pTrc300VirB1-B12 (not shown). However, growth of both strains was strongly inhibited by MTFPT concentrations of 100 μ M and 10 μ M, but lower concentrations had no significant effect. The highest concentration used in these assays was therefore 10 μ M MTFPT. The accumulation of VirB proteins in cell lysates and in exocellular high MW fractions was analyzed by SDS-PAGE and Western blotting with specific antisera. *B. suis* VirB5 was detected in pilus fraction from of UIA143 pTrcVirB1-B12 cultured in the presence of IPTG irrespective of the presence of MTFPT, whereas a weak VirB2-specific signal was only detected when the strains were cultured in the presence of IPTG and MTFPT (Fig. 40 A, lane 3-5). Cell lysis caused by the inhibitor may be an explanation for this phenomenon, but this is not likely since VirB8 was not detected in the pilus fractions (Fig. 40 A). The levels of VirB2, VirB5, VirB8 and VirB11 in IPTG-induced UIA143 pTrcVirB1-B12 were not impacted by the concentration of MTFPT (Fig. 40 B).

In virulence-induced *A. tumefaciens* A348, equal levels of VirB2 and VirB5 were detected in the pilus fraction of all strains cultured in the presence of different MTFPT concentrations. VirB8 was not detected in the exocellular fractions, which rules out that the inhibitor caused significant cell lysis under these conditions (Fig. 40 C). Similarly, MTFPT had no effect on the cell levels of VirB2, VirB5, VirB8 and VirB11 in induced A348.

In both strains, the inhibitor up to a concentration of 10 μ M did not influence the amount of cellular VirB11 and of any other VirB protein. This suggests that drastic conformational changes or disassembly of the hexamer were not caused by MTFPT, which was already suggested by the results of the crosslink analysis (Fig. 38). Thus, the inhibitory effect observed on the ATPase activities of VirB11 from *A. tumefaciens* and *B. suis* did not impact the levels of VirB proteins in the cells or the formation of high MW exocellular appendages under these conditions. At present it is not clear what caused the inhibition of the growth of *A. tumefaciens* by MTFPT, but this effect obscured the use of this model for the analysis of the impact of T4SS function(s). As alternative *in vivo* assays, T4SS models in *E. coli* were analysed next.

2.3.2.2. Effect of MTFPT on conjugative transfer of broad host range plasmids

The *In vivo* effect of MTFPT on the VirB11 orthologs of T4SS involved in transfer of the conjugative plasmids pR388, pKM101 and pRP4 to recipient cells was analyzed in conjugation assays. *E. coli* donor strain FM433 (spc^R) harbouring the broad host range plasmids pR388 (tm^R), pKM101 (carb^R) and pRP4 (kan^R) was mated to the recipient strain WL400 (cm^R , str^R) as described (Materials and Methods, 12.1.2). Concentrations of MTFPT during the conjugation assay ranged from 10 nM to 1000 μ M, and the DMSO concentration was always 10%. After serial dilution, the output donor cell number was determined by plating on LB (spc). Transconjugands resulting from pR388 transfer were selected on LB cm/ tm, from pKM101 transfer on LB cm/ carb and from pRP4 transfer on LB cm/ kan. The transfer efficiency was measured as the number of transconjugands (TC) per donor cells (D) and set to 100 % in the positive control (no MTFPT). The toxicity of MTFPT was assessed by comparison of the output donor numbers of one series of experiments with different inhibitor concentrations.

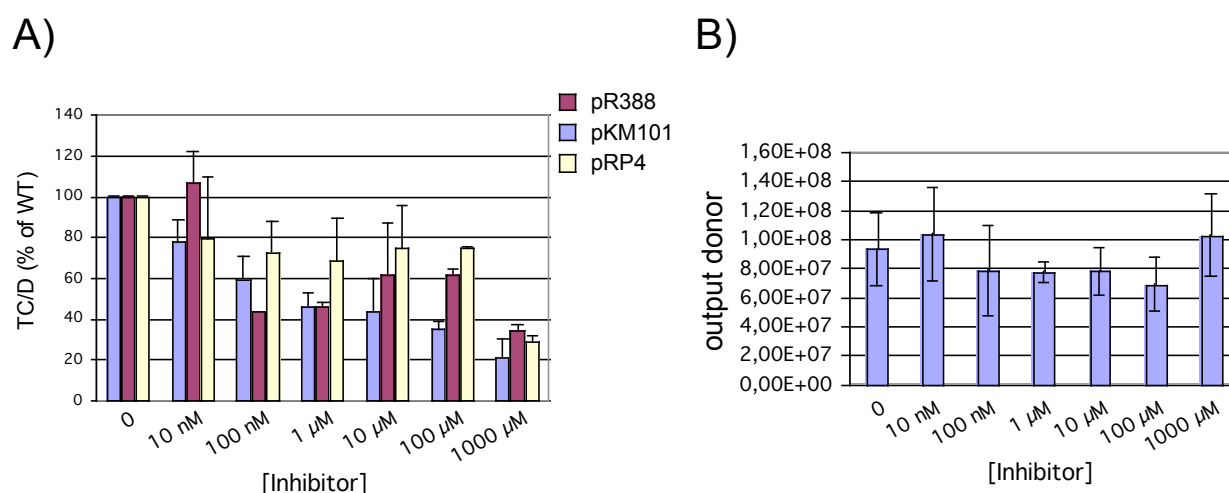


Fig. 41. MTFPT effect on conjugation and survival of IncN, -P, -W plasmid bearing cells. *E. coli* FM433 carrying the indicated plasmids was incubated with different concentrations of MTFPT and the efficiency of plasmid transfer to *E. coli* WL400 was measured. The value of transconjugand per donor (TC/D) of the uninhibited strains was set to 100% (A). The effect of MTFPT on growth of *E. coli* cells was assessed, and total output donor numbers in dependence of inhibitor concentration is shown (B). Standard deviation is from three independent experiments.

A negative effect of the inhibitor on transfer efficiency of the three plasmids was already observed at a concentration of 100 nM, which leads to a plasmid transfer efficiency of approximately 60 % of the positive control. At a MTFPT concentration of 1000 μ M, a very strong inhibitory effect on the transfer of all the plasmids strains to 30% of the level without inhibitor was observed. Inhibitor concentrations between 100 nM and 1000 μ M had intermediate effects, but there was no apparent linear relation between MTFPT concentration and inhibition of plasmid transfer (Fig. 41 A). Analysis of numbers of output donors showed that MTFPT had no toxic effect on *E. coli* at concentrations up to 1000 μ M (Fig. 41 B), showing that the inhibition of conjugative transfer was likely due to a direct effect on the plasmid-determined T4SS.

2.3.2.3. Effect of MTFPT on IncN pilus formation

An alternative assay for T4SS function in broad host range plasmids is the formation of extracellular pili, which are used by bacteriophages as entry sites. Phage infection can therefore be applied to quantify pilus formation. *E. coli* strain FM433 was used to assay effects of the inhibitor on the formation of the IncN pilus.

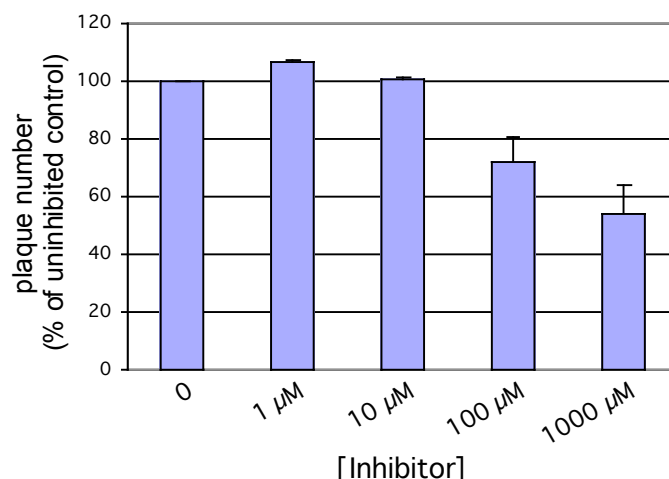


Fig. 42. Efficiency of IKE infection of an IncN plasmid-determined pilus structure. Inhibitor concentrations in μM are shown (abscissa). The plaque numbers for FM433 pKM101 incubated without MTFPT (uninhibited control) acts as a reference value and was set to 100% (ordinate). Standard deviation of three independent experiments is shown (black lines).

Pre-incubation with MTFPT affected the ability of IKE to infect FM433 pKM101. At a MTFPT concentration of 100 μM a reduction to 70% of the positive control was observed, and at a concentration of 1000 μM MTFPT the plaque number was reduced to 50% of the positive control value (Fig. 42). Obviously, incubation with MTFPT led to a change in quality and/or quantity of the primary IKE receptor on the bacterial cell surface.

2.3.3. Effects of oleic and linoleic acid on VirB11 activity

It was demonstrated by others that certain phospholipids stimulated the activity of some VirB11 orthologs (Krause *et al.*, 2000). Moreover, it could be shown that unsaturated fatty acids such as linoleic acid and oleic acid exerted an inhibitory effect on TrwD (Machon C, unpublished). The fact that fatty acids influenced the activity of at least some VirB11 orthologs raised the question whether this effect could also be observed in case of the N-terminally StrepII-tagged VirB11 orthologs.

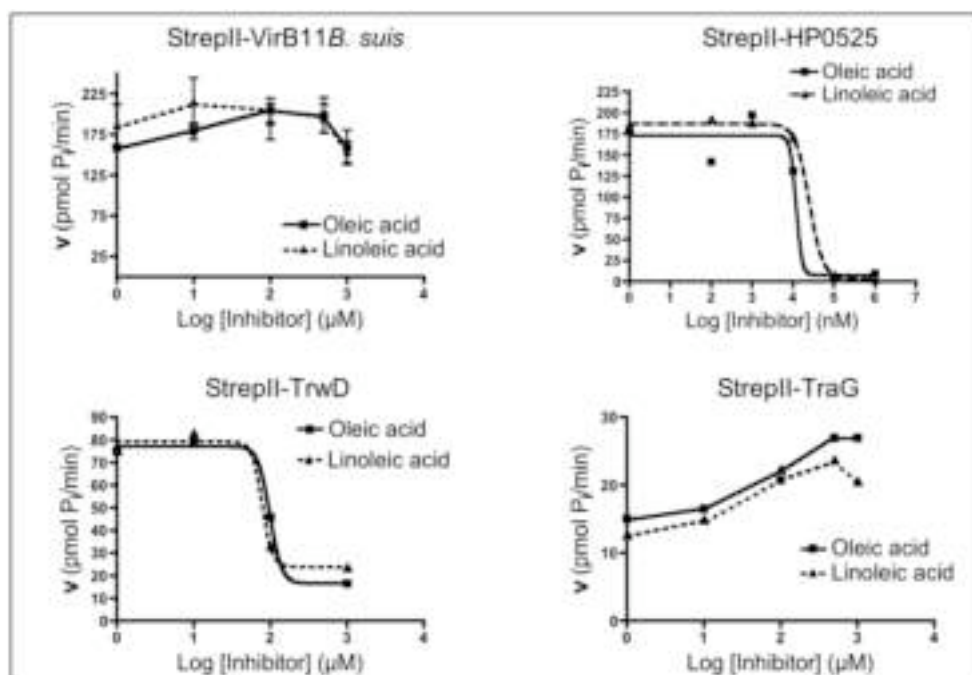


Fig. 43. The *in vitro* effect of oleic- and linoleic acid on the VirB11 orthologs. The inhibitor concentration in logarithmic scale on the abscissa is plotted against the velocity of the enzyme on the ordinate. The inhibitory effect of either oleic- or linoleic acid was determined. Lines were either drawn by hand or calculated with nonlinear regression (sigmoidal dose-response, variable slope). Experiments were performed three times with similar results.

Table 9. IC₅₀ value of different inhibitory compound's action on VirB11 orthologs

Protein	MTFPT IC ₅₀ (μM)	Oleic acid IC ₅₀ (μM)	Linoleic acid IC ₅₀ (μM)
StreptII-HP0525 <i>H. pylori</i>	189	12	25
StreptII-VirB11 <i>B. suis</i>	242	-	-
StreptII-TrwD (pR388)	8,1	99	79
StreptII-TraG (pKM101)	176	-	-
StreptII-B11A. <i>tumefaciens</i>	(38)	ND	ND

ND: not determined; -: no inhibition

(d)ATPase assays were conducted with N-terminally StreptII-tagged *B. suis* VirB11, *H. pylori* HP0525, TrwD (pR388) and TraG (pKM101) as described (2.3.1), in the presence of different concentrations of linoleic acid and oleic acid. The two compounds acted similarly when acting on the same enzyme, but between VirB11 orthologs the effect of these fatty acids varied. Whereas the ATPase activity of StreptII-VirB11 from *B. suis* remained almost constant irrespective of the fatty acid concentration, StreptII-TraG activity increased two-fold upon addition of the fatty acids. In contrast, StreptII-TrwD was inhibited in the same way as native TrwD (Machon C, unpublished), with a 6-fold reduction of activity in the presence of 1 mM linoleic or oleic acid. Interestingly, the same effect could also be observed in case of StreptII-HP0525. In the presence of 100 μM of both fatty acids P_i liberation from dATP was

strongly inhibited, and the IC_{50} values were the lowest observed in the context of this work. The IC_{50} values in the presence of fatty acids are shown in Table 9 and compared to those of MTFPT.

2.4. Complementation of an *A. tumefaciens* VirB11 mutant

In order to gain insights into the protein-protein interactions required for VirB11 functions it was tried to reconstitute a functional T4SS by heterologous complementation of the *virB11* deletion mutant PC1011 with pTrc200 expressing either *A. tumefaciens* C58 *virB11* or *B. suis* *virB11*. Ends of PCR fragments encoding full-length *virB11* were generated with the restriction enzymes *Bsp*HI and *Xba*I and inserted into vector pTrc200 treated with *Nco*I and *Xba*I. The resulting vectors pTrc200, pTrcB11 and pTrcB11s were transformed into PC1011, followed by growth under virulence gene-inducing conditions and analysis of VirB protein content in subcellular fractions (cell lysate and pilus fraction).

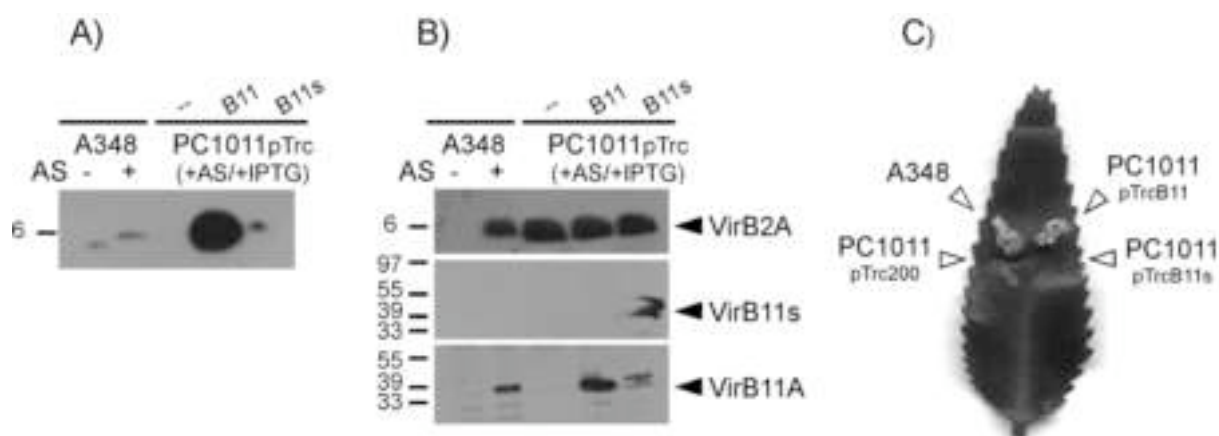


Fig. 44. Complementation of T-pilus formation and virulence by strain PC1011 expressing *virB11* orthologs. The indicated strains were cultured under virulence inducing (+AS) or non-inducing (-AS) conditions. *trc*-driven gene expression was induced with IPTG. Exocellular high-molecular mass T-pilus fractions (A) and cell lysates (B) were separated by SDS-PAGE followed by Western blotting with VirB2-, VirB11s- and VirB11A-specific antisera. Numbers on the left indicate reference proteins. Lesions on leaves of *K. diagramontiana* were inoculated with the indicated strains and tumor formation was monitored (C).

VirB11 and VirB11s in cell lysates were detected in Western blots with the respective VirB11-specific antisera, and we observed cross-reaction of the *Agrobacterium* VirB11-specific antiserum with the *Brucella* VirB11 ortholog (Fig. 44 B). *Brucella* VirB11 was apparently produced at high levels and overproduction was visible in Coomassie-stained gels (not shown). The level of VirB2 in cell lysates did not vary (Fig. 44 B), but in the pilus fractions VirB2 was only detected in the samples from A348 and PC1011 pTrcB11 cultured under virulence-inducing conditions (Fig. 44 A). Consistent with this observation, only these two strains were able to incite tumor formation in lesions of *K. diagramontiana* leaves (Fig. 44 C), showing that *Brucella* VirB11 did not complement the *virB11* defect of PC1011. A348 and PC1011 pTrcB11 were then transformed with pLS1 and their ability to transfer the IncQ-

plasmid was monitored in conjugation assays with A348 pLS1, PC1011 pTrcB11 pLS1 and PC1011 pTrcB11 spLS1 (all carb^R) as donors and UIA143 pTiA6 (ery^R) as recipient. Surprisingly, only the induced WT strain A348 was able to transfer pLS1 (not shown). This finding may be explained by the fact that PC1011 pTrcB11 did not express the *virB11* gene from the octopine-type *A. tumefaciens* A348, but the ortholog from nopaline-type *A. tumefaciens* C58. In any case, the *B. suis* VirB11 ortholog did not complement the genetic defect of PC1011 suggesting that the requirements for protein-protein interactions preclude the heterologous exchange of these two enzymes. To gain further insights into this questions VirB11 protein interactions with VirB5 were next assessed with purified proteins.

2.5. Protein-protein interactions of VirB11

2.5.1. Strep-Tactin® Sepharose® pull-down assay

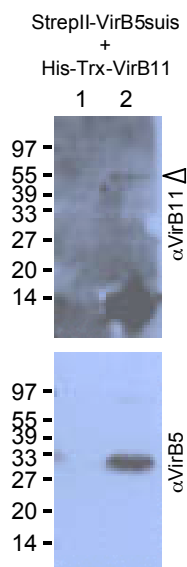


Fig. 45. *B. suis* VirB11 binds to matrix-bound StrepII-VirB5. StrepII-VirB5 was preincubated with the Strep-Tactin matrix before addition of His-Trx-VirB11. After washing, proteins were eluted from the matrix with 1 mM biotin, and analysed by SDS-PAGE and subsequent Western blot with the specific antisera indicated on the right. Lane 1: negative control where only His-Trx-VirB11 was incubated with the matrix; Lane 2: pull-down assay. White arrowhead points at the faint VirB11-specific signal. Experiments were repeated three times with consistent results.

A pull-down assay as described in 1.4.2 was performed to analyse a potential protein-protein interaction between VirB11 and the minor pilus component VirB5. Interactions of the orthologs from *A. tumefaciens* had previously been suggested by a different experimental approach (Krall, 1999). Matrix-bound *B. suis* StrepII-VirB5 (provided by A. Carle) was incubated with His-Trx-VirB11. After washing and elution, the sample was subjected to Western blot analysis with VirB11- and VirB5-specific antisera. The analysis revealed specific attachment of the recombinant ATPase to the Sepharose-matrix that displays non-covalently bound StrepII-VirB5. An implication of this result is that VirB5 may interact with VirB11 in order to be localized to the nascent pilus structure.

2.5.2. Overlay assay of VirB11 and VirB5 orthologs

L. Krall had previously observed an interaction of *A. tumefaciens* VirB11 and VirB5 using an overlay-assay. In order to reproduce this result and detect similar interactions with the different orthologs used in this work, overlay assays were performed.

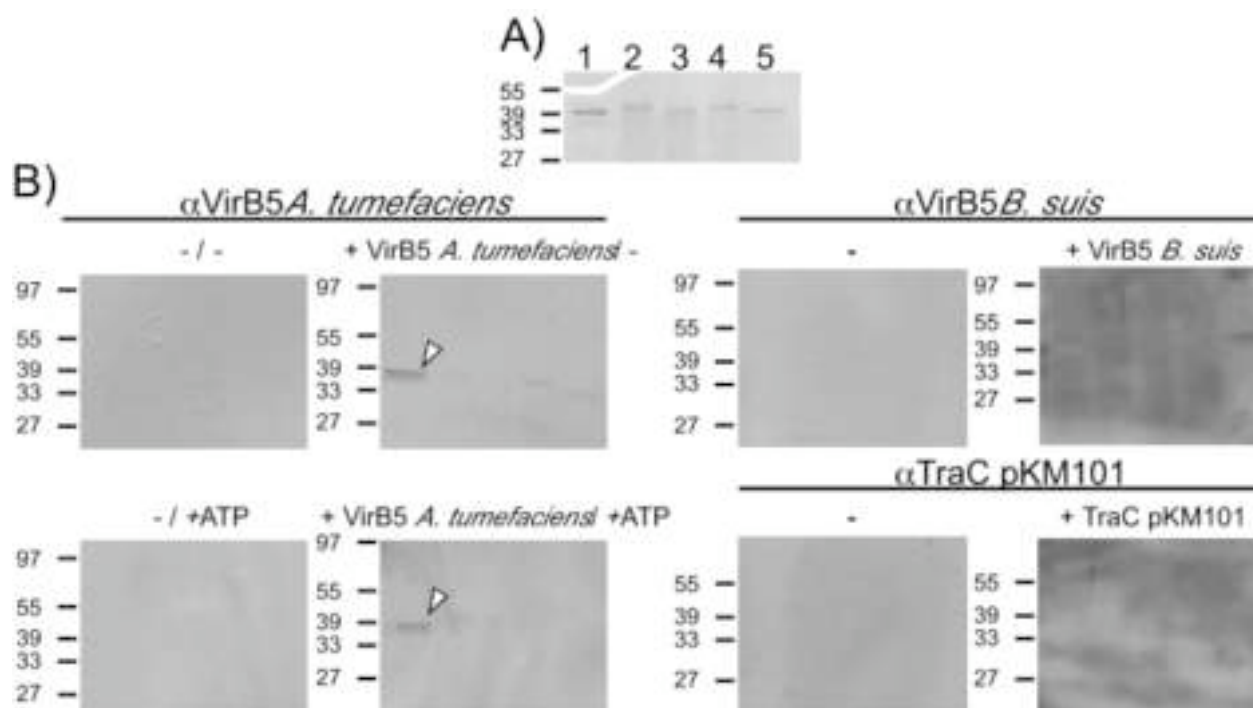


Fig. 46. Overlay-assay of PVDF-bound VirB11 orthologs with soluble VirB5 orthologs. Coomassie-stained SDS-polyacrylamide gel (A) shows the amount of VirB11 orthologs blotted onto PVDF membranes for the overlay assays. 1: VirB11 (*A. tumefaciens*); 2: StreptII-VirB11 (*B. suis*); 3: StreptII-TraG (pKM101); 4: StreptII-TrwD (pR388); 5: StreptII-HP0525 (*H. pylori*). Subsequently, these membranes were incubated with or without the indicated proteins and, only in the case of incubation with *A. tumefaciens* VirB5, with or without 1 mM ATP. Black bars indicate the specific antisera that were applied to detect bound VirB5 proteins. White arrowheads point to the detection of an *A. tumefaciens* VirB5-specific signal at a MW corresponding to the *A. tumefaciens* VirB11 monomer. Reference proteins are indicated on the left.

As our previous work had shown that it was difficult to obtain substantial amounts of the *A. tumefaciens* VirB11 ortholog in soluble form, the proteins for this assay were produced as inclusion bodies. *E. coli* strains GJ1158 harbouring pT7-StreptII-VirB11 *B. suis*, pT7-StreptII-TraG, pT7-StreptII-TrwD or pT7-VirB11 *A. tumefaciens* were cultured to an OD₆₀₀ of 0.4-0.8 and induced by addition of 5 M NaCl to final concentrations of 0.3 M. After cultivation at 37°C for 16 h, the cells were sedimented by centrifugation, suspended in PBS and lysed by passage through a French Press. After sedimentation of the lysate, large amounts (≥ 1 mg) of insoluble VirB11 orthologs were retrieved from the sedimented inclusion bodies. Proteins were boiled for 5 min in 1 ml protein sample buffer and diluted in order to separate equal amounts by SDS-PAGE (Fig. 46 A). The proteins were transferred to PVDF membranes, followed by renaturation, incubation with the putative interaction partners *Agrobacterium* StreptII-VirB5 (in the absence and in the presence of 1 mM ATP), *Brucella* StreptIIVirB5 and pKM101 TraC. The bound proteins were detected by Western blotting and specific signals were only detected on the membrane incubated with *A. tumefaciens* StreptII-VirB5 in the presence or absence of 1 mM ATP. The position of the VirB5-specific signal on

the blot corresponded to that of *A. tumefaciens* StreptII-VirB11. Binding to renatured VirB11 orthologs was not observed in case of *Brucella* StreptIIVirB5 (Fig. 46 B).

The overlay assay conducted here therefore reproduced the previous observation that VirB11 and VirB5 from *A. tumefaciens* interact. However, further evidence that this interaction occurs in other T4SS could not be provided, but data from the pull-down assay (2.5.1) demonstrated that this interaction might at least be conserved in the T4SS of *B. suis*.

Discussion

1. Interactions of VirB1 with other T4SS components

1.1. Common features of VirB1 from *B. suis* and *A. tumefaciens*

The α -proteobacteria *A. tumefaciens* and *B. suis* both live in close interaction with eukaryotes. They utilize an inducible macromolecular translocation system coined T4SS, which spans both the inner and outer membrane of the cell envelope, to support this life style. Though host characteristics and the overall way of life of both pathogens differ substantially, the *virB* operons encoding the T4SS in both organisms show a high degree of structural conservation. This becomes even more evident when single proteins of the systems are compared.

Algorithms suited for the prediction of subcellular sorting signals show that the VirB1 orthologs from *A. tumefaciens* and *B. suis* both possess N-terminal signal peptides, an observation supported by experimental evidence in the case of *A. tumefaciens* VirB1 (Llosa *et al.*, 2000). The characteristic active site signature of transglycosylase is found in both proteins. Predictions of the secondary structure show a high degree of conservation, not anticipated by the 27% identical amino acid residues in both sequences (Höppner *et al.*, 2004). The sequence that was identified as the cleavage site of *A. tumefaciens* VirB1 also shows limited conservation between the two proteins. One very interesting feature of VirB1 is that the entire C-terminal domain following the cleavage site is classified as a NORS-region. NORS-regions are likely unordered and may receive their structure through interactions with other proteins (Liu *et al.*, 2002), possibly located in the periplasma in the case of VirB1. It was previously shown that this part, denominated VirB1*, accumulates in the supernatant of virulence-induced *A. tumefaciens* cells (Baron *et al.*, 1998), and observations from this work (Fig. 17) suggest that similar processing might also occur in *B. suis* VirB1. Analysis of the efficiency of conjugative transfer into *A. tumefaciens* carrying the *B. suis* T4SS with and without VirB1 showed that this protein is non-essential but required for high-efficiency function. The finding that *B. suis* VirB1 partly complemented its *A. tumefaciens* ortholog (Höppner *et al.*, 2004) further emphasizes the similarity of the two proteins.

1.2. Interactions of VirB1 with other VirB proteins

A role of VirB1 as nucleation center was suggested before, but the many interactions with T4SS components had until now only been demonstrated in the yeast dihybrid assay (Ward *et al.*, 2002). The *B. suis* T4SS is more amenable to investigation with biochemical methods than the *Agrobacterium* T4SS. Many of its components are relatively easy to purify, because in contrast to those from *A. tumefaciens*, they can be overexpressed in a soluble

form with high yield, followed by affinity purification. This feature was exploited to conduct biochemical experiments to assess the suggested interactions. Overproduction of VirB1 with a C- or N-terminal affinity-tag resulted in a protein that was bound to GroEL, which may be due to improper folding in the cytoplasm. The C-terminally His₆-tagged variant of VirB1 could not be efficiently affinity purified with an IMAC column, suggesting that the C-terminus was inaccessible. It is likely that the chaperone GroEL bound to the NORS region of the recombinant protein. The resulting multimeric protein complex (or aggregate) had a MW larger than 600 kDa and thus eluted in the void volume of a Superdex 200 gel filtration column. Apart from that, recombinant VirB1 was mainly present in the dimeric, tetrameric and hexameric state. The above findings were demonstrated in case of VirB1-His₆ but not in case of StrepII-VirB1. The difference is probably due to a minor portion GroEL-free VirB1-His₆ in the cell lysate that is getting specifically enriched in affinity purification, since it preferentially binds to the IMAC column. In contrast to this situation StrepII-VirB1 was predominantly affinity-purified in complex with GroEL since the tag is accessible. This inhibited its protein-protein interactions.

Nevertheless, chemical crosslinking of enriched recombinant StrepII-VirB1 showed that dimeric and presumably also tetrameric forms of VirB1 exist. An attempt to map self-interacting domains of VirB1 using Peptide Array experiments was not successful, since strong binding to all VirB1-derived peptides displayed on the membrane occurred (not shown). The available data suggest that VirB1 forms homo-multimeric assemblies, probably dimers and tetramers. The molecular sieving effect of the murein layer prohibits diffusion of globular proteins or protein assemblies larger than 55 kDa. Since the permeation of the murein layer might be important for the function of lytic transglycosidase in the periplasm, the formation of dimers (approximately 50 kDa) appears to be more plausible in the natural biological context than the formation of tetramers (approximately 100 kDa), which may not permeate the murein layer.

Using a co-elution assay of proteins co-expressed from bicistron vectors we did not get any evidence for an interaction between VirB1 and VirB8, which was predicted from a previous yeast two-hybrid study (Ward *et al.*, 2002). However, this may be due to the buffer conditions used in this specific assay. Whereas the proteins did not elute from the gel filtration column together, we observed reduced amounts of supposedly GroEL-bound VirB1-His₆ in high MW assemblies. This might be explained by an interaction between VirB1 and VirB8, which may have prevented or competed with GroEL binding, but this interaction may not be stable enough to sustain cell lysis and further fractionation. In a pull-down assay with matrix-bound StrepII-VirB1 His-Trx-VirB8 was found to bind to the matrix in a non-specific

way so that this method was not suited to analyse the interaction. In contrast, chemical crosslinking of the two proteins gave evidence for interaction in a 1:1 stoichiometry. Data from the Peptide Array experiment further suggested that a set of VirB1 peptides interacts with VirB8, which supports the notion that VirB1 and VirB8 interact. The evidence is not as substantial as that in case of VirB9 discussed below, suggesting that the interaction is weaker and/or may need additional interaction partners.

The interaction between VirB1 and VirB9 was demonstrated using a pull-down assay and by chemical crosslinking of the two proteins in solution. Co-elution of the two proteins following their co-expression in a bi-cistron construct was also demonstrated with a gel filtration assay. During this experiment we also noted a reduction of the amount of high MW StrepII-VirB1 in the void volume of the gel filtration column, which further substantiates the notion that VirB9 impacts the oligomeric state of VirB1. Peptide array experiments identified VirB9-interacting peptides throughout the VirB1 sequence, and a considerable portion of them was in the C-terminus. According to the molecular masses of the co-eluting VirB1-VirB9 complexes and of the crosslinked products, VirB1:VirB9 stoichiometries of both 2:1 (80 kDa) and 2:2 (110 kDa) are likely. These data are consistent with the results of a previous study, which pursued a biochemical approach to demonstrate the interaction of the VirB1 C-terminus with VirB9 in *A. tumefaciens* orthologs (Baron *et al.*, 1997).

An interaction between VirB10 and VirB1 could neither be demonstrated with the pull-down assay nor by gel filtration. When the two proteins were subjected to cross-linking in solution no specific new products were observed. Tests of the interaction of VirB10 with a VirB1 displayed on a peptide array were therefore not conducted and we do not consider it likely that the two purified proteins interact.

In contrast to the entirely negative results in case of VirB10 some evidence for an interaction of the hexameric ATPase VirB11 with VirB1 was obtained. A pull-down assay demonstrated specific binding of His-Trx-VirB11 to StrepII-VirB1, and results of crosslinking experiments further supported this finding. However, we did not observe co-elution of the two proteins from a gel filtration column. Nevertheless, VirB11 production was enhanced upon co-expression with VirB1, which indicates an interaction and VirB11 specifically bound to certain VirB1 peptides in array experiments.

Due to the lack of VirB4-specific antisera, the interaction of the ATPase VirB4 could only be assessed in a co-elution assay following bi-cistronic expression of *streptII-virB1* and

virB4. Significant amounts of VirB4 co-eluted with StrepII-VirB1, indicating an interaction between the two proteins.

Taken together, the results suggest that VirB1 is a self-interacting protein that establishes transient contacts with other VirB proteins. In the course of biogenesis of the T4SS, VirB1 might interact with the ATPases VirB11 and VirB4, with the transmembrane channel component VirB8 and VirB9. The interaction of VirB1 and VirB10 that was postulated by a dihybrid screen (Ward *et al.*, 2002), was not observed in the experiments conducted here.

Table 10. Suggested and proven interactions of VirB1.

Protein	localization (Cascales and Christie, 2003)	dihybrid screen (Ward <i>et al.</i> , 2002)	Biochemical method			
			pull-down assay	chemical crosslink	Co-elution	peptide array
VirB1	Periplasm	+	ND	+	+	ND
VirB8	IM	+	ND	+	-	+
VirB9	OM	+	+	+	+	+
VirB10	IM	+	-	-	-	ND
VirB11	IM	+	+	+	-	+
VirB4	IM	+	ND	ND	+	ND

The data for VirB-protein localization and interactions detected with dihybrid-assays are from other publications and refer to the *A. tumefaciens* T4SS. IM: inner membrane; OM: outer membrane; ND: not defined

To assess whether the sequence stretches of VirB1 that interact with other proteins are spatially clustered or not, *E. coli* Slt70 was used as a model to approximate the structure of VirB1 (Fig. 4). The amino acid residues of *E. coli* Slt70 that correspond to amino acids from VirB1 interacting with other VirB proteins are shown in Fig. 47. The peptide array experiment yielded signals of different intensity corresponding to peptides featuring parts of the VirB1 sequence. The corresponding sequences were aligned and defined regions of interaction. For each interacting region, the intensity of the signals constituting it was categorized into four classes, from “weak” to “very strong”. This classification did not compare signal intensities between peptide array experiments with different proteins and therefore, a “strong” interaction of VirB1 peptides with VirB8 might be classified as “intermediate” in a peptide array with VirB9. The studies are therefore semi-quantitative and need to be followed up by more quantitative methods in future. VirB8 and VirB9 apparently interacted with loop regions of VirB1 that are most likely situated on different sides of the protein, and VirB11 may bind to a part of the protein that connects these two. There was no apparent interference with the active site cleft, and the amino acids identified here are not involved in the stabilization of the tertiary structure of the protein. Amino acids important for

interactions are expected to localize on the surface of a protein and this is observed here, adding credibility to the model. Most of the proposed interactions between VirB1 and VirB9 could not be visualized in this model since they map to the C-terminal part of VirB1, which lacks a counterpart in Slt70. A model, which integrates the postulated interactions with results from functional studies with *A. tumefaciens*, will be shown below (Fig. 48).

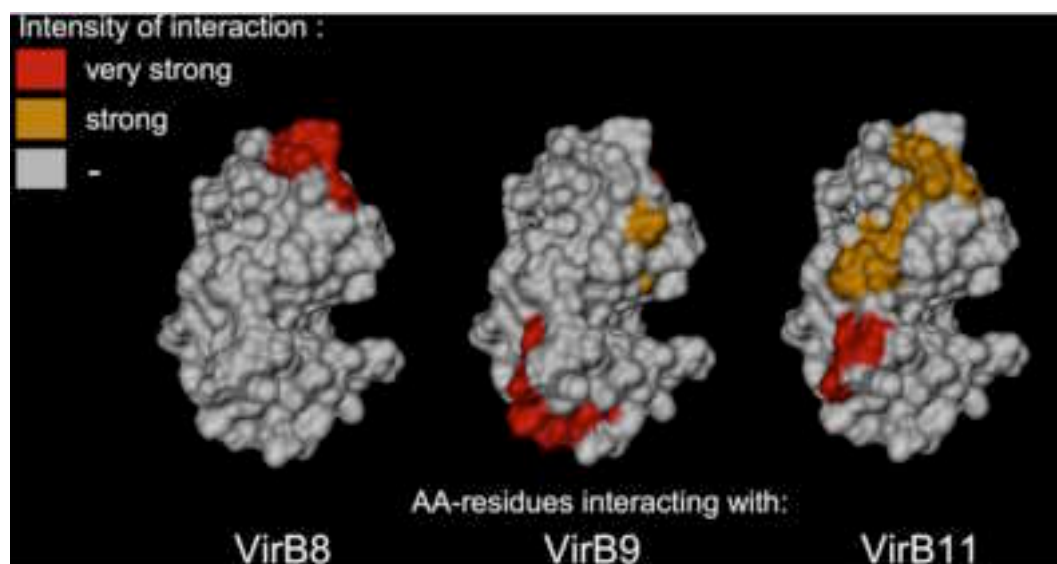


Fig. 47. Regions of *B. suis* VirB1 that are bound by VirB proteins in peptide array experiments. View of the *E. coli* Slt70 SLT domain surface structure like that shown in Fig. 4; regions of VirB1 interacting with VirB8, VirB9 and VirB11 as defined by the peptide array experiments are shown. Grey colour indicates no significant interaction, orange color indicates strong and red color very strong interaction with the different VirB proteins.

Our experiments did not provide any evidence for a direct interaction between VirB1 and VirB10. An interaction between these proteins was suggested by the finding that in Ti-plasmid-free *A. tumefaciens* expressing *virB7-virB10* the correct membrane localization of VirB10 could be achieved by expression of *virB1-virB3* but not of *virB2-virB4* (Liu and Binns, 2003). This could be explained by a direct interaction of VirB1 with VirB10 or an indirect interaction via correct localization of VirB9, which then interacts with VirB10 (Das and Xie, 2000). Alternatively, the correct localization of VirB10 could be achieved through localized cell wall lysis mediated by the transglycosylase activity of VirB1, which does not require a direct interaction. In contrast to our findings data supporting a direct interaction between VirB1 and VirB10 were obtained in a dihybrid assay (Ward *et al.*, 2002), but the results of our work did not substantiate these findings.

1.3. VirB1 is an important component of the *B. suis* T4SS

It was previously demonstrated that VirB1 orthologs play an important role in the T4SS of *A. tumefaciens* and *E. coli* strains harbouring pKM101; the efficiency of substrate transfer was reduced 10- to 1000-fold upon non-polar deletion of the encoding genes (Berger and Christie, 1994). An infection assay with signature tagged *B. abortus* mutants

demonstrated that mutagenesis of the *virB1* gene causes attenuation of virulence (Hong *et al.*, 2000). A more recent study demonstrated that survival of *B. abortus* in macrophage cell cultures was strongly attenuated in strains carrying a non-polar *virB1* mutation (Hartigh *et al.*, 2004). Taken together, the deletion of genes encoding VirB1 orthologs generally has an attenuating effect on T4SS related functions. One way to assess this effect in greater detail was enabled by the finding that VirB1 is also important for T4SS-mediated DNA uptake in *A. tumefaciens* (Liu and Binns, 2003).

Conjugation experiments proved that expression of *B. suis virB3-virB12* in *A. tumefaciens* facilitated plasmid transfer into these cells, indicating at least partly functional assembly of the heterologous T4SS. When the *virB1* gene was added to this subset of the *virB* operon, the recipient efficiency increased approximately 8-fold, which underscores the very important role of VirB1 for T4SS function. Surprisingly, the levels of VirB proteins were decreased as compared to *virB3-virB12* when *B. suis virB1-virB12* were expressed in *A. tumefaciens* and the recipient efficiency was drastically reduced. Analysis of VirB1 and VirB2 protein levels in this strain suggests that the two proteins exerted a reciprocal negative effect on each other's level in the cell. The reduced level of VirB1 in UIA143 pTrc300VirB1-B12 may be a cause for the low recipient efficiency. VirB2 from the *A. tumefaciens* T4SS requires a specific post-translational processing reaction, which leads to the formation of a 74 amino acid long cyclic peptide (Lai *et al.*, 2002). It is conceivable that similar processing of *B. suis* VirB2 may not have occurred in *A. tumefaciens* due to the substrate specificity of the involved proteases (Lanka and Haase, 1997). High amounts of improperly processed and probably misfolded VirB2 may inhibit the correct assembly of the T4SS in the *A. tumefaciens* membranes and this may explain the fact that *virB2*-expressing strains cannot serve as pLS1 recipients. This conclusion is in accord with the results of a study using crosslinking to assess VirB protein interactions in UIA143 pTrc300VirB1-B12. VirB-specific signals that corresponded to defined crosslinking products were decreased in samples from UIA143 pTrc300VirB1-B12, as compared to samples from UIA143 pTrc300VirB1-B3-B12 (Carle, 2004), suggesting major differences of T4SS assembly.

If misfolded VirB2 was responsible for impaired T4SS assembly, this could also explain the observation that UIA143 pTrc300VirB3-B12 was a much better recipient for conjugative pLS1 transfer than UIA143 pTrc300VirB1-12. An alternative explanation is that contact-promoting structures on the *A. tumefaciens* donor cell are blocked by *B. suis* VirB2 on the recipient cell. However, this possibility appears not very likely since *B. suis* VirB2 was not detected in fractions of exocellular high MW structures, whereas the putative minor pilus component VirB5 could easily be detected. This observation was exploited in another experiment, which underscored the importance of VirB1. It was shown that the active site E

residue of VirB1 was required to ensure the presence of VirB5 in exocellular high MW fractions, suggesting that the enzymatic activity of the lytic transglycosylase is necessary for pilus biogenesis of the *B. suis* T4SS.

1.4. Structure-function analysis of VirB1

Comparative analyses of structure and sequence of the soluble lytic transglycosylases Slt70 and Slt35 from *E. coli* identified general active site requirements of this enzyme family (van Asselt *et al.*, 2000). The definition of a sequence motif consisting of three significantly conserved amino acid stretches led to the identification of genes encoding lytic transglycosylases, which contribute to a variety of macromolecular secretion systems (Koraimann, 2003). In contrast to other genes from the *A. tumefaciens* *virB* operon or its orthologs, deletion of *virB1* genes has just an attenuating effect on substrate secretion in most cases. It was speculated that the localized lysis of the cell wall catalyzed by these proteins might be partly complemented by other murein-metabolizing enzymes. In spite of suggestive evidence for a role of VirB1-like proteins in murein metabolism, direct evidence for their enzymatic activity was not provided until now. The most convincing line of evidence was that overproduction of P19, the putative lytic transglycosylase from IncP plasmid RI, led to perforation of the bacterial cell envelope (Bayer *et al.*, 2001). Moreover, mutation of the active site E residues of P19 and VirB1 essentially abolished their abilities to complement the defects in their respective T4SS (Mushegian *et al.*, 1996). The notion that VirB1-like proteins likely act on the conserved murein substrate led to the hypothesis that, in contrast to other T4SS components, the exchange between different VirB1 orthologs might be possible (Koraiman, 2003).

I have applied a variety of different assays, such as T-pilus formation and IncQ-plasmid transfer, to demonstrate that despite limited sequence similarities *B. suis* VirB1 and TraL (pKM101) complemented the *virB1* defect in *A. tumefaciens* PC1001. In contrast, production of other orthologs such as F169 and HP0523 did not restore T4SS function in PC1001. Interestingly, the complementing VirB1 orthologs share a C-terminal extension, which is absent in the non-complementing proteins. In *A. tumefaciens*, this C-terminal extension (VirB1*) is removed by proteolytic processing and it exerts an important role, since its production alone partially complemented *virB1* defects (Llosa *et al.*, 2000). We suggest that the presence of a C-terminal domain in *B. suis* VirB1 and TraL (pKM101) was responsible for the outcome of the experiment. In addition, mutations were introduced into the genes at a position encoding the putative active site E residues and this abolished the complementation of TraL and *B. suis* VirB1. In contrast, *A. tumefaciens* VirB1^{E->A} retained residual activity, which further underscored the functional importance of VirB1*. Changes of the active site did not interfere with processing and secretion of VirB1*,

ruling out an autocatalytic cleavage impacted by the enzyme's transglycosylase active site (Höppner *et al.*, 2004).

Since the interaction of VirB1* with other T4SS components such as VirB9 was demonstrated *in vivo* (Baron *et al.*, 1997), it was relevant to further dissect the processing reaction by the creation of VirB1 variants with alterations of the cleavage site sequence. Seven variants surrounding this A-rich sequence motif were tested for their ability to complement strain PC1001. The amounts and molecular masses of processing products differed from VirB1* wild type in most cases. The strongest effects were observed in case of VirB1^{ΔAA}, VirB1^{A->D} and VirB1^{A->P} where alternative processing and changes of the quantities and molecular masses of the secreted products were obvious. The effect was most pronounced for VirB1^{A->D}, which altered the -1 residue respective to the cleavage site. This change had a weak but significant effect on the complementation of PC1001 T-pilus formation, IncQ-transfer and tumor formation (G. Nair, personal communication). When a Western blot using VirB1-specific antisera was performed with samples from a time course expression of VirB1^{A->D}, a number of processing products were detected, which are not commonly observed in case of the WT VirB1. Since the N-terminal SLT domain of VirB1 was never detected in Western blots (Baron *et al.*, 1997), it is reasonable to assume that these VirB1-specific signals are caused by aberrantly processed VirB1^{A->D}. Moreover, these aberrant VirB1* forms were not detected in culture supernatants of cells producing VirB1^{A->D}, indicating that efficient cleavage and secretion are likely linked.

These findings may constitute an analogy to those reported in the case of major pilus component VirB2, which is processed at a triple-A motif. The resulting C-terminal part of the protein is denominated the VirB2 pilin and it is translocated to the cell exterior and assembled into the T-pilus (Lai and Kado, 1998). Since the cleavage sites of VirB1 and VirB2 are very similar, and the cleavage products VirB1* and VirB2 pilin have the same length (73 versus 74 amino acids), it is reasonable to assume that processing occurs by the same as of yet unidentified protease. Changes of the first A of the VirB2 cleavage site to D led to a loss of pilus incorporation, detection of VirB2 propilin in cell lysates and significantly reduced virulence (Lai *et al.*, 2002). The phenotypes of such a strain and a non-polar *virB1* deletion mutant are basically identical since VirB1 is required for T-pilus formation (Lai *et al.*, 2000). Thus, the effect of a VirB1 cleavage site variant could be explained by interference of the unprocessed protein with T4SS biogenesis. Propeptides from other processed and secreted virulence factors like elastase and subtilisin assist folding of the protease before they are proteolytically removed (Mclver *et al.*, 1995). VirB1* might exert a similar function on the VirB1 SLT domain and/or VirB2.

The results of the analysis of cleavage site variants support the notion that F169 and HP0523 did not complement PC1001 because they do not possess a VirB1*-like region. To test this hypothesis, a hybrid protein was created comprising the *A. tumefaciens* VirB1 signal peptide, the SLT domain of HP0523 and C-terminal VirB1*. SP-HP0523-VirB1* was processed to yield VirB1* and partially complemented pilus formation. However, pilus fractions from strains expressing *sp-hp0523-virB1** contained trace amounts of VirB8, which suggests lysis of the cells upon production of the hybrid protein. This leaves the possibility that the extracellular localization of VirB2 may be caused by limited cell lysis and not by pilus assembly. In contrast to pilus formation, other bioassays performed with PC1001 pTrcSP-HP0523-B1 delivered no evidence for functional complementation. Taken together, the results suggest that the hybrid protein may be able to complement pilus biogenesis, but not the full T4SS function.

An overview of the properties of *A. tumefaciens* strains expressing different *virB1* constructs is shown in Table 10.

Table 10. Relative efficiency of PC1001 complementation by different VirB1 variants.

Strain:	PC1001 ¹⁾	PC1001 pTrcB1 ¹⁾	PC1001 pTrcB1 ^{E→A 1)}	PC1001 pTrcB1-N (SLT)	PC1001 pTrcB1 ^{A→D 1)}	PC1001 pTrcB1*
<i>virB1</i> -genotype:	$\Delta virB1$	WT	<i>virB1 E60A</i>	<i>virB1</i> Δ 173-252	<i>virB1 A172D</i>	<i>virB1</i> Δ 29-172
Transfer efficiency (%)	9,4 +/- 4,7	100 +/-47	18,8 +/- 9,4	8,2 +/- 2,4 ³⁾	40 +/- 20	14 +/- 2,4 ³⁾
Tumor formation:	+	+++	++	++ ²⁾	+++	++ ²⁾
T-pilus:	-	+++	-	- ³⁾	++	- ³⁾

The relative efficiency of the indicated donor strain to transfer IncQ-plasmid pLS1 to UIA143 pTiA6 was determined in at least three independent experiments. SLT: soluble lytic transglycosylase domain; +++: strong, ++: significant, +: weak, -: absent. Data are taken from: this work ¹⁾; (Llosa et al, 2000) ²⁾; (Höppner, 2000) ³⁾

1.5. Multiple roles of VirB1

A large amount of information on the role of VirB1 was collected in previous studies. Together with this analysis of protein interactions of VirB1 from the *B. suis* T4SS and the results from functional studies conducted with both the *A. tumefaciens* and *B. suis* T4SS, a model can be designed describing the function(s) of VirB1 as follows.

Upon expression of the *virB* operon, all VirB proteins possessing a N-terminal signal peptide are exported into the periplasm or partially traverse the inner membrane. By self-interaction of its C-terminal NORS-region, VirB1 forms a 50 kDa homo-dimer, which may render the active site inaccessible. The predicted pore size of the peptidoglycan layer

permits diffusion of globular proteins larger than 55 kDa (Dijkstra and Keck, 1996), and therefore, VirB9, VirB7, VirB5, VirB2 and the VirB1 dimer freely diffuse in the periplasm (Fig. 48a). The contact between VirB1 and VirB9 is mediated via the C-terminus of VirB1 and leads to activation of the lytic transglycosylase activity of VirB9-bound VirB1. This step may lead to a conformational change, followed by processing of VirB1 at its VirB1* cleavage site by signal peptidase I (SPI), which also cleaves the VirB2 propilin. Interactions with inner membrane proteins such as the NTPases VirB11 and VirB4 may localize subunits of the T4SS to the site of peptidoglycan degradation (Fig. 48b). Assembly of VirB7 and VirB9, which subsequently recruit other channel components such as VirB10 and VirB8, accompanies the opening of the cell wall. Next, VirB10 exerts its proposed role to bridge the periplasm between the NTPases of the inner membrane and the VirB9-VirB7 subassembly. The N-terminal part of VirB1 is subsequently degraded in order to protect cellular integrity, whereas the C-terminal domain remains attached to VirB9 (Fig. 48c). The VirB2 pilin may next interact with VirB1*, which may facilitate correct folding and/or passage to the extracellular space through the nascent pilus channel. This scenario is supported by results from a chemical crosslinking assay with isolated Ti-pili, which showed interaction of VirB2 and full-length VirB1 (Krall, 2004). In addition, in a non-polar *virB1*-mutant decreased level of VirB2 was detected in the cell whereas deletions of all other *virB* genes did not have such an effect (Lai *et al.*, 2000), which further supports a functional interaction between the two proteins. While interactions between the other VirB proteins promote T4SS assembly (Fig. 48d), VirB2/VirB1* and VirB5 are translocated to the exterior of the cell, VirB1* is released, triggering assembly of the pilus components (Fig. 48e). VirB1* may exert an additional function in host cell recognition, but the model proposed here accounts for its contribution to T4SS assembly and its accumulation in the extracellular space.

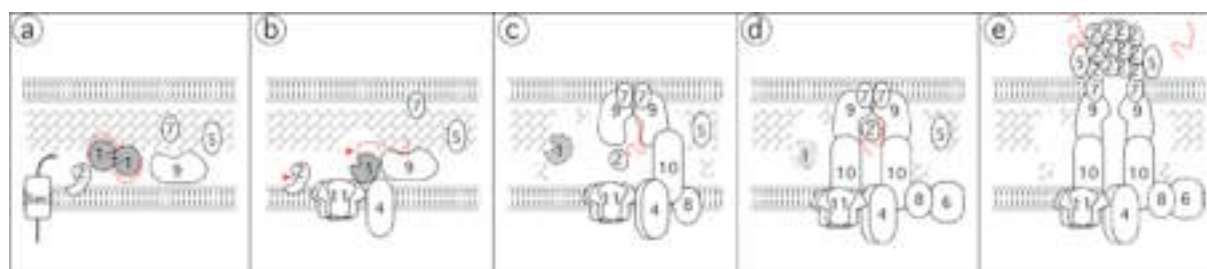


Fig. 48. Model of T4SS assembly emphasizing the role of VirB1. The model is based on all the data available on T4SS subunit contacts and assembly (Cascales and Christie, 2003). The VirB1 SLT domain is labeled in grey, the unordered C-terminal NORS region in red. Red arrowheads symbolize action of a protease, possibly signal peptidase I (SPI). The VirB proteins are indicated by their respective numbers in the *A. tumefaciens* or *B. suis* *virB* operon. Bottom: cytoplasmic side, Sec: machinery of the general secretion pathway.

VirB1 orthologs are not present in all T4SS, but they obviously play an important role. T4SS without VirB1-like components may benefit from coordinated induction of the *virB* genes with the up-regulation of genes responsible for peptidoglycan metabolism, which ensures the formation of openings in the cell wall. This would require coordinated expression of genes located at different positions in the genome and an example of this principle is *Caulobacter crescentus*. This organism possesses a lytic transglycosylase, which permits assembly of the flagellar basal body hook complex at the cell pole of swarmer cells. The protein PleA is transcriptionally autonomous and upregulated only for a short time period in the predivisional cell when this activity is needed (Viollier and Shapiro, 2003). Taken together, it is evident that the localized lysis of the murein layer is important for the efficient assembly of the T4SS. In many systems this is achieved through coordinated expression of the lytic transglycosylase genes with those of the components of the membrane spanning structure. However, the presence of naturally occurring openings in the murein layer or the activity of cell wall metabolic enzymes may be sufficient to allow limited assembly of functional T4SS. This explains the severely attenuated phenotype of *virB1* mutants, which might not be able to assemble sufficient amounts of T4SSs for wildtype-like effector secretion.

2. VirB11, the hexameric traffic (d)NTPase from T4SS

2.1. Structural conservation in diverse systems

VirB11 orthologs are indispensable for correct assembly and function of T4SS. Five different orthologs from well-characterized T4SS were analyzed in the context of this work to gain insights into their structure, biochemical properties and inhibition by different small molecules. The VirB11 ortholog from *H. pylori* consists of two domains with approximately equal length and both are comprised of extended central β sheets (Savvides *et al.*, 2003). The connecting linker region close to residue I134 is in close structural proximity to the Walker A motif, which is responsible for nucleotide binding and hydrolysis. A notable feature discovered upon alignment of sequences of VirB11 orthologs is that conserved residues are not evenly distributed in the N- or C-terminal domain. The HP0525 N-terminal domain comprises 133 amino acids, which constitutes 40.3% of the entire protein. Only 25.7% of the amino acids, which are identical among the five analyzed VirB11 orthologs, and only 24.8% of all amino acids scored from 7 to A in an AMAS alignment (indicating high conservation), localize in this domain. The conservation of amino acids is therefore much higher in the C-terminus of the proteins. The significance of this finding is evident knowing that the more rigid C-terminus of this inner membrane protein was suggested to be inserted in the inner membrane and to mediate the oligomerization (Yeo and Waksman, 2004). In contrast, the more flexible N-terminus may be in contact with the periplasm and may be involved in

diverse protein-protein interactions as suggested by dihybrid analysis with the *A. tumefaciens* ortholog (Ward *et al.*, 2002). Two prominent stretches in the N-terminal part of VirB11 ortholog do not contain any conserved residues. They correspond to the HP0525 residues M1 to L35, which constitute an α -helical region, and E64 to R80, which constitutes an extended loop region. Together, these domains form structurally adjacent parts of the N-terminus that likely face the periplasm. The lower degree of conservation can be explained assuming that the N-terminal part interacts with T4SS components that vary between the different organisms using these secretion machineries. In contrast to that, the highest degree of sequence conservation was found in case of amino acids that are parts of the substrate binding cleft or contribute to catalytic activity, tertiary structure and homomultimer formation. Those features of VirB11 are presumably more conserved between the orthologs.

2.2. Similar enzymology of VirB11 orthologs from T4SS

The hexameric VirB11 orthologs were purified as N-terminally StrepII-tagged proteins from *E. coli* cell lysates. The enzymologies of all proteins were very similar, and they had a strong preference for ATP or dATP hydrolysis at the pH value of 7.5. In a previous study, the native proteins VirB11 from *A. tumefaciens* and TrwD from plasmid pR388 were analyzed with a different assay relying on Phosphorimager/storage phosphor technology, utilizing radioactively labeled NTPs and a competition assay to establish substrate preference (Krause *et al.*, 2000). The results of the present study differ from the previous one concerning the optimal pH value, the utilized substrates and v_{MAX} . These differences may be a result of the different assay methods, buffer conditions and protein purification protocols, but many results were entirely consistent in both studies.

For example, the formation of hexamers, the requirement for divalent cations, the substrate preference for ATP and dATP and the inefficient utilization of dTTP and dCTP were observed in both studies (Krause *et al.*, 2000). In Krause *et al.*, the pH value promoting maximum substrate turnover was found to be 9.5 for HP0525 and TrbB, the latter having a second maximum at pH 7.5. In this work pH 7.5 was found to be the optimal pH for all VirB11 orthologs and the activity of StrepII-HP0525 was higher than the activity described for native HP0525. The results of this work therefore prove that the addition of N-terminal StrepII and TrxA tags did not impair hexamer formation of the VirB11 orthologs, and the tags have greatly facilitated protein purification. The high degree of conservation of the active site region was reflected by similar substrate requirements. One observation that had not been described until now is the positive cooperativity of substrate conversion, which was indicated by the sigmoidal shape of the curve when substrate concentration was plotted versus the enzyme velocity. This is a characteristic feature of cooperative enzymes whose kinetics cannot be described by the classic Michaelis-Menten equation (Stryer, 1997).

2.3. Inhibitors act on all VirB11 orthologs

The *in vitro* effect of the novel inhibitory compound MTFPT, originally denominated CHIR-1, was not specific although the molecule was identified in a high-throughput-screen for inhibitors of the native hexameric HP0525 (Chiron Diagnostics, unpublished). I showed here that this effect extends to a number of orthologs from different T4SS. The potency of MTFPT was analyzed *in vivo* in a *H. pylori* tissue culture infection model and with purified HP0525 without an N-terminal tag. The inhibition occurred at significantly lower concentrations than those found in this study (this work; W. Pansegrau, Chiron personal communication). In spite of the quantitative differences, the data presented here are qualitatively similar to those obtained by our collaborators. In addition, the results are very similar in case of the two VirB11 orthologs analyzed in most detail, *H. pylori* StrepII-HP0525 and *B. suis* StrepII-VirB11.

For both enzymes very similar IC₅₀ values were determined, and the fact that changes of the substrate concentration did not alter this value constitutes convincing evidence against a competitive mode of inhibition. The data were analyzed using a *Dixon plot*, which is a plot of 1/v against [Inhibitor] and a *Cornish-Bowden plot* of S/v against [Inhibitor], and the results strongly suggest a non-competitive or mixed-uncompetitive mode of inhibition in case of both enzymes (Cortés *et al.*, 2001). This type of analysis was not carried out for the other VirB11 orthologs, but inhibitory effects were observed and the IC₅₀-values were within the same range of 10 to 200 micromolar.

It was reported previously that phospholipids such as cardiolipin and phosphatidylglycerol stimulate the ATPase activity of VirB11 orthologs (Krause *et al.*, 2000). Others reported that unsaturated fatty acids inhibit the enzymatic activity of TrwD in a non-competitive manner (C. Machón, unpublished). This question was analyzed here and to this end, oleic acid and linoleic acid were added to the ATPase assays with VirB11 orthologs. The effect of both fatty acids on TrwD was confirmed since the activity of StrepII-TrwD decreased similar to previous reports. In contrast, StrepII-TraG and StrepII-VirB11 were not inhibited. Remarkably, a strong negative effect of both oleic and linoleic acid on the activity of the *H. pylori* ortholog was observed and these results suggest interesting follow-up work. Oleic and linoleic acid are non-toxic and water-insoluble components found in plants and they are not only utilized in a number of processes in the food industry but also are enriched in many products such as cottonseed or olive oil. We suggest that the search for a non-toxic pharmaceutical product to cure *Helicobacter* infections should be viewed in the light of the ability of oleic and linoleic acid to disable the Cag-PAI *via* HP0525 inhibition. In any case, good pharmacokinetic properties of biologically active compounds are important for its further

development and in the case of MTFPT the *in vitro* effect had to be assessed in a number of suitable *in vivo* assays.

When conjugation assays with *A. tumefaciens* were conducted to assess the effect of MTFPT, it became apparent that it has a bacteriostatic or even bactericidal effect on *Agrobacterium* cells at concentrations higher than 10 μ M under these conditions. Therefore, we could not assess the effect on the T4SS in this organism. The growth inhibition of *Agrobacterium* was only tested on minimal media since this is required for *virB* induction. MTFPT may have no effect on *Agrobacterium* when is cultured on rich media, but this was not tested. Instead, we exploited the ability of MTFPT to inhibit IncP, -W and -N conjugation between *E. coli* cells. The inhibitor did not have toxic effects on this organism at concentrations up to 1 mM. For all tested plasmids, the T4SS-mediated conjugative transfer was significantly reduced in the presence of more than 100 μ M MTFPT, which confirmed the results of the *in vivo* analysis. The pKM101-determined pilus serves as receptor for the lytic bacteriophage IKe. I conducted an assay exploiting this fact and showed that decreased conjugation efficiency correlated with decreased availability of the pilus phage receptor. The data obtained *in vitro* were thus confirmed by the *in vivo* experiments. Inhibition of the ATPase had the consequence that the *tra* operon-determined T4SS could not elaborate a pilus structure, and MTFPT had similar effects on the secretion machineries encoded on pR388 and pRP4. Major obstacles that became apparent in the course of these experiments are the insolubility of MTFPT in water and the high concentrations that were needed to cause an effect. It is nevertheless reasonable to assume that this component may serve as a lead compound for development in a medicinal chemistry program, which may lead to potent broad-spectrum T4SS-inhibitors.

3. Complementation of a VirB11 mutant

The observation that VirB proteins from different T4SSs complement each other's function was encouragement to perform a complementation experiment with the VirB11 orthologs from *A. tumefaciens* and *B. suis*. However, expression of the *virB11* gene from *B.suis* did not complement the *virB11* defect in *A. tumefaciens* PC1011. The amino acid identity between the proteins is only 33%, and many of the conserved residues are likely part of the active site pocket and homo-multimerization domain. The protein interface responsible for interactions with other T4SS components such as VirB9, VirB10 and VirB4 (Ward *et al.*, 2002; Zhou and Christie, 1997), seems to be more variable, which explains why complementation was not observed in this case.

In contrast to that, it was a very unexpected finding that VirB11 from *A. tumefaciens* strain C58 did not complement IncQ plasmid transfer in the *A. tumefaciens* strain A348

derivative PC1011. In contrast to that, tumor development following infection of *K. diagrammontiana* leaves and the amount of Ti-pili were undistinguishable between the complemented strain and the WT. These observations are reminiscent of previous reports showing that heterologous production of VirB11 from *A. tumefaciens* strain A348 with certain amino acid substitutions uncoupled pilus production from the ability to transfer T-DNA and IncQ plasmids (Sagulenko *et al.*, 2001).

VirB11 from *A. tumefaciens* strains C58 and A348 have an overall amino acid identity of 90%, and all but one of the residues, which were proven to be important for the complementation of PC1011 in previous studies (Sagulenko *et al.*, 2001), were identical. Earlier, it was shown that expression of strain A348 *virB11*Q135E in PC1011 complemented pilus production and T-DNA transfer, while IncQ-transfer was attenuated 4,5-fold (Sagulenko *et al.*, 2001). The C58 VirB11 protein used in the present work carries H instead of a Q in position 135, and this may explain the complementation phenotype described here. Moreover, results from the cited publication show that stronger expression of A348 *virB11* WT resulted in decreased efficiency of IncQ transfer. It is therefore assumed that the strong, *trc* promotor-driven expression of C58 *virB11* carrying a substitution at the position corresponding to Q135 is even less supportive for complementation of IncQ-transfer. Taken together, the above findings give a clear indication as to why strain C58 VirB11 does not substitute in the pLS1 transfer assay for its very similar ortholog from strain A348.

4. Interaction of VirB11 and VirB5

Like all other proteins encoded by the *A. tumefaciens virB* operon, VirB11 is required for T-DNA transfer and T-pilus elaboration (Lai *et al.*, 2000). Many interactions of this protein with other components of the T4SS have been proposed (Ward *et al.*, 2002; Zhou and Christie, 1997). The absence of pili in a *virB11* deletion mutant was always regarded as a consequence of the loss of T4SS assembly caused by the absence of the energy provided by the ATPase. In the course of previous studies on VirB11, certain variants of the conserved His box (258-270) were found to uncouple the contribution of VirB11 to pilus formation and substrate translocation. Most significantly, the protein VirB11^{I265T} mediated transfer of T-DNA and IncQ-plasmids at wild type levels but T-pili were not detected (Sagulenko *et al.*, 2001). Western blot analysis demonstrated that quantity of the pilus-associated protein VirB7 (Krall *et al.*, 2002) in exocellular fractions of a VirB11^{I265T}-producing *virB11* mutant was indistinguishable from the WT, whereas correct localization was impaired in a non-polar *virB11* mutant (Sagulenko *et al.*, 2001). As the mutation has an effect exclusively on pilus biogenesis, it was hypothesized that VirB11 may guide VirB2 folding and pilus assembly. Overlay assays did not give evidence for direct interaction between VirB11 and VirB2, but in

contrast, an interaction of the minor pilus component VirB5 and VirB11 was detected (Krall, 1999), which prompted further analysis of this question. The original result was confirmed in this study, but only in case of the *A. tumefaciens* T4SS. Neither the orthologs from *B. suis* nor IncN-plasmid pKM101 interacted in a comparable manner with their respective VirB11 orthologs. Since this method relies on re-naturation of membrane-bound VirB11 orthologs and interaction with soluble VirB5 orthologs, there are many possible explanations for our inability to observe interactions, such as not suited buffer conditions, refolding times or temperatures. Other biochemical methods need to be applied in future to assess whether the interaction between *A. tumefaciens* VirB5 and VirB11 reflects a biologically relevant phenomenon.

Summary

The aim of this study was to unravel general properties of two VirB proteins that participate in the biogenesis of T4SS in the human and animal pathogenic bacterium *B. suis* and the plant pathogen *A. tumefaciens*. Using biochemical and functional studies and the comparative analysis of orthologs from different T4SSs we gained novel insights into the mechanism of these macromolecular translocation systems. The work focused on VirB1, a lytic transglycosylase present in many but not all T4SS, and on VirB11, a hexameric ATPase ubiquitously present in all type II and type IV secretion systems.

VirB1 orthologs share a conserved active site signature. A C-terminal domain, classified as structurally unordered NORS-region, characterizes some members of this family. In *A. tumefaciens*, this region is proteolytically cleaved, possibly by action of periplasmatic proteases or of SPI, and it is then secreted. Functional studies showed that a highly conserved active site E is crucial for its activity and that VirB1-like proteins are to some extent interchangeable between different T4SSs. In *A. tumefaciens*, an active site variant of VirB1 partially complemented the non-polar *virB1* mutant. This may be explained by the fact that the C-terminal VirB1* domain is involved in stabilizing interactions with other T4SS components. Not surprisingly, variations of the C-terminal processing site reduced the complementation of the *virB1* deletion strain, showing that the processing event is functionally important.

Different biochemical techniques were applied to characterize interactions of *B. suis* VirB1 with other T4SS components. Genes from the *B. suis virB* operon were cloned into expression vectors, and large amounts of affinity-tagged *Brucella* proteins were purified and applied to various assays. VirB1 interacted with itself, possibly forming dimers, and the binding of GroEL, likely to the VirB1 C-terminus, was observed. Subsequent experiments demonstrated interactions of VirB1 with VirB9 and VirB11, whereas tests of the VirB8 interaction yielded contradictory results and VirB10 did not interact with VirB1. Mapping of VirB1 peptides that interact with other VirB proteins underscored the importance of the C-terminus, especially for the VirB1-VirB9 interaction. Heterologous expression of different *B. suis virB* operon constructs in *A. tumefaciens* revealed functional assembly of the T4SS, but also emphasized the importance of the contribution of VirB1. Taken together, the data suggested a refined model of VirB1 action in T4SS biogenesis.

The VirB11 orthologs from two mammalian pathogens, a plant pathogen and two broad-host-range plasmids were cloned into vectors suited for protein overproduction. The

active hexameric ATPases were purified as N-terminal fusion proteins and their enzymatic properties were characterized. The effect of MTFPT, a putative lead for novel anti-infective drugs targeting the *H. pylori* ortholog of VirB11, was tested both *in vitro* and *in vivo*. Enzyme assays demonstrated non-competitive inhibition of all tested ATPases and similar effects on T4SS function were observed *in vivo*. The unsaturated fatty acids oleic- and linoleic acid also inhibited some of the VirB11 orthologs *in vitro*, among them HP0525 from *H. pylori*, and this finding may be relevant for anti-*Helicobacter* drug discovery programs.

The complexity of VirB11 functions was illustrated by the fact that an ortholog with 90% sequence identity failed to fully complement a non-polar *virB11* mutant, thereby uncoupling T-pilus formation and transfer of only one of the substrates (pLS1). Direct interaction of the pilus component VirB5 with VirB11 was demonstrated in case of the *A. tumefaciens* orthologs in an overlay assay. Using this assay it was not possible to demonstrate similar interactions of the respective orthologs from the pKM101 *tra* region and *B. suis*. Nevertheless, the interaction of VirB11 and VirB5 from *B. suis* was demonstrated in a pulldown assay.

The results in this work did not confirm all the data from the first characterization of MTFPT, which suggested a considerably lower IC₅₀ in the nano-molar range. Nevertheless, the results presented here are qualitatively consistent with previous reports. Since the effects of this inhibitor extend to many VirB11 orthologs it appears to be very promising to further pursue this line of research. Further development of this molecule may lead to the creation of new drugs to fight bacterial infectious diseases, and the characterisation of VirB11 inhibitors gained in this work may contribute to reach this goal in future.

References

- Alksne L. and S. Projan** (2000). "Bacterial virulence as a target for antimicrobial chemotherapy." Curr. Opin. Biotechnol. 11(6): 625-36.
- Balsiger S., Ragaz C., Baron C., Narberhaus F.** (2004) "Replicon-specific regulation of small heat shock genes in *Agrobacterium tumefaciens*." J. Bacteriol. 186(20):6824-9
- Baron C., Llosa M., Zhou S., Zambryski PC.** (1997). "C-terminal processing and cellular localization of VirB1, a component of the T-complex transfer machinery of *Agrobacterium tumefaciens*." J. Bacteriol. 179: 1203-10.
- Baron C., O'Callaghan D., Lanka E.** (2002). "Bacterial secrets of secretion: EuroConference on the biology of type IV secretion processes." Mol. Microbiol. 43: 1359-66.
- Bayer M., Iberer R., Bischof K., Rassi E., Stabentheimer E., Zellnig G., Koraimann G.** (2001). "Functional and mutational analysis of P19, a DNA transfer protein with muramidase activity." J. Bacteriol. 183: 3176-83.
- Berger B. R. and P. J. Christie** (1994). "Genetic complementation analysis of the *Agrobacterium tumefaciens* *virB* operon: *virB2* through *virB11* are essential virulence genes." J. Bacteriol. 176: 3646-60.
- Bhandari P. and J. Gowrishankar** (1997). "An *Escherichia coli* host strain useful for efficient overproduction of cloned gene products with NaCl as the inducer." J. Bacteriol. 179: 4403-06.
- Binns A. N.** (2002). "T-DNA of *Agrobacterium tumefaciens*: 25 years and counting." Trends in Plant Science 7(5): 231-33.
- Blake CC., Koenig DF., Mair GA, North AC., Phillips DC., Sarma VR.** (1965) "Structure of hen egg-white lysozyme. A three-dimensional Fourier synthesis at 2 Ångstrom resolution." Nature 206(986):757-61
- Bloom H., Beier H., Gross H.J.** (1987) Electrophoresis 8:93-9
- Bohne J., Yim A., Binns A.N.** (1998). "The Ti plasmid increases the efficiency of *Agrobacterium tumefaciens* as a recipient in *virB*-mediated conjugal transfer of an IncQ plasmid." Proc. Natl. Acad. Sci. USA 95: 7057-62.
- Boschirolu ML., Ouahrani-Bettache S., Foulongne V., Michaux-Charachon S., Bourg G., Allardet-Servent A., Cazevielle C., Liautard JP., Ramuz M., O'Callaghan D.** (2002) "The *Brucella suis virB* operon is induced intracellularly in macrophages." Proc. Natl. Acad. Sci. 99(3):1544-9
- Breitschwerdt E. and D. Kordick** (2000). "*Bartonella* infection in animals: carriership, reservoir potential, pathogenicity, and zoonotic potential for human infection." Clin. Microbiol. Rev. 13(3): 428-38.
- Burlingham BT. and TS. Widlanski** (2003). "An intuitive look at the relationship of K_i and IC_{50} : A more general use for the Dixon plot." J. Chem. Ed. 80(2):214-18
- Cao T. B. and M. R. J. Saier** (2001). "Conjugal type IV macromolecular transfer systems of Gram-negative bacteria: organismal distribution, structural constraints and evolutionary conclusions." Microbiology 147: 3201-14.
- Carle, A.** (2004). Doctoral thesis. Department I. Munich, LMU.
- Cascales E. and P.J. Christie** (2004). "Definition of a bacterial type IV secretion pathway for a DNA substrate." Science. 304(5674): 1170-3.
- Cascales E. and P. J. Christie** (2003). "The versatile bacterial type IV secretion systems." Nature Rev. Microbiol. 1: 137-49.
- CDC** (2003). Epidemiology and prevention of vaccine-preventable diseases, Centers for Disease Control and Prevention.
- CDC** (2004). Pertussis Disease, Centers for Disease Control and Prevention. 2004.
- The Carter Center** (2002-2003). The Carter Center. Annual Report 2002-2003:18.
- Christie P. J. and J. P. Vogel** (2000). "Bacterial Type IV secretion: conjugation systems adapted for delivery of effector molecules to host cells." Trends Microbiol. 8: 354-60.
- Cogan E.B., Birrell G.B., Griffith O.H.** (1999) "A robotic-based automated assay for inorganic and organic phosphates". Anal. Biochem. 271:29-35
- Comerci D. J., Martinez-Lorenzo M.J., Sieira R., Gorvel J.P., Ugalde R.A.** (2001). "Essential role of the VirB machinery in the maturation of the *Brucella abortus*-containing vacuole." Cell. Microbiol. 3: 159-68.
- Corbel M.** (1997). "Brucellosis: an overview." Emerg. Infect. Dis. 3(2): 213-21.
- Cortes A., Cascante M., Cardenas ML., Cornish-Bowden A.** (2001). "Relationships between inhibition constants, inhibitor concentrations for 50% inhibition and types of inhibition: new ways of analysing data." Biochem. J. 357(1): 263-8.

- Covacci A., Telford J.L., Del Giudice G., Parsonnet J., Rappuoli R.** (1999) "*Helicobacter pylori* virulence and genetic geography." Science 284:1328-33
- Dang T. A., Zhou X.-R., Graf B., Christie P.J.** (1999). "Dimerization of the *Agrobacterium tumefaciens* VirB4 ATPase and the effect of ATP-binding cassette mutations on the assembly and function of the T-DNA transporter." Mol. Microbiol. 32: 1239-53.
- Das, A. and Y.-H. Xie** (2000). "The *Agrobacterium* T-DNA transport pore proteins VirB8, VirB9 and VirB10 interact with one another." J. Bacteriol. 182: 758-63.
- Datta, N. and R. W. Hedges** (1972). "Trimetoprim resistance conferred by W plasmids of *Enterobacteriaceae*." J. Gen. Microbiol. 72: 349-55.
- Dehio, C.** (2001). "*Bartonella* interactions with endothelial cells and erythrocytes." Trends Microbiol. 9: 279-85.
- Demchick P. and A. Koch** (1996). "The permeability of the wall fabric of *Escherichia coli* and *Bacillus subtilis*." J. Bacteriol. 178(3): 768-73.
- den Hartigh AB., Sun YH., Sondervan D., Heuvelmans N., Reinders MO., Ficht TA., Tsolis RM.** (2004). "Differential requirements for VirB1 and VirB2 during *Brucella abortus* infection." Infect. Immun. 72(9): 5143-9.
- Dijkstra A. J. and W. Keck** (1996). "Peptidoglycan as a barrier to transenvelope transport." J. Bacteriol. 178: 5555-62.
- Eisenbrandt R., Kalkum M., Lai E.M., Lurz R., Kado C.I., Lanka E.** (1999). "Conjugative pili of IncP plasmids, and the Ti plasmid T pilus are composed of cyclic subunits." J. Biol. Chem. 274: 22548-55.
- Evenson R.E. and V. Santaniello** (2004) "The regulation of agricultural biotechnology". CABI Publishing
- FAO** (2004). FAOSTAT Statistical Databases, Food and Agriculture Organization of the United Nations.
- FAO** (1986). WHO Expert Committee on Brucellosis. Geneva, World Health Organization.
- Fiedler S. and R. Wirth** (1988). "Transformation of bacteria with plasmid DNA by electroporation." Anal. Biochem. 170(1): 38-44.
- Galazka A.** (1991). Pertussis mortality, Methods for estimation of number of deaths due to pertussis. EPI Research and Development Group Meeting, Geneva, Switzerland.
- Garfinkel D. J., Simpson R.B., Ream L.W., White F.F., Gordon M.P., Nester E.W.** (1981). "Genetic analysis of crown gall: fine structure map of the T-DNA by site-directed mutagenesis." Cell 27: 143-53.
- Halling SM. Bricker BJ.** (1994). "Characterization and occurrence of two repeated palindromic DNA elements of *Brucella* spp.: Bru-RS1 and Bru-RS2." Mol. Microbiol. 14(4): 681-9.
- Harb O., Gao LY., Abu Kwaik Y.** (2000). "From protozoa to mammalian cells: a new paradigm in the life cycle of intracellular bacterial pathogens." Environ. Microbiol. 2(3): 251-65.
- Higgins D.** (1994). "CLUSTAL V: multiple alignment of DNA and protein sequences." Methods Mol. Biol. 25: 307-18.
- Hoerauf A., Mand S., Volkmann L., Buttner M., Marfo-Debrekyei Y., Taylor M., Adjei O., Buttner DW.** (2003). "Doxycycline in the treatment of human onchocerciasis: Kinetics of *Wolbachia* endobacteria reduction and of inhibition of embryogenesis in female *Onchocerca* worms." Microbes Infect. 5(4): 261-73.
- Hofreuter D., Odenbreit S., Haas R.** (2001). "Natural transformation competence in *Helicobacter pylori* is mediated by the basic components of a type IV secretion system." Mol. Microbiol. 41: 379-91.
- Höltje JV.** (1998). "Growth of the Stress-Bearing and Shape-Maintaining Murein Sacculus of *Escherichia coli*". Microb. Mol. Biol. Rev. 62(1):181-203
- Homann H.E., Willenbrink W., Buchholz C.J., Neubert WJ.** (1991) Sendai virus protein-protein interactions studied by a protein-blotting protein-overlay technique: Mapping of domains on NP protein required for binding to P protein. J. Virol. 65:1304-09
- Hong P., Tsolis R., Ficht TA.** (2000). "Identification of genes required for chronic persistence of *Brucella abortus* in mice." Infect. Immun. 68(7): 4102-7.
- Höppner C.** (2000). Diploma thesis. Department I. Munich, LMU.
- Höppner C., Liu Z., Domke N., Binns A.N., Baron C.** (2004). "VirB1 orthologs from *Brucella suis* and pKM101 complement defects of the lytic transglycosylase required for efficient type IV secretion from *Agrobacterium tumefaciens*." J. Bacteriol. 186(5): 1415-22
- Hwang HH. and SB. Gelvin** (2004) "Plant proteins that Interact with VirB2, the *Agrobacterium tumefaciens* pilin protein, mediate plant transformation." Plant Cell. 16(11):3148-67
- Jakubowski S.J., Krishnamoorthy V., Christie PJ.** (2003) *Agrobacterium tumefaciens* VirB6 protein participates in formation of VirB7 and VirB9 complexes required for type IV secretion. J. Bacteriol. 185(9):2867-78

- Jones, D. A., M. H. Ryder, B. G. Clare, S. K. Farrand, Kerr A.** (1991) "Biological control of crown gall using *Agrobacterium* strains K84 and K1026". In H. Komada, K. Kiritani, and J. Bay-Petersen (ed.), The biological control of plant diseases. 42:161-170
- Kathoon H., Iyer RV., Iyer VN.** (1972). "A new filamentous bacteriophage with sex-factor specificity." Virology 48(145-55).
- Kempf V., Volkmann B., Schaller M. Sander CA., Alitalo K., Riess T., Authenried IB.** (2001). "Evidence of a leading role for VEGF in *Bartonella henselae*-induced endothelial cell proliferations." Cell Microbiol. 3(9): 623-32.
- Killick V.** (2004). Behind the Frieze - Sir David Bruce (1855-1931), London School of Hygiene & Tropical Medicine. 2004.
- Krall L.** (1999). Diploma thesis. Department I. Munich, LMU.
- Krall L.** (2004). Doctoral thesis. Department I, Microbiology. Munich, LMU.
- Krall L., Wiedemann U., Unsin G., Weiss S., Domke N., Baron C.** (2002). "Detergent extraction identifies different VirB protein subassemblies of the type IV secretion machinery in the membranes of *Agrobacterium tumefaciens*." Proc. Natl. Acad. Sci. USA 99: 11405-410.
- Krause S., Pansegrau W., Lurz R., de la Cruz F., Lanka E.** (2000a). "Enzymology of Type IV macromolecule secretion systems: the conjugative transfer regions of plasmid RP4 and R388 and the *cag* pathogenicity island of *Helicobacter pylori* encode structurally and functionally related nucleoside triphosphate hydrolases". J. Bacteriol. 182: 2761-70
- Krause S., Barcena S., Pansegrau W., Lurz R., Carazo JM., Lanka E.** (2000b). "Sequence-related protein export NTPases encoded by the conjugative transfer region of RP4 and by the *cag* pathogenicity island of *Helicobacter pylori* share similar hexameric ring structures." Proc. Natl. Acad. Sci. USA 97: 3067-72.
- Kromayer M., Wilting R., Tormay P., Böck A.** (1996). "Domain structure of the prokaryotic selenocysteine-specific elongation factor SelB." J. Mol. Biol. 262: 413-20.
- Kuldau GA., De Vos G., Owen J., McCaffrey G., Zambryski P.** (1990) "The virB operon of *Agrobacterium tumefaciens* pTiC58 encodes 11 open reading frames." Mol Gen Genet. 221(2):256-66.
- Laemmli U. K.** (1970). "Cleavage of structural proteins during the assembly of the head of bacteriophage T4." Nature 227: 680-85.
- Lai E.-M. and C. I. Kado** (1998). "Processed VirB2 is the major subunit of the promiscuous pilus of *Agrobacterium tumefaciens*." J. Bacteriol. 180: 2711-17.
- Lai E.-M. and C. I. Kado** (2000). "The T-pilus of *Agrobacterium tumefaciens*." Trends Microbiol. 8: 361-369.
- Lai E. M., Chesnokova O., Banta L.M., Kado C.I.** (2000). "Genetic and environmental factors affecting T-pilin export and T-pilus biogenesis in relation to flagellation of *Agrobacterium tumefaciens*." J. Bacteriol. 182: 3705-16.
- Langer P. J. and G. C. Walker** (1981). "Restriction endonuclease cleavage map of pKM101: relationship to parental plasmid R46." Mol. Gen. Genet. 182: 268-72.
- Leung AK, D. H., Honek JF, Berghuis AM.** (2001). "Crystal structure of the lytic transglycosylase from bacteriophage lambda in complex with hexa-N-acetylchitohexaose." Biochemistry 40(19): 5665-73.
- Liu J. and B. Rost** (2003). "NORSp: Predictions of long regions without regular secondary structure." Nucleic Acids Res. 31(13): 3833-5.
- Liu J., Tan H., Rost B.** (2002). "Loopy proteins appear conserved in evolution." J. Mol. Biol. 322(1): 53-64.
- Liu Z. and A. N. Binns** (2003). "Functional subsets of the VirB type IV transport complex proteins involved in the capacity of *Agrobacterium tumefaciens* to serve as a recipient in virB-Mediated conjugal transfer of plasmid RSF1010." J. Bacteriol. 185: 3259-69.
- Livingstone C. and G. Barton** (1993). "Protein sequence alignments: a strategy for the hierarchical analysis of residue conservation." Comput. Appl. Biosci. 9(6): 745-56.
- Llosa M., Zupan J., Baron C., Zambryski P.C.** (2000). "The N- and C-terminal portions of the *Agrobacterium* VirB1 protein independently enhance tumorigenesis." J. Bacteriol. 182: 3437-45.
- LSHTM** (2004) "Behind the Frieze-Sir David Bruce (1855-1931)." London School of Hygiene & Tropical Medicine, <http://www.lshtm.ac.uk/library/archives/bruce.html>
- Lutzmann M., Kunze R., Buerer A., Aebi U., Hurt E.** (2002). "Modular self-assembly of a Y-shaped multiprotein complex from seven nucleoporins." EMBO J. 21(3): 387-97.
- Machon C., Rivas S., Albert A., Goni FM., de la Cruz F.** (2002). "TrwD, the hexameric traffic ATPase encoded by plasmid R388, induces membrane destabilization and hemifusion of lipid vesicles." J. Bacteriol. 184(6):1661-8.
- Madigan M. M., Martinko J., Parker J.** (1997). Brock Biology of Microorganisms, Prentice Hall.

- Masui S., Sasaki T., Ishikawa H.** (2000). "Genes for the type IV secretion system in an intracellular symbiont, *Wolbachia*, a causative agent of various sexual alterations in arthropods." J. Bacteriol. 182(22): 6529-31.
- McGraw E. and S. O'Neill** (2004). "*Wolbachia pipiens*: intracellular infection and pathogenesis in *Drosophila*." Curr. Opin. Microbiol. 7(1): 67-70.
- McIver K.S., Kessler E., Olson J.C., Ohman D.E** (1995) "The elastase propeptide functions as an intramolecular chaperone required for elastase activity and secretion in *Pseudomonas aeruginosa*." Mol. Microb. 18:877-89
- Mushegian A. R., Fullner K.J., Koonin E.V., Nester E.W.** (1996). "A family of lysozyme-like virulence factors in bacterial pathogens." Proc. Natl. Acad. Sci. USA 93: 7321-26.
- Nagai H. and C. R. Roy** (2003). "Show me the substrates: modulation of host cell function by type IV secretion systems." Cell. Microbiol. 5: 373-83.
- Needleman S. and C. Wunsch** (1970). "A general method applicable to the search for similarities in the amino acid sequence of two proteins." J. Mol. Biol. 48(3): 443-53.
- Olsen R. H., Siak J.-S., Gray R.H.** (1974). "Characteristics of PRD1, a plasmid-dependent broad host range DNA bacteriophage." J. Virol. 14: 689-99.
- O'Callaghan D., Cazeville C., Allardet-Servent A., Boschirolu M.L., Bourg G., Foulongne V., Frutus P., Kulakov Y., Ramuz M.** (1999). "A homologue of the *Agrobacterium tumefaciens* VirB and *Bordetella pertussis* Ptl type IV secretion systems is essential for intracellular survival of *Brucella suis*." Mol. Microbiol. 33: 1210-20.
- Pansegrau W., Lanka E., Barth P.T., Figurski D.H., Guiney D.G., Haas D., Helinski D.R., Schwab H., Stanisich V.A., Thomas C.M.** (1994). "Complete nucleotide sequence of Birmingham IncP alpha plasmids. Compilation and comparative analysis." J. Mol. Biol. 239: 623-63.
- Parsonnet, J.** (1998). "*Helicobacter pylori*: the size of the problem." Gut. 43(1): 6-9.
- Paulsen I. T. et al.** (2002). "The *Brucella suis* genome reveals fundamental similarities between animal and plant pathogens and symbionts." Proc. Natl. Acad. Sci. USA 99: 13148-153.
- Petit A., Delhaye S., Tempé J., Morel G.** (1970) "Recherches sur les guanidines des tissus de crown gall. Mise en évidence d'une relation biochimique spécifique entre les souches d'*Agrobacterium tumefaciens*, et les tumeurs qu'elles induisent." Physiol. Veg. 8:205-13
- Pisani P., Parkin DM., Munoz M., Ferlay J.** (1997). "Cancer and infection: estimates of the attributable fraction in 1990." Cancer Epidemiol. Biomarkers Prev. 6(6): 387-400.
- Planet P. J., Kachlany S.C., DeSalle R., Figurski D.H.** (2001). "Phylogeny of genes for secretion NTPases: identification of the widespread *tadA* subfamily and development of a diagnostic key for gene classification." Proc. Natl. Acad. Sci. USA 98: 2503-8.
- Possot O. and T. Pugsley** (1994). "Molecular characterization of PulE, a protein required for pullulanase secretion." Mol. Microbiol. 12(2): 287-99.
- Rabel C., Grahn AM., Lurz R., Lanka E.** (2003) "The VirB4 family of proposed traffic nucleoside triphosphatases: Common motifs in plasmid RP4 TrbE are essential for conjugation and phage adsorption." J Bacteriol. 185(3):1045-58
- Ragan V. and M. Gilsdorf** (2001). Animal and Plant health inspection services: STATUS REPORT - FISCAL YEAR 2001, Cooperative State-Federal Brucellosis Eradication Program.
- Rivas S., Bolland S., Cabezon E., Goni FM., de la Cruz F.** (1997). "TrwD, a protein encoded by the IncW plasmid R388, displays an ATP hydrolase activity essential for bacterial conjugation." J. Biol. Chem. 272(41): 25583-90.
- Rost B.** (1996). "PHD: predicting one-dimensional protein structure by profile-based neural networks." Methods Enzymol. 266: 525-39.
- Rust R. and T. Worrell** (2004). Brucellosis, University of Virginia Hospital and Clinics. 2004.
- Sagulenko E., Sagulenko V., Chen J., Christie P.J.** (2001). "Role of *Agrobacterium* VirB11 ATPase in T-pilus assembly and substrate selection." J. Bacteriol. 183: 5813-25.
- Saint Andre A., Blackwell NM., Hall LR., Hoerauf A., Bratting NW., Volkmann L., Taylor MJ., Ford L., Hise AG., Lass JH., Diaconu E., Pearlman E.** (2002). "The role of endosymbiotic *Wolbachia* bacteria in the pathogenesis of river blindness." Science 295(5561): 1892-5.
- Sakai D., Horiuchi T., Komano T.** (2001). "ATPase activity and multimer formation of PilQ protein are required for thin pilus biogenesis in plasmid R64." J. Biol. Chem. 276(21): 17968-75.
- Sambrook J., Fritsch J.E., Maniatis T.** Eds. (1989). Molecular cloning: a laboratory manual. Cold Spring Harbor, NY, Cold Spring Harbor Laboratory.
- Sanger F., Nicklen S., Coulson AR.** (1977). "DNA sequencing with chain-terminating inhibitors." Proc. Natl. Acad. Sci. U S A 74(12): 5463-7.

- Sauer F. G., Futterer K., Pinkner J.S., Dodson K.W., Hultgren S.J., Waksman G.** (1999). "Structural basis of chaperone function and pilus biogenesis." *Science* 285: 1058-61.
- Savvides S. N., Yeo H.J., Beck M.R., Blaesing F., Lurz R., Lanka E., Buhrdorf R., Fischer W., Haas R., Waksman G.** (2003). "VirB11 ATPases are dynamic hexameric assemblies: new insights into bacterial type IV secretion." *EMBO J.* 22: 1969-80.
- Schägger H. and G. von Jagow** (1987). "Tricine-sodium dodecyl sulfate-polyacrylamide gel electrophoresis for the separation of proteins in the range of 1 to 100 kDa." *Anal. Biochem.* 166: 368-79.
- Schmidt-Eisenlohr H., Domke N., Angerer C., Wanner G., Zambryski P.C., Baron C.** (1999a). "Vir proteins stabilize VirB5 and mediate its association with the T pilus of *Agrobacterium tumefaciens*." *J. Bacteriol.* 181: 7485-92.
- Schmidt-Eisenlohr H., Domke N., Baron C.** (1999b). "TraC of IncN plasmid pKM101 associates with membranes and extracellular high molecular weight structures in *Escherichia coli*." *J. Bacteriol.* 181: 5563-71.
- Schmidt-Eisenlohr H., Rittig M., Preithner S., Baron C.** (2001). "Biomonitoring of pJP4-carrying *Pseudomonas chlororaphis* with Trb protein-specific antisera." *Environ. Microbiol.* 3: 720-30.
- Shamaei-Tousi A., Cahill R., Frankel G.** (2004). "Interaction between protein subunits of the type IV secretion system of *Bartonella henselae*." *J. Bacteriol.* 186(14): 4796-801.
- Siber G. and M. Samore** (1998). Pertussis. *Harrison's Principles of Internal Medicine*. A. Fauci. New York, McGraw Hill: 933-35.
- Sieira R., Comerchi D.J., Sanchez D.O., Ugalde R.A.** (2000). "A homologue of an operon required for DNA transfer in *Agrobacterium* is required in *Brucella abortus* for virulence and intracellular multiplication." *J. Bacteriol.* 182: 4849-55.
- Smith T. and M. Waterman** (1981). "Overlapping genes and information theory." *J. Theor. Biol.* 91(2): 379-80.
- Sonnenberg A. and J. Everhart** (1997). "Health impact of peptic ulcer in the United States." *Am. J. Gastroenterol.* 92: 614-20.
- Stahl L. E., Jacobs A., Binns A.N.** (1998). "The conjugal intermediate of plasmid RSF1010 inhibits *Agrobacterium tumefaciens* virulence and VirB-dependent export of VirE2." *J. Bacteriol.* 180: 3933-39.
- Stryer L.** (1995). *Biochemistry*, Freeman.
- Tabor S. and C. Richardson** (1985). "A bacteriophage T7 RNA polymerase /promotor system for controlled exclusive expression of specific genes." *Proc. Natl. Acad. Sci. USA* 82(4): 1074-78.
- Taylor M. and A. Hoerauf** (1999). "Wolbachia bacteria of filarial nematodes." *Parasitol. Today* 15(11): 437-42.
- Thanassi DG. and S.J. Hultgren** (2000). "Multiple pathways allow protein secretion across the bacterial outer membrane." *Curr. Opin. Cell Biol.* 12(4): 420-30.
- Tsolis RM.** (2002) "Comparative genome analysis of the alpha -proteobacteria: relationships between plant and animal pathogens and host specificity." *Proc Natl Acad Sci.* 99(20):12503-5.
- Viollier P.H. and L. Shapiro** (2003) "A lytic transglycosylase homologue, PleA, is required for the assembly of pili and the flagellum at the *Caulobacter crescentus* cell pole". *Mol. Microb.* 49(2):331-45
- Wallace L., Ward J., Bennett PM., Robinson M.K., Richmond MH.** (1981). "Transposition immunity." *Cold Spring Harb. Symp. Quant. Biol.* 45(1): 183-8.
- Walsh C.** (2003). "Where will new antibiotics come from?" *Nat. Rev. Microbiol.* 1(1): 65-70.
- Ward D., Draper O., Zupan J.R., Zambryski P.C.** (2002). "Peptide linkage mapping of the *A. tumefaciens* vir-eN coded type IV secretion system reveals novel protein subassemblies." *Proc. Natl. Acad. Sci. USA* 99: 11493-500.
- Weiss A. A., Johnson F.D., Burns D.L.** (1993). "Molecular characterization of an operon required for pertussis toxin secretion." *Proc. Natl. Acad. Sci. USA* 90: 2970-74.
- WHO/TDR** (2002). Onchocerciasis. Disease burden and epidemiological trends, World Health Organization/Tropical disease research.
- Williams-Woodward J.** (2002). Georgia Plant Disease Loss Estimates, Cooperative Extension Service;The University of Georgia College of Agricultural and Environmental Sciences. 2004.
- Winans S., Kerstetter RA., Nester EW.** (1988). "Transcriptional regulation of the *virA* and *virG* genes of *Agrobacterium tumefaciens*." *J. Bacteriol.* 170(9): 4047-54.
- Winans S. C., Burns D.L., Christie P.J.** (1996). "Adaption of a conjugal system for the export of pathogenic macromolecules." *Trends Microbiol.* 4: 64-68.
- Winstead E. R.** (2002). Potential bioweapon, *Brucella suis*, is sequenced, Genome News Network. 2004.

- Woodcock D., Crowther P., Doherty J., Jefferson S., DeCruz E., Noyer-Weidner M., Smith SS., Michael MZ., Graham MW.** (1989). "Quantitative evaluation of *Escherichia coli* host strains for tolerance to cytosine methylation in plasmid and phage recombinants." Nucleic Acids Res. 17(9): 3469-78.
- Yanisch-Perron C., Viera J., Messing J.** (1985). "Improved M13 phage cloning vectors and host strains: nucleotide sequence of the M13mp18 and pUC18 vectors." Gene 33: 103-19.
- Yeo H. J., Savvides S. N., Herr A.B., Lanka E., Waksman G.** (2000). "Crystal structure of the hexameric traffic ATPase of the *Helicobacter pylori* type IV secretion system." Mol. Cell 6: 1461-72.
- Yeo H.-J. and G. Waksman** (2004). "Unveiling molecular scaffolds of the type IV secretion system." J. Bacteriol. 186(7):1919-26
- Yeo H.-J., Yuan Q., Beck M.R., Baron C., Waksman G.** (2004). "Structural and functional characterization of the VirB5 protein from the type IV secretion system encoded by the conjugative plasmid pKM101." Proc. Natl. Acad. Sci. USA, in press.
- Zambryski P.C.** (1992). "Chronicles from the *Agrobacterium*-plant cell DNA transfer story." Ann. Rev. Plant Physiol. Plant Molec. Biol. 43: 465-90.
- Zhou X. and P.J. Christie** (1997). "Suppression of mutant phenotypes of the *Agrobacterium tumefaciens* VirB11 ATPase by overproduction of VirB proteins." J. Bacteriol. 179(18): 5835-42.
- Zinoni F., Heider J., Böck A.** (1990). "Features of the formate dehydrogenase mRNA necessary for decoding of the UGA codon as selenocysteine." Proc. Natl. Acad. Sci. USA 87: 4660-64.
- Zupan J., Muth TR., Draper O., Zambryski P.** (2000) "The transfer of DNA from *Agrobacterium tumefaciens* into plants: a feast of fundamental insights." Plant J. 23(1):11-28.

Danksagung

Bei Herrn Prof. Dr. C. Baron bedanke ich mich sehr herzlich für die Vergabe eines interessanten Themas, für sein stetes Interesse am Fortgang der Arbeit, seine Geduld und dafür, dass er mir bei klar definierten Zielvorgaben immer große Freiheit gewährt hat.

I am indebted to all collaborators in the EU frame program 5, especially Prof. Dr. David O'Callaghan who was an excellent, humorous but not very French supervisor during my work with a BL3 pathogen that (as I understand) can best be distinguished from *E. coli* by its characteristic smell. Special thank to Annette Vergunst, Felix Sangari, Doris Zahrl and Günther Koraimann for lively discussions.

Vielen Dank besonders auch an Herrn Prof. Dr. A. Böck für ein offenes Ohr und das professionelle und vorbildliche Verhalten welches er Studenten, Doktoranden und Professoren gegenüber gezeigt hat.

Besonderer Dank geht an meine liebe Kollegin Anna. Ihre aktive Unterstützung, ihre Fachkenntnisse, ihr charmanter Zynismus und ihre gelegentlich auftretende, viel zu schlechte Laune, haben den Laboralltag stark bereichert.

Danke an alle ehemaligen und aktuellen Mitglieder der AG Baron, besonders Qing für seine stets außerordentlich gute Laune und Natalie für Hilfe bei der praktischen Umsetzung des Projektes. Danke an Lili für die Definition des Begriffes "Optimismus" und vielen Dank an Heike für ihre kopierenswerte Zielstrebigkeit. Thank you Durga and Khaled for nice protocols and occasional moral support.

Für das gute Arbeitsklima bedanke ich mich bei den Mitarbeitern des Instituts für Genetik und Mikrobiologie, für musikalische Aufmunterungen danke ich der Hit-Rotation von Antenne Bayern und Phil Collins.

Danke an die Mitarbeiter der Städtischen Kinderkrippe Schachenmeierstraße und an Nicolas Leonid, dafür dass er immer so gerne dort hingeht.

Vielen Dank meiner Familie, besonders meiner Frau Bine für die fachliche Hilfe in Fragen der Strukturbioologie, moralische Unterstützung und das gelegentliche Kopf-Zurechtrücken.

Lebenslauf

Persönliche Daten

Name: Christoph Höppner
Geburtsdatum: 7. 1. 1975
Geburtsort: München
Familienstand: verheiratet
Kinder: Nicolas Leonid Höppner
Staatsangehörigkeit: Deutschland, USA

Ausbildung

1985-1994 Werner-Heisenberg-Gymnasium in Garching,
mathematisch-naturwissenschaftlicher Zweig

8/94-10/95 Zivildienst

11/95-3/01 Studium der Biologie an der Ludwig- Maximilians-
Universität in München und der Universidad der
Concepción, Chile; Diplom

seit 9/01 Bearbeitung der vorliegenden Dissertation am Lehrstuhl
für Mikrobiologie der Ludwig-Maximilian-Universität
München und am INSERM U431 in Nîmes, Frankreich
unter Leitung von Prof. Dr. C. Baron